TU DELFT – MULTIDISCIPLINARY PROJECT CIE4061

Afsluitdijk Project
"The Monument" Location

Final Report

Sien Liu, Jun Huang, Sebastian Rayo, Tai Yan Lim

21/12/2012



CONTENTS

1 Introduction 3
1.1 Background 3
1.2 Problem Description 3
1.3 Document Scope 3
1.4 Documents Lists 3
2 Data Collection and Analysis 4
2.1 Site Appreciation Analysis 4
2.2 Wave Climate Definition 6
2.3 Definition of Relevant Cross Sections 6
2.4 Location and Dimensions of Obstacles on Dike's Crest 8
2.5 Comments 9
3 Problem Analysis 10
3.1 Overtopping 10
3.1.1 Cross Section Selection 10
3.1.2 Overtopping rate 10
3.1.3 Flow depth and flow velocity 11
3.2 Flow distribution 11
3.2.1 Assumptions 12
3.2.2 Figures of places of interest 12
3.3 Diagnosis 16
3.3.1 Critical Spots Definition 16
3.3.2 Analysis 17
3.4 Recommendations 18
4 Definition of Alternatives 19
4.1 Alternatives 19
4.1.1 Reinforcing of Outer Protection 19
4.1.2 Wall on Top 19
4.1.3 Berm 20
4.1.4 Submersed Breakwater 20
4.1.5 Reinforced Grass with Small Wall 21
4.1.6 Energy Converter Device 22
4.1.7 Increase in Roughness 23
4.2 Pre-Dimensioning 24
4.3 Investment Cost 24
4.3.1 General Information 24
4.3.2 Cost Estimation 24
4.4 Final Comments 24
5 Multi – Criteria Analysis 25
5.1 Methodology 25
5.2 Criteria Definition 25
5.3 Alternatives 26
5.4 Evaluation 27
5.5 Result 27
6 Development of Selected Alternative 28
6.1 Overtopping retaining wall 28
6.1.1 Gravity wall 28

6.1.2 Design of Cantilever Retaining Wall 28
6.2 Construction of Cantilever Retaining Wall 31
6.3 Final Comments 32
7 Final Conclusions 33
8 References 34

1 INTRODUCTION

1.1 Background

The Afsluitdijk (Enclosure Dam) is a main dam that forms the fundamental part of the larger Zuiderzee Works that separates the Zuiderzee, a salt water inlet of the North Sea, and turning it into the fresh water lake of the IJsselmeer. It protects the central Netherlands from the effects of the North Sea. It was constructed between 1927 and 1933, and runs from Den Oever on Wieringen to the village of Zurich in Friesland. It is 32 km long and 90 meters wide, rising to 7.25 meters above sea-level, with an incline of 25% on each side.

At the location along the Afsluitdijk where the final water passage was closed ('De Vlieter'), a lookout tower known as 'The Monument' was built in 1933. It was presented by the Zuiderzee Works Construction Company and designed by architect W.M. Dudok. The site has a statue of a "Steenzetter", and also marks the inscription 'A living nation builds for its future'. A statue of Cornelis Lely has also been erected near Den Oever on the Barrier Dam itself.

The Afsluitdijk with The Monument are currently managed by the Ministry of Infrastructure and the Environment ("The client"). There is a restaurant at The Monument where the client has sublet it for private operator to manage it.

1.2 Problem Description

With the anticipation of increase storm intensity and sea level rise in the future, the client had previously engaged a consultant to analyze the existing design of Afsluitdijk for a design storm of 1:10,000 years. According to the client, the result of the study concluded that the standard cross-section of Afsluitdijk is not sufficient to withstand the design storm of 1:10,000 years, hence, modifications of it are required. The study also found that during the design storm, there is a significant overtopping over the dike.

The client is concerned about the significant overtopping found from the previous study may have adverse impact on the non-standard cross-section of the dike where The Monument is located. Therefore, the client has requested our design team to look into the dike section at The Monument location.

1.3 Document Scope

The main objective of this document is:

- To present a summary with the different phases of the Afsluitdijk project.

1.4 Documents Lists

The following documents are part of this package:

- Literature Review
- Data Collection and Analysis
- Problem Analysis
- Definition of Alternatives
- Multi – Criteria Analysis
- Overtopping Wall Design

2 DATA COLLECTION AND ANALYSIS

2.1 Site Appreciation Analysis

Relevant information to the developing of the project is presented in Figures 2.1 to 2.5.

Figure 3.1 shows the seaside slope of the Afsluitdijk at The Monument location. Relevant characteristics are the presence of a toe made of rocks, the slope has a basalt revetment with presence of grass and on the upper part of the slope exist a steep section, which in some parts appears to be vertical.



Figure 2.1. Seaside slope of Afsluitdijk at The Monument location

Figure 2.2 shows the seaside slope of the Aflsuitdijk at the standard cross section, outside The Monument location. Relevant characteristics are the presence of a toe made of rocks, the slope has a partial revetment of basal (lower part) while the upper part has grass cover. The crest of the dike is also has a grass cover.



Figure 2.2. Seaside slope of Afsluitdijk at the standard cross section

The cross section at The Monument location is different than the standard cross section. The Afsluitdijk has two transition sections. Those sections are characterised by a variable height of the wall, a variable level of the bicycle lane and a variable width of the dike's crest. Figure 2.3 shows a photograph of the south transition section.



Figure 2.3. Southern transition between standard cross section and The Monument cross section

During the visit, on the crest of the dike at The Monument location, several obstacles were found. These obstacles corresponds to a statue (A), an information wall (B), a scale dike of basalt (C) and a bridge for pedestrians (D). Figures 2.4 presents photographs of these singularities.


(a)


(b)

(c)

(d)

Figure 2.4. a) Statue; b) Information wall; c) Scale dike of basalt; d) Bridge for pedestrians

Finally, the rear slope of the dike at The Monument location presents two main characteristics: the presence of a large platform that serves as a parking area for vehicles; and a building with a tower (includes a restaurant).


(a)

(b)

Figure 2.6. a) Parking area; b) Building with tower

2.2 Wave Climate Definition

Tables 2.1 present part of the information for the selected wave climate scenario.

Table 2.1. Wave climate for year 2050, model HYDRA-K2012

Location	Sea elevation	Significant wave height	Mean wave period
	[m+NAP]	*[m]*	*[s]*
East	5.54	3.02	5.70
Middle	5.61	3.90	6.18
West	5.69	3.08	5.72

Table 2.1 presents information for three locations. Neither of it includes The Monument (location approximately at 7 kilometres from the beginning of the dike). Therefore, it will be considered the "Middle" location because its related data is more conservative.

Hence, wave climate is defined as:

- Future sea level elevation = 5.61 m + NAP
- Significant wave height = 3.90 m
- Mean wave period = 6.18 s

Finally, this table do not provide information about direction of the waves. To estimate the overtopping, a wave approaching perpendicularly to the dike will be considered, because the values under this situation are more conservative.

2.3 Definition of Relevant Cross Sections

Overtopping rate will be calculated for several relevant cross sections. Those cross sections are:

- Cross section at The Monument location (section A)
- Standard cross section (section B)
- Transition cross section 1 (closer to standard cross section) (section C)
- Transition cross section 2 (closer to The Monument cross section) (section D)

Figure 2.6 presents a plan view with the location of the defined cross sections.

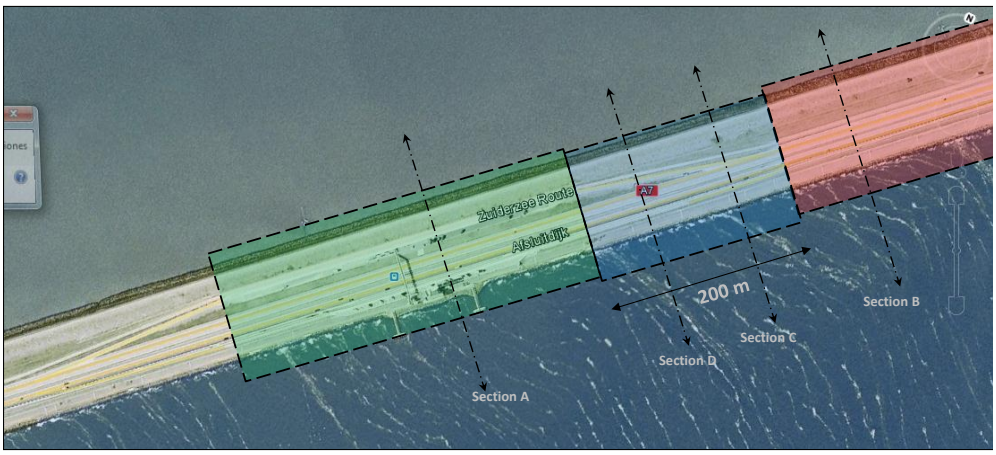

Figure 2.6. Plan view with location of cross sections.

Although section B is outside of the area of study, it is important to obtain an overtopping estimation in order to compare it with previous overtopping results. Transition sections are important because they are not part of the previous study and the field visit revealed that these sections are covered with grass (dike crests and rear slope) and the crest width is thinner than in the standard cross sections.

Figures 2.7 and 2.8 present typical cross sections of The Monument and standard dike, respectively.

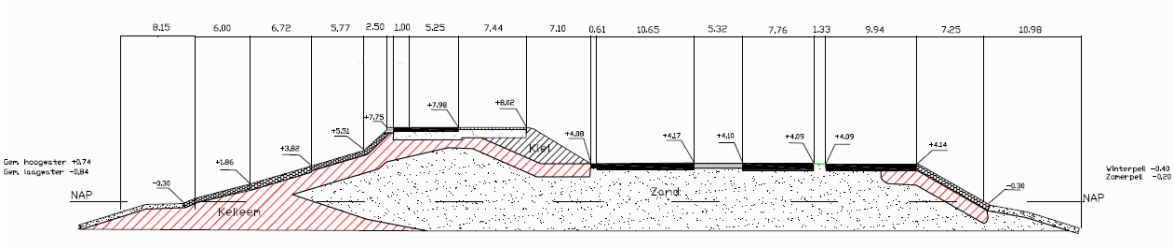

Figure 2.7.Cross section at The Monument location

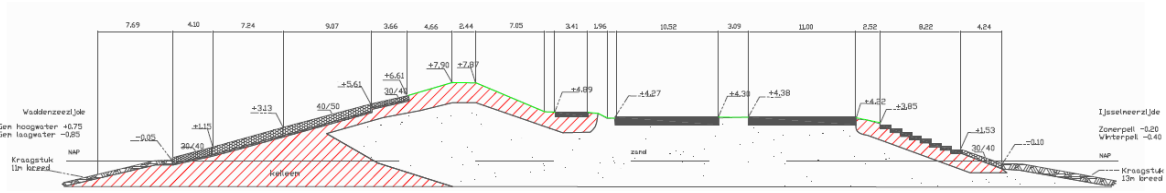

Figure 2.8. Afsluitdijk standard cross section

According with the information obtained from these Figures, at The Monument location the crest elevation is +7.75 m while the standard cross section is slightly taller (+7.9 m). Another important feature that was seen during the visit is the presence of a small wall at The Monument location, which is not present in Figure 2.7.

There is no direct information about cross sections for the transition area. Therefore, it is necessary to recreate it from the available information. The site visit allowed seeing that variation of the crest elevation, the width of the crest and the height of the seawall varied linearly from section A to section B. Hence, sections C and D were constructed assuming that linear variation between known sections. Figures 2.9 and 2.10 present the front slope of sections C and D, respectively.

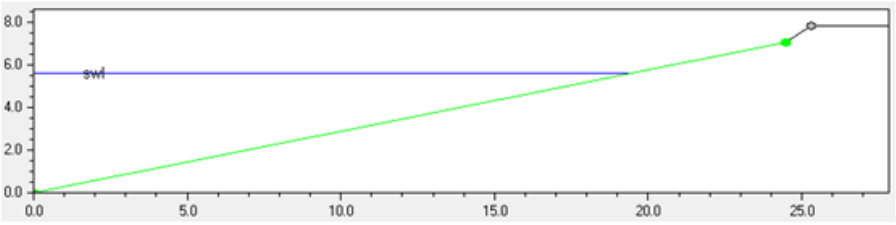

Figure 2.9. Transition cross section C

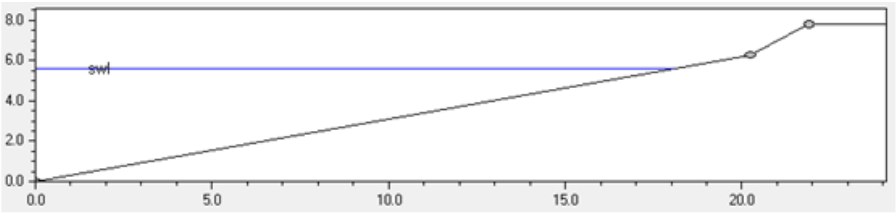

Figure 2.10. Transition cross section D

2.4 Location and Dimensions of Obstacles on Dike's Crest

The field visits revealed the existence of several obstacles at The Monument location. Figure 2.11 shows a plan view of The Monument location. Several obstacles are highlighted: statue (A), information wall (B), scale dike of basalt (C) and building on the rear part (D).

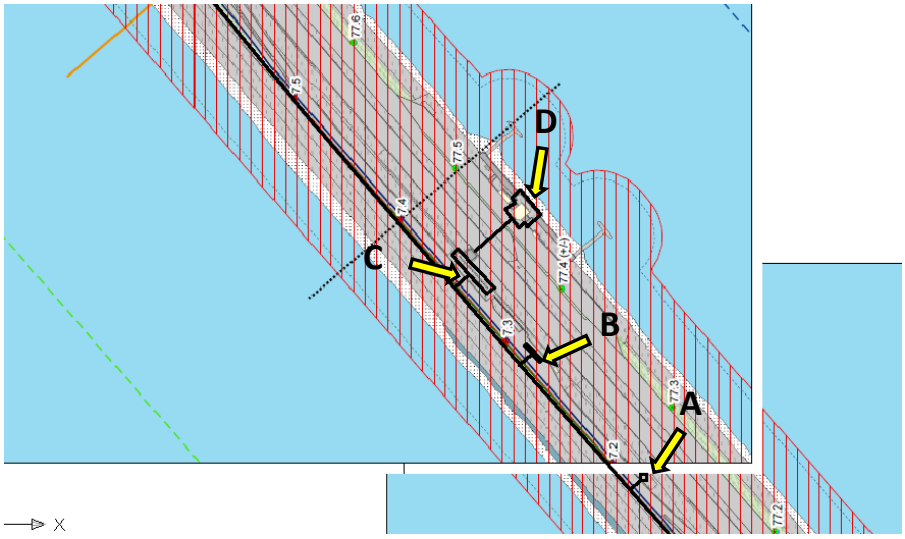

Figure 2.11. Transition cross section D. Source: reference [5]

All of these obstacles are located in the regular section of The Monument area (i.e. they are not located in any of the transition areas or the standard cross section of the Afsluitdijk). Therefore, the overtopping rate that will be produced in front of these obstacles can be considered as uniform; hence, the relative position of each obstacle along the dike is not relevant.

The important parameters related with each obstacle are the dimensions (width) and distance to the top of the dike at the defence line. Dimensions were obtained with software Autocad and are approximated. Table 2.2 presents a summary with relevant dimensions and distances.

Table 2.2. Relevant dimensions and distances of obstacles at The Monument area

Obstacle	Denomination	Width	Distance to defence line
		[m]	*[m]*
Statue	A	5 (1)	9
Information wall	B	14	11
Scale dike of basal	C	34	13
Building	D	21	33 (2)

(1) The statue is not aligned with the dike's axis, but it is rotated with an estimated angle of 45°. Presented width corresponds to the projection of two sides of a square, which has a side of 3.8 m.
(2) Because the building is located in the rear slope of the dike, the presented distance corresponds to the horizontal distance to the bottom of the first rear slope, which is basically the width of the highway plus the parking width plus existing tolerances.

2.5 Comments

Regarding with the analysis of available information, the following comments are made:

- Site visits allowed the visualization and detection of several obstacles. In this analysis, only the most important (largest) obstacles were considered. Some minor obstacles, like fences, bus stops, steps and small platforms were not considered because it is considered that their effect is not significant.
- The model to estimate wave conditions under a storm of 1:10,000 years is considered to be valid. Hence, no further verification of its results will be made.
- However, it is important to emphasize that it is assumed that the results of wave propagation from deep water are considered at the top of the toe. Hence, future calculation of overtopping flow rate will consider a cross section that does not include the toe of the dike.
- Cross sections considered are obtained from a well-known reference. Nevertheless, there are some visual differences that are not perfectly explained by these cross sections. More specifically, the presence of a sea wall at The Monument area is not clearly seen in Figure 2.7, which may generate results more conservative than reality. However, in accordance with the client, this section will be considered as a basis of the hydraulic calculations.
- There are no cross sections available at the transition areas. Therefore, the linearization procedure is the best possible assumption that can be made. However, there are uncertainties about these cross sections, which can generate errors in overtopping estimation. A future definition of overtopping at these locations necessarily will need a proper survey of these sections.
- Location and dimensions of the obstacles are on the basis of available layouts and the field visits. However, there is no detailed information about these obstacles. Therefore, dimensions are only approximations based on available information.
- Finally, the available information does not include anything related with foundations of the structures. Considering that dimensions of the visible part of these structures are only approximations, it is not possible to assume any dimension and/or shape of their foundations. Therefore, a calculation of resistance against overturning will be possible to make only in future stages of engineering.

3 PROBLEM ANALYSIS

3.1 Overtopping

3.1.1 Cross Section Selection

In this procedure, 4 cross-sections are chosen to calculate based on the particular shape respectively. The first cross-section is the standard cross-section, the second cross-section is the monument cross-section, and the third and the fourth cross-section are two transition cross-sections from the standard cross-section to the monument cross-section.

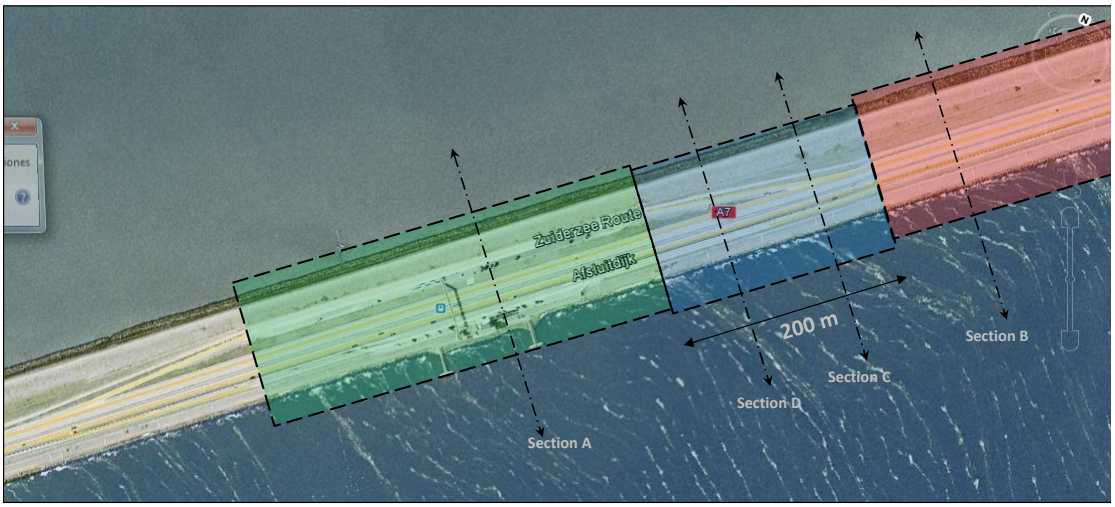

Figure 3.1 Plan view with location of cross sections

3.1.2 Overtopping rate

The overtopping rates and maximum wave overtopping volume are calculated by using computer program 'PCOverslag'. The storm duration is considered to be 6h, and the incident wave angles are considered to be 0 in order to obtain a conservative result. There are only two different kinds of materials on the seaward slope, basalt and grass. The influence factors of roughness are $\gamma_f = 0.9$ and $\gamma_f = 1$ respectively. The seaward slopes consist of several segments with different $\tan\alpha$, this effects are also taken into consideration in 'PCOverslag'.

The results in Table 3.1 show the output of 'PCOverslag'. Several important parameters like wave run-up, mean wave overtopping rates and maximum wave overtopping volume are selected. The maximum wave overtopping volume has high uncertainty and highly depends on the storm duration. However, it an important parameter to evaluate the hazard on buildings and infrastructure caused by wave overtopping.

Table 3.1. PC overtopping software results

Parameters	Standard cross section	Monument cross section	Transition 1	Transition 2
R_c (m+NAP)	7.90	7.75	7.90	7.75
$Z_{2\%}$ (m+NAP)	12.48	14.2	14.163	12.635
$Z_{2\%}$- R_c	4.58	6.45	6.263	4.885
q (l/s/m)	270.88	579.82	549.036	289.168
V_{max} (l/m)	32349.17	59066.09	56573.1	33503.66

3.1.3 Flow depth and flow velocity

The flow depth and flow velocity are important to estimate the erosion rate of the grass and clay which will be the cause of dike breaching. Base on the newly developed theory by Bosman, the overtopping flow depth and flow velocity can be calculated, but under following assumptions:

- Dike crest is horizontal.
- Vertical flow velocity to the dike slope can be neglected.
- Pressure term is constant over dike crest.
- Viscous effects in flow direction are small and bottom friction is constant over dike crest.

The formula that we use to calculate the flow depth and flow velocity are further development by Bosman based on formula of Schüttrumpf and Van Gent (2003). The results with some important parameters are shown in Table 3.2. Same consideration is taken to obtain conservative results, so the influence factors of roughness are considered to be 1.

Table 3.2. Flow velocity and flow depth on crest

Parameters	Standard cross section	Monument cross section	Transition 1	Transition 2
$H_{(0)}$ [m]	0.46	0.41	0.40	0.41
$V_{(0)}$ [m/s]	6.6	6.2	6.1	6.2
Crest width [m]	2.5	19	18	3
$H_{(end)}$ [m]	0.24	0.03	0.004	0.19
$V_{(end)}$ [m/s]	4.3	0	0	3.2

3.2 Flow distribution

Based on the result from the data analysis, the flow distributions through the following obstacles were calculated:

- Statue
- Monument Tower (Building with restaurant and tower)
- Information Wall
- Mini- Dike (Scale dike of basalt)

These obstacles around The Monument location were the only possible obstacles from the analysis to generate a 'concentration' of overtopping flow both in the top and in the rear slope of the Afsluitdijk.

3.2.1 Assumptions

The following five assumptions were made on the flow of the water after it overtop the crest and travel through the inner and encounter obstacles.

- Flow reduction of 1/2 L is used to estimate the overtopping flow just in front of obstacle, q_2.
- Flow distribution coefficient, W_1/W_2 varies to max 1.00. => $q_3 = 2 \times q_2$, where Max W_2 = 5m
- For long obstacle, flow from edge to W_1 m is assumed to be diverted to the sides of obstacle.
- For long obstacle, flow that is between W_1 m away from both edges is assumed to be reflected.
- For Monument Tower, no flow reduction is applied to q_2 (i.e. 61.03 l/s/m), after it passes down from the inner slope.

One important point to note is that these assumptions were conservative in nature and thus will overestimate the actual amount of flow that passed the obstacle. More research is required in future to validate these assumptions and obtain a more cost effective design.

For more details about these assumptions, see document 'Problem Analysis'.

3.2.2 Figures of places of interest

Statue

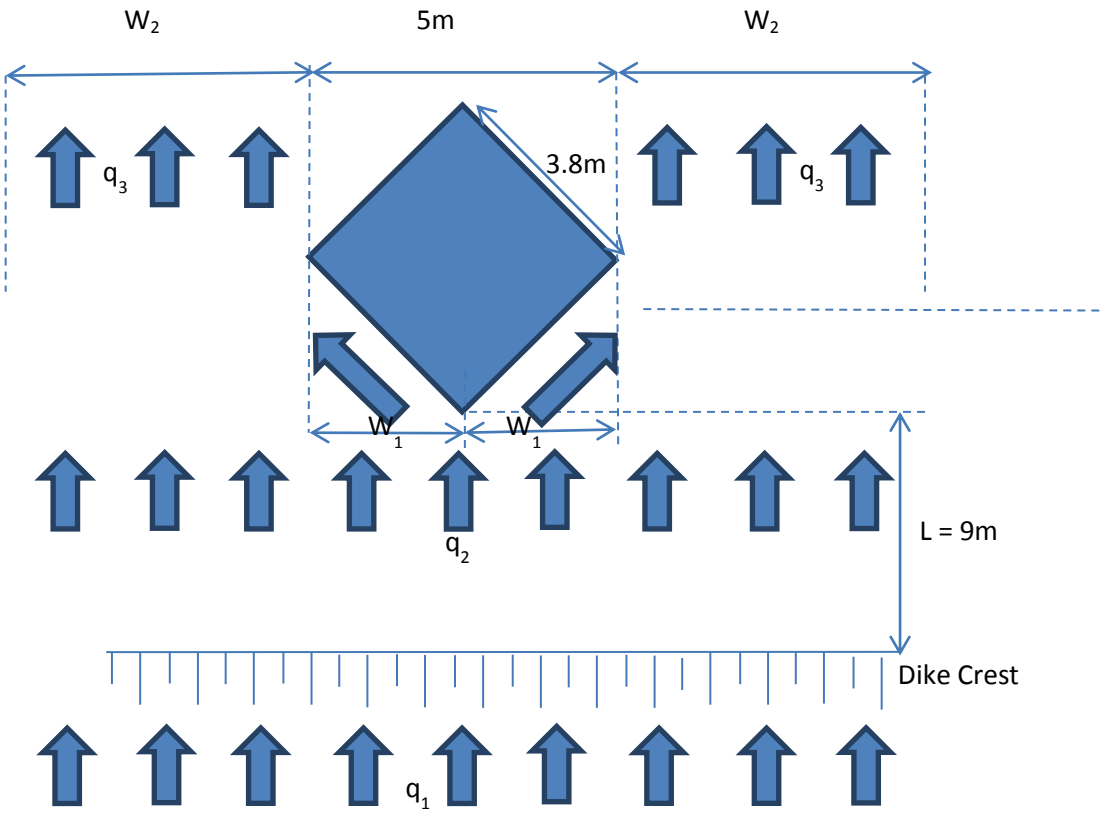

Figure 3.2 Flow distribution of statue

The corresponding data is listed in Table 3.3 below.

Table 3.3. Relevant parameter for location of statue

q1	579.82	l/s/m
L	9.00	m
x	0.50	
q2	128.85	l/s/m
W1	2.50	m
W2	2.5 - 5	m
W1/W2	0.5 - 1	
q3	193.27 -257.70	l/s/m

Monument tower

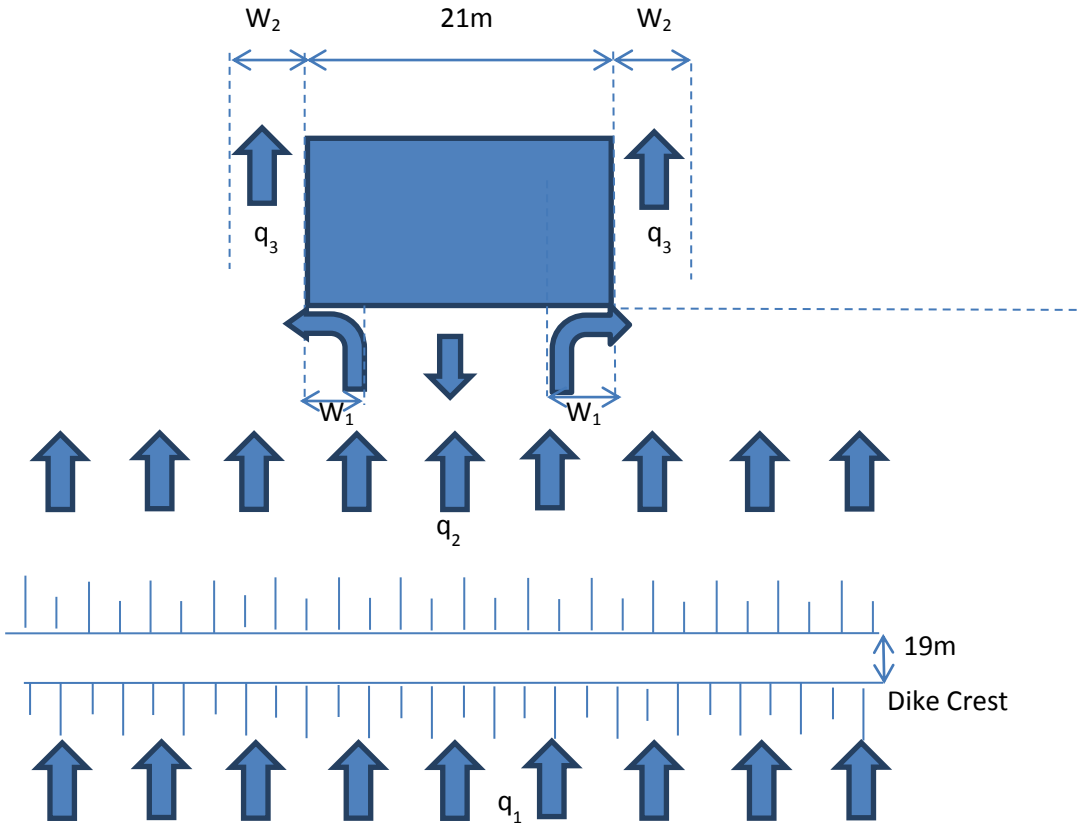

Figure 3.3 Flow distribution of Monument tower

The corresponding data is listed in Table 3.4 below.

Table 3.4 Relevant parameter for location of monument tower

q1	579.82	l/s/m
L	19.00	m
x	0.50	
q2	61.03	l/s/m
W1	1.00	m
W2	1.0 - 5.0	m
W1/W2	0.2 - 1.00	
q3	73.24 - 122.07	l/s/m

Information Wall

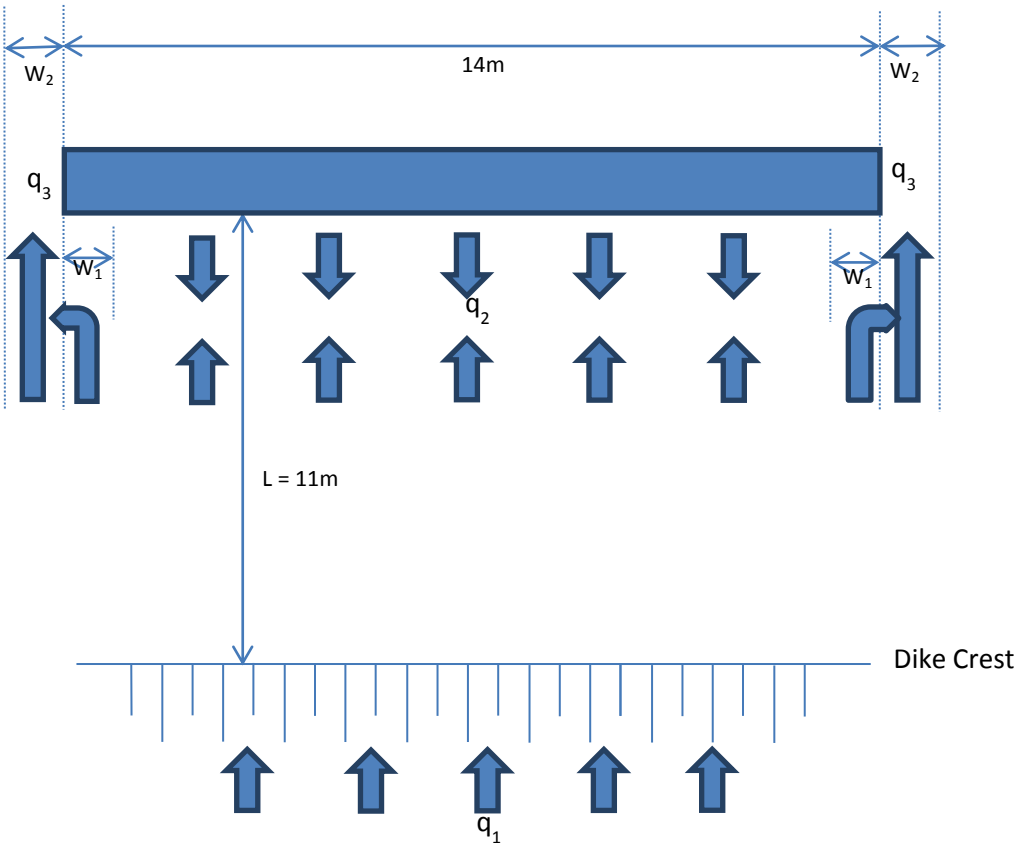

Figure3.4 Flow distribution of Information Wall

The corresponding data is listed in Table 3.4 below.

Table 3.4. Relevant parameter for location of information wall

q1	579.82	l/s/m
L	11.00	m
x	0.50	
q2	105.42	l/s/m
W1	1.00	m
W2	1.0 - 5.0	m
W1/W2	0.2 - 1.00	
q3	126.51 - 210.84	l/s/m

Mini dike

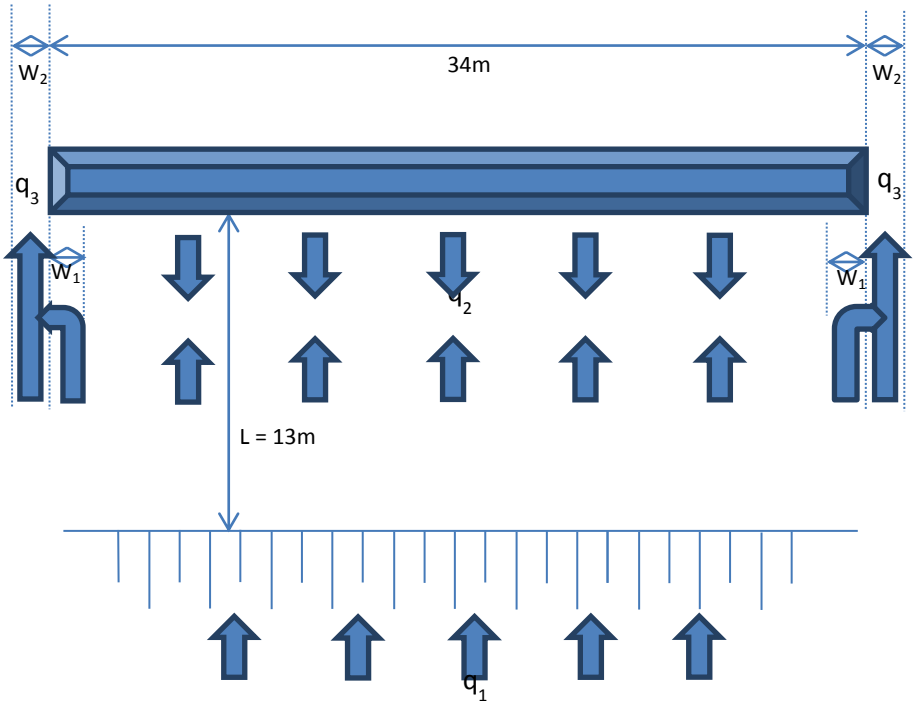

Figure 3.5 Flow distribution of mini dike

The corresponding data is listed in Table 3.5 below.

Table 3.5. Relevant parameter for location of mini dike

q1	579.82	l/s/m
L	13.00	m
x	0.50	
q2	89.20	l/s/m
W1	1.00	m
W2	1.0 - 5.0	m
W1/W2	0.2 - 1.00	
q3	107.04 - 178.41	l/s/m

3.3 Diagnosis

3.3.1 Critical Spots Definition

The calculation of overtopping flow rate and its spatial distribution at the top of the dike have revealed several areas that might be in risk of breaching if there is a storm of 1:10,000 years. The critical spots are presented in Figure 3.6.

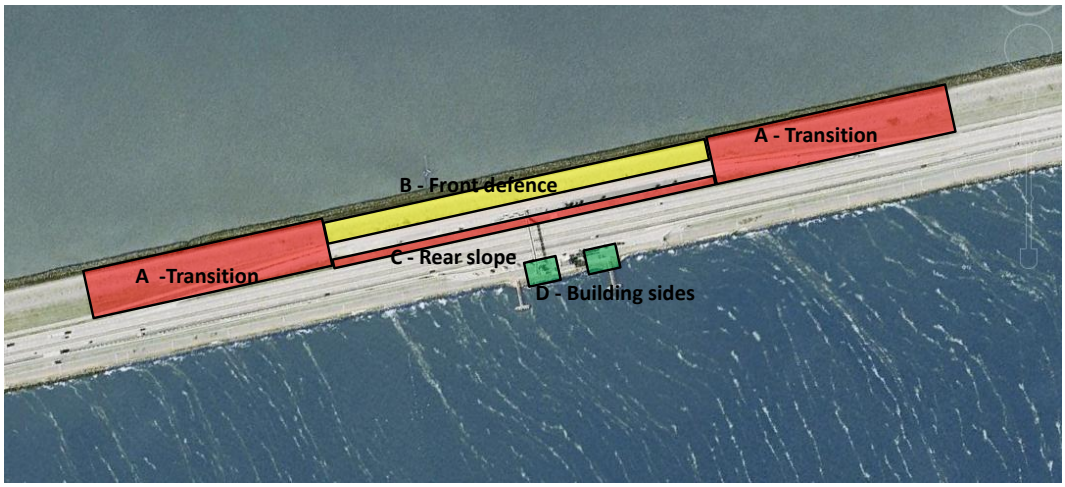

Figure 3.6. Critical spots at The Monument location

The critical spots are:

- Spot A: both transitions (north and south sides) from The Monument cross section to standard cross section.
- Spot B: front defence at The Monument area (part of the high parking area closer to the seaside slope).
- Spot C: rear slope at The Monument area (from parking area to highway platform).
- Spot D: sides of the tower building (rear slope from low parking area to lake side).

3.3.2 Analysis

Spot A: transitions

Previously the overtopping flow rate was calculated at two different cross sections (transition 1 and 2). The values obtained were 549 l/s/m and 289 l/s/m, respectively. Considering that the boundaries of both transitions are The Monument and the standard dike, the overtopping flow rate at those points is 271 l/s/m and 580 l/s/m, respectively.

At both transitions, on the front slope the dike has a revetment with basalt. Nevertheless, the top and rear slope of the dike has grass revetment. The strength of grass is quite small, especially when there are large velocities of overtopping. Calculations of overtopping velocities are in the range of 6 to 6.5 m/s, which are larger than the maximum allowed velocities for grass. Figure 3.7 shows the maximum permissible duration of grass coverage depending on the flow velocity and the quality of the grass coverage.

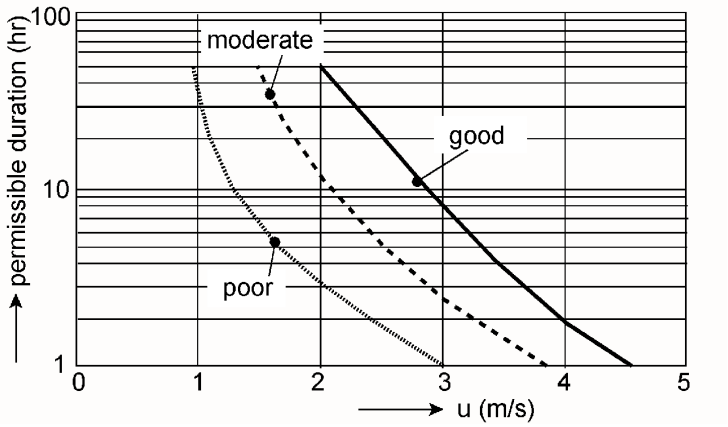

Figure 3.7. Permissible flow duration on grass cover. Source: Schiereck, G. J., 'Introduction to Bed, Bank and Shore Protection'

The overtopping velocities exceed the maximum allowed in this graph, which means that the permissible duration of a storm will be less than one hour. Therefore, it can be concluded that the resistance of the grass for overtopping flow rate in the range 271 to 580 l/s/m is very limited.

Below the grass cover there is a clay layer. If there is no grass cover anymore, the clay layer will have a limited resistance against overtopping load. Applying the Parthenade method (suitable for cohesive soils) and assuming the clay layer has a critical shear stress equal to 5 Pa, the erosion process in this layer will take about 1.5 hours. Hence, it can be stated that the resistance of this layer is low when the outer protection has been removed.

Considering that the resistance of both the grass cover and the clay layer are quite low against the overtopping loads, diagnosis indicates that an improvement in this spot is required.

Spot B: Front defence at The Monument

The overtopping flow rate is fixed and is equal to 590 l/s/m. In this spot, the dike's rear slope has a basalt revetment, while on top of the dike there is a small concrete wall. The overtopping rate is large but there is a strong revetment at this location. The main assumption is that behaviour of concrete and asphalt against large overtopping flow rates (especially for erosion) is good. Hence, no further improvements are considered to protect the front defence.

It is important to emphasize that further research of asphalt under very large flow velocities is required, in order to define if this material may have risk of failure.

Spot C: Rear slope at The Monument

The rear slope located behind the high parking area at The Monument has a variable overtopping flow rate, which is influenced by the presence of obstacles at The Monument area. These obstacles generate flow concentrations at some areas. In addition, there are some other areas that does not have overtopping flow rate because they are just behind this obstacles.

The overtopping flow rate is variable, from 0 l/s/m to 260 l/s/m. The average overtopping flow rate along the rear slope is equal to 60 l/s/m.

The rear slope has grass coverage. Characteristics overtopping flow rate (average and maximum) are larger than the maximum allowed overtopping flow rate for a grass cover (30 l/s/m).

Considering that the resistance of the grass cover is limited, diagnosis indicates that an improvement in this spot is required.

Spot D: Sides of tower building

At both sides of the tower building, overtopping flow rate is concentrated. The maximum overtopping flow rate will be 120 l/s/m.

On this spot, the rear slope of the dike has a revetment made of basalt. The strength of the rear slope of the dike at this location is sufficient for a overtopping flow rate of 120 l/s/m. Therefore, improvement at this spot is not required.

3.4 Recommendations

Based on the previous diagnosis, several recommendations should be considered:

- Both transition areas and the rear slope behind the high parking area at The Monument require improvements to withstand a design storm of 1:10,000 years.
- Improvements should be an increase of dike's resistance, a diminishing of the load (reduction of overtopping flow rate) or a combination of both measures.
- The diagnosis is made on the basis of several assumptions made to determine distribution of overtopping flow rate at The Monument.
- Diagnosis considers the limit state of the dike is the removal of the outer protection (grass cover, asphalt or concrete). The resistance of the clay layer can be considered as very small, which means that in case of the design storm, the erosion of the clay layer will be sufficiently rapid to generate a breaching on the dike.

4 DEFINITION OF ALTERNATIVES

4.1 Alternatives

General improvements may be an increase of the dike's strength, a diminishing of the overtopping flow rate (reduced load) or a combination of both. A brainstorm workshop and suggestion from the Client defined several alternatives for both spots.

4.1.1 Reinforcing of Outer Protection

This alternative considers that the outer protection of the dike (grass cover) should be improved by replacing it with a material that stands for very large overtopping flow rate, especially without erosion. It is considered that some materials that have an important resistance against large overtopping flow rates are block revetment and asphalt.

Figure 4.1 shows a scheme with the outer protection's reinforcing. On the transition areas, grass cover of the top and rear slope of the dike are replaced by block revetment; on The Monument area, grass cover of the rear slope is replaced by block revetment.

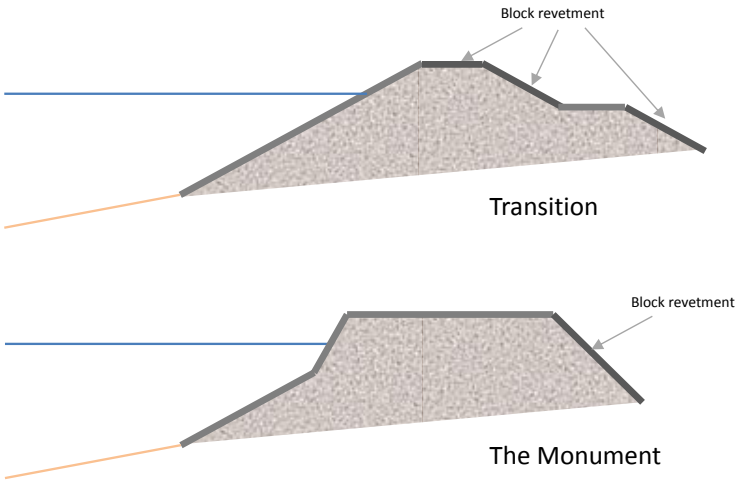

Figure 4.1. Scheme of reinforcing of outer protection

Considering that this alternative does not reduce the load, then the overtopping flow rate at the transition areas and the rear slope of The Monument are those defined in the diagnosis.

4.1.2 Wall on Top

This alternative considers that the overtopping flow rate on the dike will be reduced by the construction of a wall on top of the dike. Reduction of the overtopping flow rate will be to values that a grass cover can stand without significant damage. According to literature review, the selected maximum overtopping flow rate for a grass cover is 30 l/s/m.

Figure 4.2 shows a scheme with the location of the constructed wall. The wall should be constructed with a material with large resistance against direct impacts of overtopping, like concrete. On both areas, the existing grass covers are not modified.

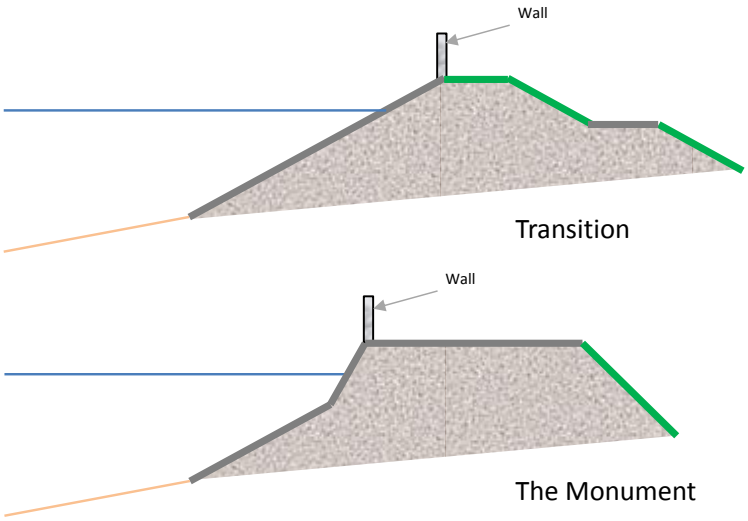

Figure 4.2. Scheme of wall on top

4.1.3 Berm

This alternative considers that the overtopping flow rate on the dike will be reduced by the construction of a berm on the sea side slope of the dike. Reduction of the overtopping flow rate will be to values that a grass cover can stand without significant damage. According to literature review, the selected maximum overtopping flow rate for a grass cover is 30 l/s/m.

Figure 4.3 shows a scheme with the location of the berm. The berm should be constructed with a material with large resistance against waves, like rocks. On both areas, the existing grass covers are not modified.

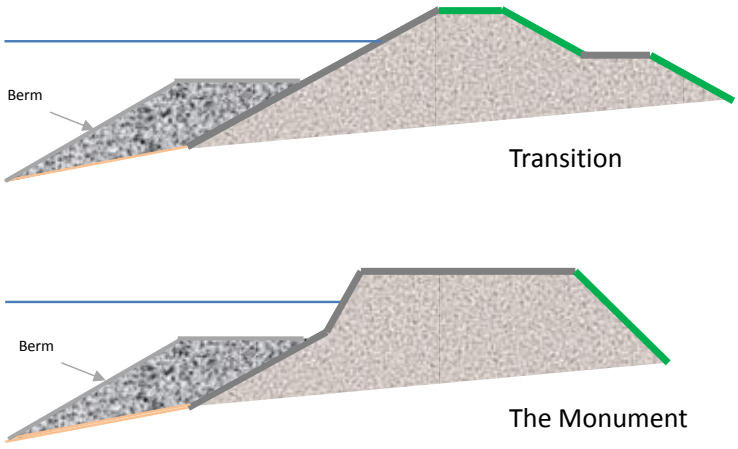

Figure 4.3. Scheme of berm

4.1.4 Submersed Breakwater

This alternative considers that the significant wave height will be reduced by the presence of a submersed breakwater. The transmitted waves will have a significant wave height smaller, which will finally reduce the overtopping flow rate on the dike. Final reduction of the overtopping flow rate will be to values that a grass cover can stand without significant damage. According to literature review, the selected maximum overtopping flow rate for a grass cover is 30 l/s/m.

Figure 2.4 shows a scheme with the location of the submersed breakwater. It is important to emphasize that during the design storm (1:10,000 years), the sea level will rise to a certain elevation. The proposed breakwater will be 'submersed' only during this type of events. The rest of the time the crest of the breakwater will be over the sea surface, which means that the armour layer of this structure must be designed for direct wave impacts.

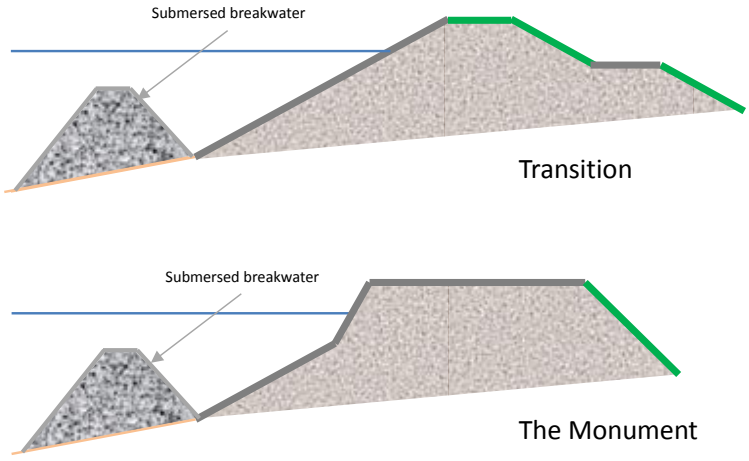

Figure 4.4. Scheme of submersed breakwater

4.1.5 Reinforced Grass with Small Wall

This alternative considers that the strength of the outer protection of the dike will be increased and, at the same time, the load on the dike will be reduced (partially). The existing grass cover will be replaced by a reinforced grass cover (with geo-membrane) that has a better behaviour against erosion caused by overtopping flow rate. Nevertheless, there is no available information about maximum overtopping flow rates for this type of protection. Maximum allowed overtopping flow rate will be estimated based on the increase of the maximum significant wave height and its relation with overtopping flow rate.

Figure 4.5 presents a graph that indicates increase of allowed significant wave height in terms of the grass cover status.

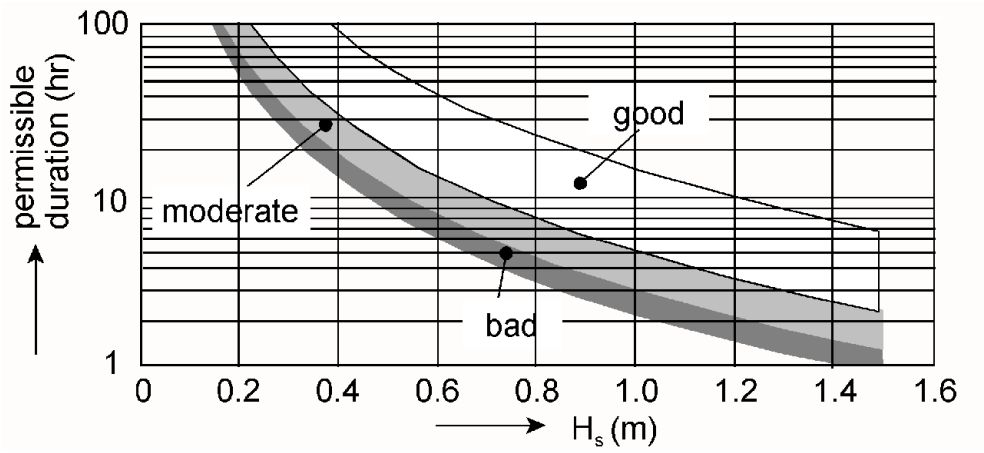

Figure 4.5. Permissible flow duration on grass cover. Source: Schiereck, G. J., 'Introduction to Bed, Bank and Shore Protection'

Assuming typical storm duration of 5 hours, an increase of the grass status from moderate to good is reflected in an increase of the maximum significant wave height from 1.0 m to 1.5 m, which is an increment of 50%. By using software 'Overslag', it is possible to estimate that the maximum overtopping flow rate increases from 30 to 150 l/s/m when there is an increment of maximum allowed significant wave height of 50%. Nevertheless, it is important to emphasize that this method is only an assumption and further research should be made in order to estimate more accurately the real resistance of reinforced grass.

Because the maximum overtopping flow rate for reinforced grass is smaller than the overtopping flow rate estimations, it is necessary to reduce the load on the dike. This partial reduction will be made by constructing a small wall on top of the dike.

Figure 4.6 shows a scheme with the location of the reinforced grass and the small wall. While the reinforced grass will have a geo-membrane to increase resistance against erosion, the wall will be made of a material with sufficient resistance against overtopping flow, like concrete.

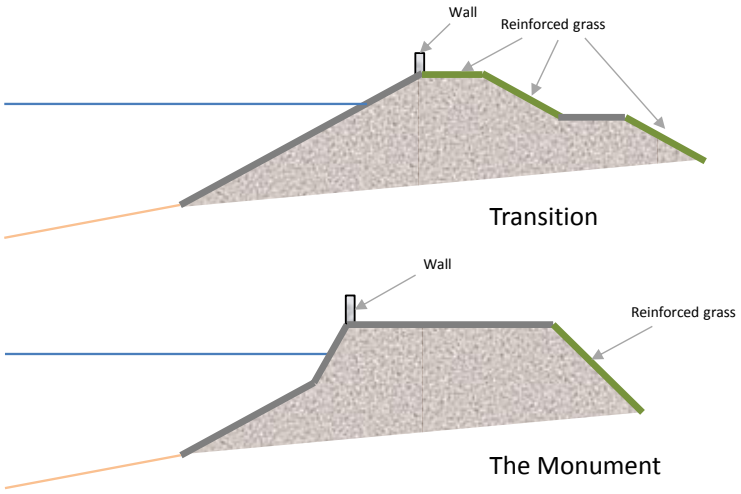

Figure 4.6. Scheme of reinforced grass and small wall

4.1.6 Energy Converter Device

This alternative considers that the load on the dike will be reduced by several energy converter devices. These devices extract part of the wave energy, transform it into electric energy and reduce the wave energy that reaches the dike. Therefore, the significant wave height is reduced and in this way, the overtopping flow rate also reduces. Final reduction of the overtopping flow rate will be to values that a grass cover can stand without significant damage. According to literature review, the selected maximum overtopping flow rate for a grass cover is 30 l/s/m.

Figure 4.7 shows a scheme with the location of the energy converter device. Considering that there are many different type of energy converter (floating or bottom-placed units), the pre-selected units will be Oyster (bottom-placed units). On both areas the existing grass covers are not modified.

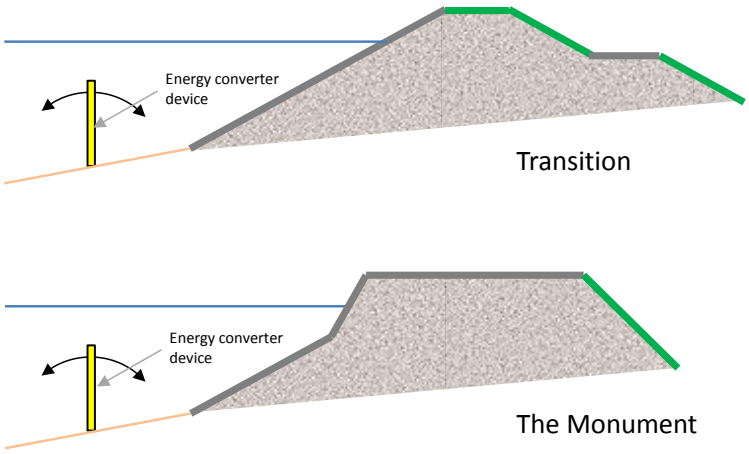

Figure 4.7. Scheme of energy converter device

4.1.7 Increase in Roughness

This alternative considers that the overtopping flow rate on the dike will be reduced by an increase of the roughness at the dike's seaside slope. A larger roughness generates a reduction in the overtopping flow rate. Nevertheless, the reduction in the overtopping flow rate is not sufficient to obtain values smaller than the maximum allowed for grass covers. An increase in roughness will be obtained by replacing the basalt cover with a more rough material, for example, rocks.

Because the maximum overtopping flow rate for reinforced grass is smaller than the overtopping flow rate, it is necessary to reduce the load on the dike. This partial reduction will be made by constructing a small wall on top of the dike.

Figure 4.8 shows a scheme with the location of the increased roughness of the dike. On both areas the existing grass covers are not modified.

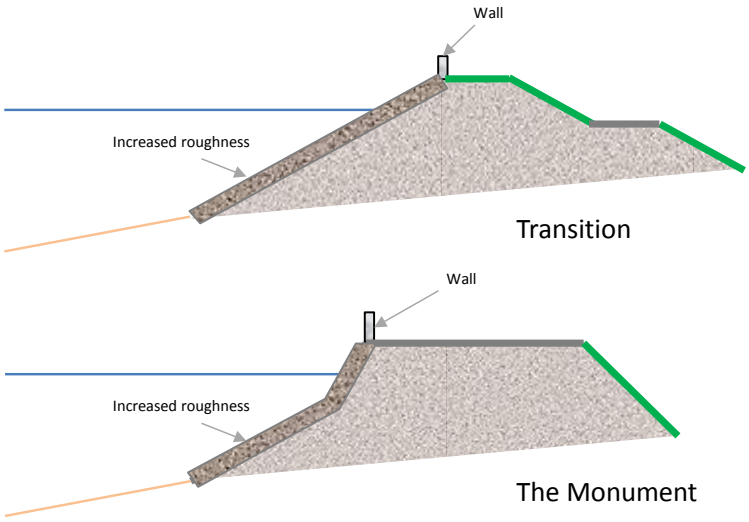

Figure 4.8. Scheme of increased roughness in seaside slope

4.2 Pre-Dimensioning

To evaluate the different alternatives, a rough dimensioning for each one is completed. For details of these calculations, see document 'Definition of Alternatives'.

4.3 Investment Cost

4.3.1 General Information

To estimate the investment cost for each alternative, the following unitary prices are assumed:

- Block revetment: 7 US$/yd^2 = **58** euros/m^2. Source: US Army Corps of Engineers, 'Design of Coastal Revetments, Seawalls and Bulkheads'.
- Concrete: 260 US$/m^3 = **200** euros/m^3. Source: own assumption.
- Rocks: 60 US$/yd^3 = **55** euros/yd^3. Source: US Army Corps of Engineers, 'Design of Coastal Revetments, Seawalls and Bulkheads'.
- Reinforced grass: **14** euros/m^2. Source: own assumption.
- Energy converter device: 33 x 10^6 euros/unit. Source: www.aquamarinepower.com

4.3.2 Cost Estimation

Table 4.1 presents a summary with the cost estimation per alternative per critical spot.

Table 4.1. Summary of investment cost estimation

Spot	Alternative	Quantity	Total cost *(euros)*
Transition	A1 – Reinforcing of outer protection	Block revetment: 8,640 m^2	500,000
	A2 – Wall on top	Concrete: 288 m^3	35,000
	A3 – Berm	Rocks: 54,600 m^3	3,000,000
	A4 – Submersed breakwater	Rocks: 37,094 m^3	2,000,000
	A5 – Reinforced grass with small wall	Reinforced grass: 8,640 m^2 Concrete: 140 m^3	150,000
	A6 – Energy converter device	Oyster: 56 units	1,850,000,000
	A7 – Increase in roughness	Rocks: 5,000 m^3 Concrete: 56 m^3	550,000
The Monument	B1 – Reinforcing of outer protection	Block revetment: 2,800 m^3	162,000
	B2 – Wall on top	Concrete: 224 m^3	58,000
	B3 – Berm	Rocks: 42,875 m^3	2,400,000
	B4 – Submersed breakwater	Rocks: 18,547 m^3	1,500,000
	B5 – Reinforced grass with small wall	Reinforced grass: 2,800 m^3 Concrete: 56 m^3	50,000
	B6 – Energy converter device	Oyster: 40 units	1,350,000,000
	B7 – Increase in roughness	Rocks: 3,640 m^3 Concrete: 28 m^3	400,000

4.4 Final Comments

Regarding with the definition of alternatives and its investment costs, the following comments are made:

- Most of the proposed alternatives are improvements that by themselves solve the overtopping problems at the critical spots (transition areas and rear slope of The Monument). Nevertheless,

the utilisation of reinforced grass and an increase in roughness of the seaside slope of the Afsluitdijk necessarily require a partial reduction of the load. This partial reduction is obtained with the construction of a small seawall.

- Dimensioning of each alternative is preliminary. It obeys to an intention to estimate roughly the investment cost, information that is necessary in order to discard any possible alternative because of economic unfeasibility.
- For the transition spot, the cheapest alternatives are A2 (wall on top) and A5 (reinforced grass with small wall), with investment costs equal to 35,000 and 150,000 euros, respectively. The investment cost for the rest of the alternatives exceeds several times the cheapest costs, therefore, the rest of the alternatives are considered as economical unfeasible and discarded from this analysis.
- For The Monument spot, the cheapest alternatives are B1 (reinforcing of outer protection), B2 (wall on top) and B5 (reinforced grass with small wall), with investment costs equal to 162,000, 58,000 and 50,000 euros, respectively. The investment cost for the rest of the alternatives exceeds several times the cheapest costs, therefore, the rest of the alternatives are considered as economical unfeasible and discarded from this analysis.
- Pre-selected alternatives (A2 and A5; B1, B2 and B5) will be analysed in a Multi-Criteria workshop. Results of this workshop will define the best alternative for each spot.

5 MULTI – CRITERIA ANALYSIS

5.1 Methodology

The multi-criteria analysis is a sub-discipline of operations research that explicitly considers multiple criteria in decision-making environments. Various criteria are taken into consideration; cost can be the most important criterion.

It were considered 10 criteria which are listed below: Investment costs, Maintenance costs, Common practice, Aesthetic, Environment, Ease of construction, Overtopping reduction, Flexibility, Additional benefit, Public safety. And for each criterion, a certain weight factor is given based on the importance and preference of it. The weight varies from 0 to 1.

For each criterion, different methods are evaluated and given certain scores based on how much the criterion is fulfilled. The scores vary from 0 to 1 and have a sum of 1.

From the basic analysis, 3 alternatives for position A, and 2 alternatives for position B. For position A, the 3 alternatives are A1 reinforced dike, A2 wall in top and A5 reinforced grass and wall respectively, and for position B, B2 wall in top and B5 reinforced grass and wall are chosen.

After the procedures, each method is evaluated by adding the score multiplied by the weight together. The method with the largest value is the best one.

5.2 Criteria Definition

Investment cost

The total investment cost is very important for the designer and stakeholder to take into concern.

Maintenance cost

Maintenance should be reduced to as low as possible, and for some alternatives, it is quite difficult to maintain, so the cost will be very high.

Common practice

Common practice measures whether the alternative is commonly used by the public, if it is, it will reduce the difficulty of construction.

Aesthetic

Aesthetic is a very important criterion since the monument place is also a very famous tourist place.

Environment

Environment is always an important around coastal areas including factors like sediment transport, it should be concerned.

Ease of construction

The ease of construction is defined to measure how easy it is to construct the certain construction or to install the particular devices. Including the adjustment of the design and construction technology for the certain location; the amount of waste and abortive work; the ease for the local construction industry participants are able to read construction documentation, including all drawings and specifications.

Overtopping reduction

Large overtopping rate will increase the failure probability of the inner slope and also will largely affect the monument and the restaurant. So the criteria of the overtopping reduction is essential here to measure the influence of the allowable overtopping.

Flexibility

With time increase, the construction will need some maintenance as well as some improvement. Even the construction will be replaced by some more effective ones with modern technology. Here the criteria is to measure the ease of that.

Additional benefits

For methods with special devices there will be some additional benefits such as income from wave energy converter.

Public safety

The public safety concerns about people who may be in danger caused by overtopping, as well as the vehicles in the parking area, and the restaurant's safety.

5.3 Alternatives

Based on the diagnosis the section A and the section B are chosen to be analyzed.

For section A, six methods are analyzed, which are:

- A1: reinforce dike with revetment
- A2: seawall in dike's crest
- A3: construct a berm,
- A4: construct a submerged breakwater
- A5: replace grass with reinforced grass and construct seawall in dike's crest

- A6: install energy converter device

For section B, the alternatives are the same.

According to the previous document in alternatives, A1, A2 and A5 are pre-selected for location A; B2 and B5 are selected for location B.

5.4 Evaluation

For details on the scoring of each alternative, see document 'Multi – Criteria Analysis'.

5.5 Result

For the multiple criteria analysis the weight and the score are put in the Tables 5.1 and 5.2.

Table 5.1. Results of Multi – Criteria Analysis for location A

Criterion	Weight	Methods	
		A2	A5
Investment costs	1.0	0.60	0.40
Maintenance costs	1.0	0.60	0.40
Common practice	0.7	0.65	0.35
Aesthetic	0.5	0.40	0.60
Environment	0.7	0.55	0.45
Ease of construction	0.8	0.65	0.35
Overtopping reduction	0.2	0.60	0.40
Flexibility	0.5	0.50	0.50
Additional benefit	0.3	0.50	0.50
Public safety	0.8	0.60	0.40
Total Score		**3.76**	**2.74**

Table 5.2. Results of Multi – Criteria Analysis for location B

Criterion	Weight	Methods		
		B1	B2	B5
Investment costs	1.0	0.12	0.44	0.44
Maintenance costs	1.0	0.37	0.37	0.26
Common practice	0.7	0.38	0.38	0.24
Aesthetic	0.5	0.20	0.30	0.50
Environment	0.7	0.13	0.50	0.38
Ease of construction	0.8	0.31	0.38	0.31
Overtopping reduction	0.2	0.15	0.50	0.35
Flexibility	0.5	0.20	0.40	0.40
Additional benefit	0.3	0.33	0.33	0.33
Public safety	0.8	0.13	0.50	0.38
Total Score		**1.52**	**2.68**	**2.30**

It can be seen clearly from the table above, build a wall on top of the dike for both locations can be found to be the chosen choices.

6 DEVELOPMENT OF SELECTED ALTERNATIVE

6.1 Overtopping retaining wall

6.1.1 Gravity wall

Figure 6.1 presents a scheme of a gravity wall.

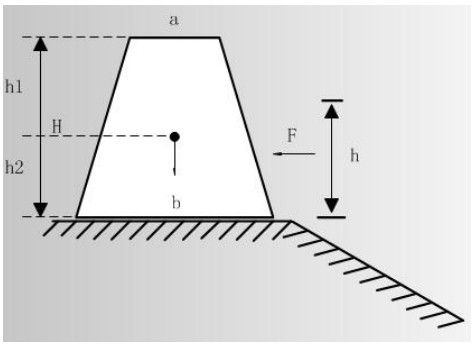

Figure 6.1. Gravity wall

Table 6.1 presents a rough calculation of dimension for this type of wall.

Table 6.1. Rough calculation of dimension of gravity wall

Parameter	Value
F [N]	20639
a [m]	0.5
B [m]	0.8
G [N]	*13759*
F [N]	*4128*
Conclusion : f << F	

It can be seen from the first estimation of dimensions of gravity wall, the friction force is much less than the flow force ($F \approx 5f$). In addition, the dimension of gravity wall is already very large with a=0.5 m and b-0.8m. If gravity wall is designed as a solution for overtopping reduction, a large structure is in need and that is much costly. Consequently, a smaller structure with strong resistant to wave overtopping is preferred. Cantilever Retaining Wall is a good approach for this design.

6.1.2 Design of Cantilever Retaining Wall

There are three main failure mechanisms for cantilever retaining wall, they are sliding, overturning and bearing (see Figures 6.2).

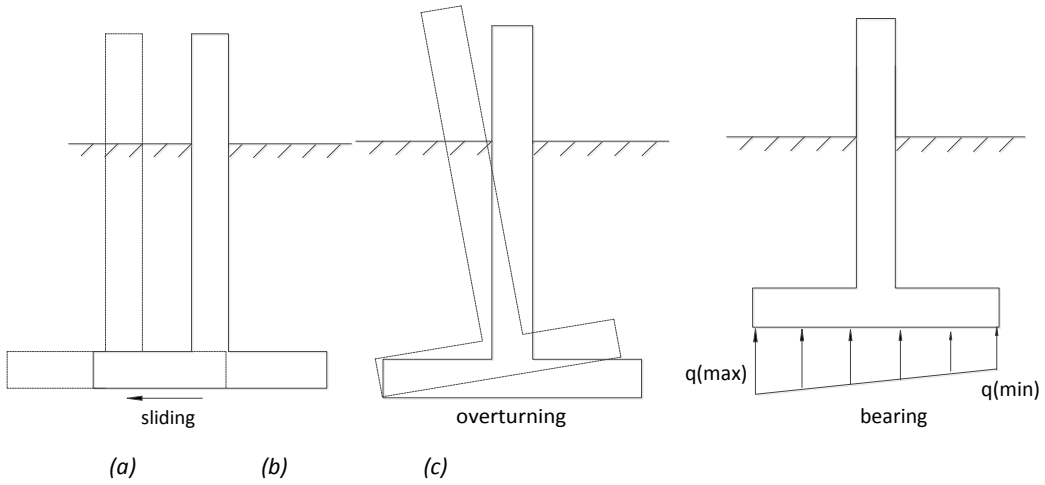

Figure 6.2. Failure patterns

First, a force diagram is drawn below for design of Cantilever Retaining Wall. Figure 6.3 shows all the main forces executing on the structure and Table 6.2 shows interpretation of each force.

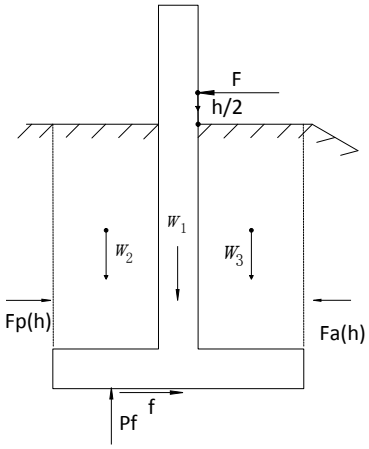

Figure 6.3. Force diagram

Table 6.2. Interpretation of force

Parameter	Interpretation
F	Flow impact force
W1	Gravity of structure
W2 & W3	Gravity of clay
Fa(h)	Horizontal component of Fa
Fp(h)	Horizontal component of Fp
f	Friction force
Pf	Uplift force

For failure pattern of sliding, the horizontal force balance and vertical force balance are important. Details of these balances are presented in document 'Development of Best Alternative'.

Based on the theory given above, after several trail and error the final dimension of the structure has been determined. See Figure 6.4 and Table 6.3.

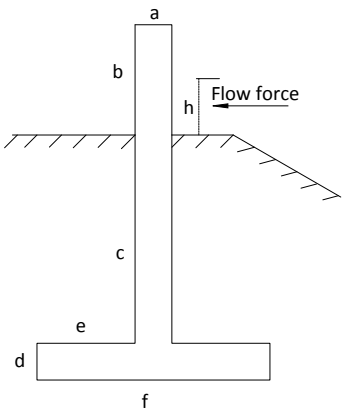

Figure 6.4. Dimensions of retaining wall

Table 6.3. Dimensions of Cantilever Retaining Wall

Parameter	Value
a [m]	0.3
b [m]	0.9
c [m]	1.7
d [m]	0.3
e [m]	0.8
f [m]	1.9

The final stability is checked and the procedure of calculation is presented in Table 6.4.

Table 6.4. Stability of structure

SECTION	AREA	ρ	W_i	Arm of force	M_i
1	1.35	2400	19110	0.95	18154.5
2	1.36	1800	23990	0.4	9596
3	1.36	1800	23990	1.5	35985
$\sum Mi$ =63735.5					
Lateral earth pressure (Left side)					
D	K_p	P_p	F_p	Arm of force	M_p
2	2.62	963	963	0.67	645.2
Lateral earth pressure (Right side)					
D	K_a	P_a	F_a	Arm of force	M_a
2	0.38	140	140	0.67	93.8
Overturning					
$M_r = M_p + \sum Mi = 645.2 + 63735.5 = 64380.7$ $M_d = M_F + M_a = 20639 \cdot 2.23 + 93.8 = 46118.8$ Safty factor $= M_r/M_d = 1.40$ (limit 1.3)					
W_1	W_2	W_3	μ	F	P_f
19110	23990.4	23990.4	0.4	20639	67090.8
Sliding					
$F_{net} = F + F_a - F_p = 20639 + 140 - 963 = 19816$ $f = \mu \cdot P_f = 26836.3$ Safety of factor $= f/F_{net} = 1.35$ (limit 1.3)					
Bearing					
$q_{max} = q'_{max} + q' = 35311 + 142698 = 178009 = 178$kPa $q_{allowable} = 300kPa$ (Source: British Code) Safety factor $= q_{allowable}/q_{max} = 1.68$ (limit 1.5)					

6.2 Construction of Cantilever Retaining Wall

Here a rough estimation of the construction time is given; the starting time of the whole project is set to be on 20th, March, 2013.

The whole project construction is set to contain two phases. The first phase starts from 20th, March, 2013 and ends at 23rd, April, 2013, including the task of construction preparation, foundation excavation, gravel cushion, steel processing, the scaffold ride demolition template group demolition, concrete pouring. The second part starts from 25th, May, 2013 and ends at 11th, May, 2013, including wall the Backfill compacted, mortared rubble slope protection, Mortar rubble draining system, and concrete curing.

Table 6.5. Construction procedure of cantilever retaining wall

Name of procedure	Duration
Preparation for construction	3 days
Reinforced steel bending preparation	9 days
Foundation excavation	7 days
Gravel mattress	7 days
Concrete stepping stone layer	4 days
Steel banding	14 days
Scaffolding erection	6 days
Template installation	11 days
Pouring concrete	9 days
Template removal	3 days
Backfill compacted	10 days
Mortar rubble slope protection	16 days
Mortar rubble draining system	16 days
Cleaning the area	2 days

Figure 6.5 presents a Gantt chart with the construction of a Cantilever Retaining Wall.

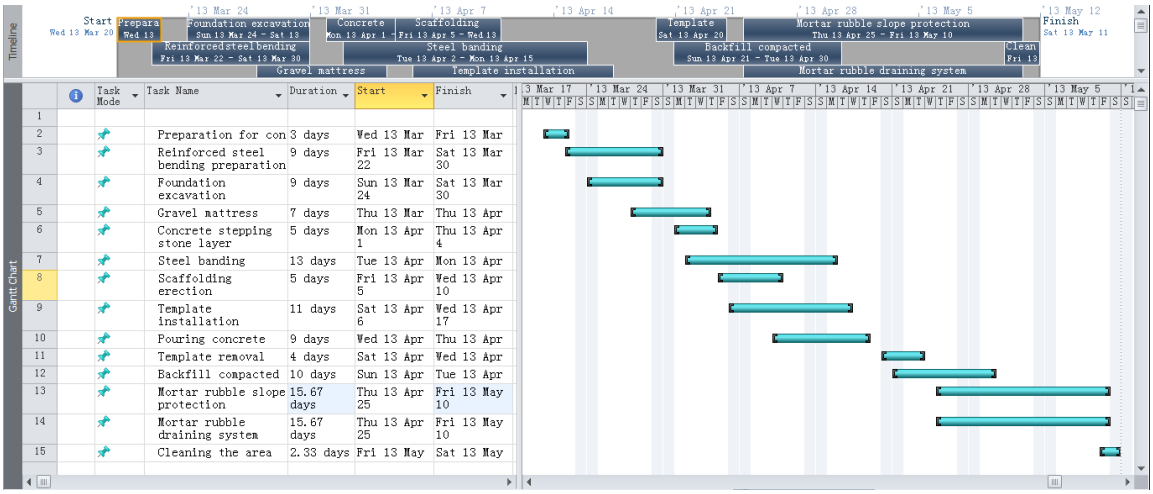

Figure 6.5. Gantt chart for construction of Cantilever Retaining Wall

6.3 Final Comments

- Two kinds of retaining walls have been considered in this design, Gravity Wall and Cantilever Retaining Wall. However, it requires too much material of concrete for Gravity Wall. Hence, the Cantilever Retaining Wall is chosen as the optimum alternative.
- The height of wall (b=0.9m) above the ground is determined by certain degree of overtopping rate reduction. This is calculated by PCOverslag software and not included in the part of wall design.
- The foot of the wall is symmetric as a simple design. It is suggested to adjust the foot of the structure to make further design.
- Three failure patterns are checked in the wall design including overturning, sliding, and bearing of earth. However, the bending failure of the structure is not considered in the design. This kind of failure pattern can always be avoided by increasing the number of rebar in the wall.

7 FINAL CONCLUSIONS

The following conclusions are obtained from this project:

- On the dike crest, The Monument location, several obstacles were found. These obstacles can create a distribution and/or concentration of the overtopping flow rate.
- Overtopping results were computed using PCOverslag software.
- Calculated overtopping for the standard cross-section is very close (i.e. 271 l/s/m) to that given by the Client (i.e. 272 l/s/m).
- For results of flow distribution, several conservative assumptions for flow reduction and flow distribution have been made to obtain the flow beside the four critical obstacles (statue, information wall, scale dike and building). The maximum flow is 258 l/s/m at the statue.
- In the diagnosis, 4 critical spots were identified. They were (1) the transition area, (2) front defence, (3) rear slope and (4) building sides.
- The limit state definition is the occurrence of 'potential' breaching, i.e., the removal of the outer protection.
- Analysis shown that only two spots required improvement, i.e. (1) the transition area and (2) rear slope.
- Several alternatives were identified with the aims to reduce loading on the existing dike or to increase the strength of the dike.
- Based on the result from the Multi – Criteria Analysis in both critical spots, the alternative to build a seawall on top of the crest has the highest value (i.e. most preferred option).
- A Cantilever Retaining Wall was selected instead of a Gravity Wall. The second one requires a large volume of concrete.
- For designing the Cantilever Retaining Wall, three failure patterns were considered: i) overturning; ii) sliding; iii) buring. Bending of concrete was not considered because it depends on the strength of concrete, which can be improved by increasing the amount of steel.

8 REFERENCES

- CIRIA, CUR, CETMEF (2007), 'The Rock Manual. The Use of Rock in Hydraulic Engineering' . 2nd edition, C683, CIRIA, London.
- Eijgenraam, C., Brekelmans, R., den Hertog, D., Roos, K. (2010), 'Safe Dike Heights at Minimal costs: The Homogeneous Case'. Submitted to Management Science. Available on http://www.tilburguniversity.edu/research/institutes-and-research-groups/center/ graduate-school/chp/opmaast/dike1.pdf
- Inspectie Verkeer en Waterstaat (2006), 'Assessment of Primary Flood Defences in The Netherlands, National Report on 2006'. Available on http://www.safecoast.nl/editor/databank/File/Assessment%20primary%20flood%20defences%20in%20NL.pdf
- Jonkman, S., Jongejan, R., Maaskant, B., Vrijling, H. (2010), 'New Safety Standards for Coastal Flood Defences in The Netherlands'. 32nd International Conference on Coastal Engineering, ICCE 2010, June 30 – July 5 2010, Shanghai, China.
- Kim, H., Lee, J. et al (2012). 'Numerical Analysis of Flood Risk Change Due to Obstruction'. KSCE Journal of Civil Engineering 16 (2). 207-214.
- OFFE, OFAT and OFEFP (1997), 'Prise en compte des dangers dus aux dans le cadre des activities del'amenagement du territoire'. Bienne, 1997, Office Federal de l'Economie des Aux (OFFE), Office Federal de l'Amenagement du Territoire (OFAT), Office Federal de l'Environnent, Desforets, et du Paysage (OFEFP).
- Pullen, T., Allsop, N. W. H., Bruce, T., Kortenhaus, A., Schüttrumpf, H., Van der Meer, J. W. (2007), 'EurOtop – Wave Overtopping of Sea Defences and Related Structures: Assessment Manual'. Environment Agency, UK, Expertise Netwerk Waterkeren, NL and Kuratorium für Forshung im Küsteningenieurwessen, DE.
- Roos, A., Riedstra, D. (2010), 'Safety Standards in The Netherlands'. Rijkswaterstaat Centre for Water Management. Presentation of March 17th, 2010.
- Syme, W. (2008), 'Flooding in Urban Areas – 2D Modelling Approaches for Buildings and Fences'. 9th National Conference on Hydraulics in Water Engineering. Engineers Australia. Darwin Convention Centre, Australia.
- Szydlowski, M. (2011), 'Numerical Simulation of Open Channel Flow Between Bridge Piers'. TASK Quarterly 15 (3-4). 271-282.
- Testa, G., Zuccala, D. et al (2007), 'Flash Flood Flow Experiment in a Simplified Urban District'. Journal of Hydraulic Research 45 (supl. 1). 37-44.
- Lin, P.Z., Liu, P.L.F., 1999. Internal wave-maker for Navier-Stokes equations models. Journal of Waterway Port Coastal and Ocean Engineering 125 (4), 207‐215.
- Guidance on erosion resistance of inner slopes of dikes from three years of testing with the Wave Overtopping Simulator, Van der Meer, Schrijver, Hardeman, Van Hoven, Verheij and SteendamW. Allsop, MICE, T. Bruce, J. Pearson BEng and P. Besley 'Wave overtopping at vertical and steep seawalls'. Maritime Engineering 158 September 2005 Issue MA3,103–114
- Dr J.W. van der Meer (2002), 'Technical Report Wave Run-up and Wave Overtopping at Dikes', Technical Advisory Committee on Flood Defence

TU DELFT – MULTIDISCIPLINARY PROJECT CIE4061

Afsluitdijk Project
"The Monument" Location

Literature Review

Sien Liu, Jun Huang, Sebastian Rayo, Tai Yan Lim

21/12/2012



CONTENTS

1 Introduction 2
1.1 Background 2
1.2 Problem Description 2
1.3 Document Scope 2
2 Interaction Between Waves and Structures 3
2.1 Definitions 3
2.2 Types of Overtopping 3
3 Safety Standards 5
3.1 Hazards 5
3.2 Existing Criteria 5
3.2.1 Return Period 5
3.2.2 Tolerable Discharges 7
3.2.3 Overtopping Velocities 8
4 Overtopping Modelling 9
4.1 Description 9
4.2 Factors of Influence 9
4.2.1 Various slopes ($\tan\alpha$) 9
4.2.2 Shallow foreshore (h_m/H_{m0}) and breaking parameter (ξ_0) 9
4.2.3 Incident wave angle (γ_β) 10
4.2.4 Berms (γb) 10
4.2.5 Roughness of elements (γf) 12
4.2.6 Vertical wall on slope (γv) 12
4.2.7 Slope with composite roughness elements (γf) 12
4.3 Mean overtopping discharge 13
4.4 Maximum over topping volume 13
4.5 Overtopping flow velocity and flow depth 13
4.5.1 On seaward slope 14
4.5.2 On crest of dike 15
4.5.3 On the landward slope 16
4.5.4 Spatial distribution of the overtopping water 17
5 Overtopping Flow Encountering Obstacles 24
5.1 Effect of Obstacle on Flow 24
5.2 Effect of Flow when encountering obstacle 27
6 References 32

1 INTRODUCTION

1.1 Background

The Afsluitdijk (Enclosure Dam) is a main dam that forms the fundamental part of the larger Zuiderzee Works that separates the Zuiderzee, a salt water inlet of the North Sea, and turning it into the fresh water lake of the IJsselmeer. It protects the central Netherlands from the effects of the North Sea. It was constructed between 1927 and 1933, and runs from Den Oever on Wieringen to the village of Zurich in Friesland. It is 32 km long and 90 meters wide, rising to 7.25 meters above sea-level, with an incline of 25% on each side.

At the location along the Afsluitdijk where the final water passage was closed ('De Vlieter'), a lookout tower known as 'The Monument' was built in 1933. It was presented by the Zuiderzee Works Construction Company and designed by architect W.M. Dudok. The site has a statue of a "Steenzetter", and also marks the inscription 'A living nation builds for its future'. A statue of Cornelis Lely has also been erected near Den Oever on the Barrier Dam itself.

The Afsluitdijk with The Monument are currently managed by the Ministry of Infrastructure and the Environment ("The client"). There is a restaurant at The Monument where the client has sublet it for private operator to manage it.

1.2 Problem Description

With the anticipation of increase storm intensity and sea level rise in the future, the client had previously engaged a consultant to analyze the existing design of Afsluitdijk for a design storm of 1:10,000 years. According to the client, the result of the study concluded that the standard cross-section of Afsluitdijk is not sufficient to withstand the design storm of 1:10,000 years, hence, modifications of it are required. The study also found that during the design storm, there is a significant overtopping over the dike.

The client is concerned about the significant overtopping found from the previous study may have adverse impact on the non-standard cross-section of the dike where The Monument is located. Therefore, the client has requested our design team to look into the dike section at the Monument location.

1.3 Document Scope

The main objectives of this document are:

1. To introduce the typical processes related to the interaction between waves and a hydraulic structure.
2. To establish the state-of-art of safety standards of dikes in the Netherlands.
3. To establish a methodology to model wave overtopping and its characteristics discharge, height and velocity) on top and the rear slope of a dike.
4. To look for research related with 2D distribution of un-steady flow when there are some obstacles in front of it.

2 INTERACTION BETWEEN WAVES AND STRUCTURES

2.1 Definitions

CIRIA et al (2007) defines that the interaction between waves and hydraulic structures (such as dikes) can be classified into: wave run-up (and run down), wave overtopping, wave transmission and wave reflection.

Definitions for each interaction process are:

- Wave conditions are defined by incident wave height (usually significant wave height), the wave period, the angle of incidence and the local depth.
- Wave run-up and run-down are defined as the extreme levels that a wave can reach on a sloping structure.
- Wave overtopping occurs when wave run-up exceeds the crest level.
- Wave transmission occurs when a structure has a permeable core, which permits the transmission of part of the wave energy through the structure.
- Wave reflection is when part of the wave energy returns towards the sea because of the influence of a hydraulic structure.

Figure 2.1 presents schemes of different type of interaction between waves and a dike.

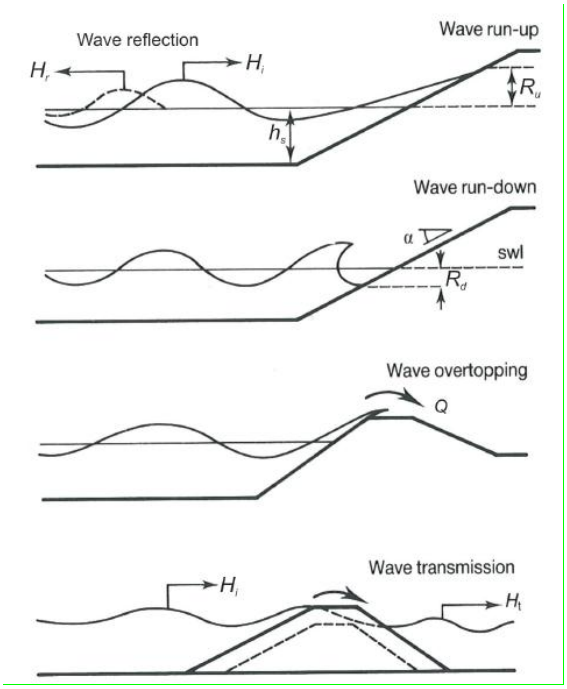

Figure 2.1. Different type of interaction between waves and a dike. Source: CIRIA et al (2007)

2.2 Types of Overtopping

According to Pullen et al (2007), two different types of overtopping are distinguished:

- ‘Green water’, which is related with complete sheets of water that run over the crest of a defence;
- ‘White water’, which is related with waves that break at the seaside, generating an important amount of spray and a non-continuous overtopping flow.

Spray generated by wind can generate some hazards for people and vehicles near the dike, due to lack of visibility. Nevertheless, it is not considered as an overtopping flow like the previous definitions.

3 SAFETY STANDARDS

3.1 Hazards

According to Pullen et al (2007), overtopping effects and its related consequences can be classified within four different categories:

a) *Direct hazard of injury or death to people immediately behind the defence;*
b) *Damage to property, operation and/or infrastructure in the area defended, including loss of economic, environmental or other resource, or disruption to an economic activity or process;*
c) *Damage to defence structure(s), either short-term or longer-term, with the possibility of breaching and flooding;*
d) *Low depth flooding (inconvenient but no dangerous).*

According to Pullen et al (2007), the main responses to these hazards are three:

a) *Move human activities away from the area subject to overtopping and/or flooding hazard, thus modifying the land use category and/or habitat status;*
b) *Accept hazard at a given probability (acceptable risk) by providing for temporary use and/or short-term evacuation with reliable forecast, warning and evacuation systems, and/or use of temporary/demountable defence systems;*
c) *Increase defence standard to reduce risk to (permanently) acceptable levels probably by enhancing the defence and/or reducing loadings.*

3.2 Existing Criteria

3.2.1 Return Period

The return period for which a defence is designed is usually determined in accordance with local and national guidelines, as well as is related with local circumstances, a balance between risk and benefits and the level of overall exposure. Table 3.1 presents some typical values of design life and levels of protection.

Table 3.1. Hazard type

Hazard type and reason	Design life *(years)*	Level of protection *(years)*
Temporary or short term measures	1 – 20	5 – 50
Majority of coast protection or sea defence walls	30 – 70	50 – 100
Flood defences protecting large areas at risk	50 – 100	100 – 10,000
Special structure, high capital cost	200	Up to 10,000
Nuclear power stations, etc.	-	10,000

Source: Pullen et al (2007)

According to Pullen et al (2007), the design life in Netherlands for flood defences is 50 years. However, for special structures with high capital cost, the design life can be extended to 200 years.

Roos and Riesdstra (2010) give more detailed information. In the Netherlands, every ring has a specific safety standard. West and North Netherlands have safety standards of 1:10,000 and 1:4,000, respectively. Figure 3.1 shows details of safety standard definition in the Netherlands.

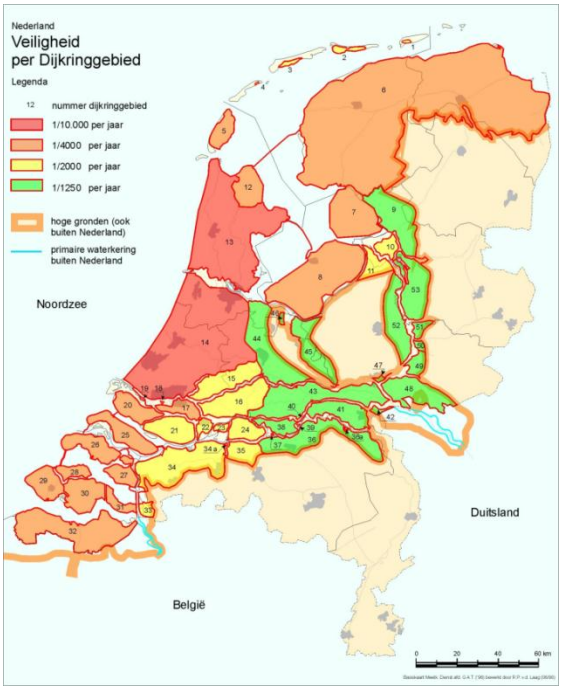

Figure 3.1. Details of safety standards definition in the Netherlands. Source: Roos and Riedstra (2010)

Nevertheless, because of climate change, a discussion started in 2006 with respect to the definition of safety standards, which will be updated in 2017. Figure 2.3 shows a map of the Netherlands with detailed information about safety standard achievement for several locations. Particularly, the Aflsluitdijk does not comply with the standard.



Figure 2.2. Results second safety assessment primary flood defences, 1 January 2006. Source: Inspectie Verkeer en Waterstaat (2006)

Jonkman et al (2010) mention that in the Netherlands, current safety standards are based on cost – benefits analysis, but they do not incorporate casualties in a proper way. Hence, they propose that a research on risk definition should be made, considering both individual (probability of death of a person in one year) and societal risks (probability of occurrence of an event with several fatalities).

Eijgenraam et al (2010) propose a numerical method to determine optimal dike heights, considering a risk analysis definition. They conclude that in the Netherlands there is a need to increase safety standards, which will increase expenses of the Dutch government for the protection against flooding item.

3.2.2 Tolerable Discharges

Information available in Pullen et al (2007) gives several limits of overtopping (flow discharges and volumes) for pedestrians, vehicles and properties behind the defence. Tables 3.2 to 3.4 present that information.

Table 3.2. Limits for overtopping for pedestrians

Hazard type and reason	Mean discharge	Max volume
	q (l/s/m)	V_{max} *(l/m)*
Trained staff, well shod and protected, expecting to get wet, overtopping flows at lower levels only, no falling jet, low danger of fall from walkway.	1 – 10	500 at low level
Aware pedestrian, clear view of the sea, not easily upset or frightened, able to tolerate getting wet, wider walkway.	0.1	20 – 50 at high level or velocity

Source: Pullen et al (2007)

Table 3.3. Limits for overtopping for vehicles

Hazard type and reason	Mean discharge	Max volume
	q (l/s/m)	V_{max} *(l/m)*
Driving at low speed, overtopping by pulsating flows at low flow depths, no falling jets, vehicle not immersed.	10 – 50	100 – 1,000
Driving at moderate or high speed, impulsive overtopping giving falling or high velocity jets.	0.01 – 0.05	5 – 50 at high level or velocity

Source: Pullen et al (2007)

Table 3.4. Limits for overtopping for property behind the defence

Hazard type and reason	Mean discharge	Max volume
	q (l/s/m)	V_{max} *(l/m)*
Significant damage or sinking of larger yachts	50	5,000 – 50,000
Sinking small boats set 5 – 10 m from wall. Damage to larger yachts.	10	1,000 – 10,000
Building structure elements	1	-
Damage to equipment set back 5 – 10 m	0.4	

Source: Pullen et al (2007

Information available in Pullen et al (2007) indicates that the work realized by Goda and other researchers gave some guidelines of setting limits for the defence structures. That information is summarized in Table 3.5.

Table 3.5. Limits for overtopping for damage to the defence crest or rear slope

Hazard type and reason	Mean discharge *q (l/s/m)*
Embankment seawalls / sea dikes	
No damage if crest and rear slope are well protected	50 – 200
No damage to crest and rear face of grass covered embankment of clay	1 – 10
No damage to crest and rear face of embankment if not protected	0.1
Promenade or revetment seawalls	
Damage to paved or armoured promenade behind seawall	200
Damage to grassed or lightly protected promenade or reclamation cover	50

Source: Pullen et al (2007)

Further research was done in Netherlands during year 2007. Wave overtopping tests were developed on existing dikes (both made of clay and covered with grass). Results indicated that the resistance of these dikes is higher than the values defined by Goda. Particularly, the resistance of a dike covered with grass was good enough for overtopping rates up to 50 l/s/m.

3.2.3 Overtopping Velocities

Information available in Pullen et al (2007) indicates that maximum velocities of 5 – 8 m/s can occur for overtopping discharges in the range 10 – 30 l/s/m.

4 OVERTOPPING MODELLING

4.1 Description

The dikes in Netherlands normally consist of a toe structure, a gentle slope with a berm, a crest of a certain width, outer and inner crest lines and inner slope. For some special dikes, transport infrastructure like bicycle lanes and highways may lie behind the inner slope. The configurations of dikes described above all have influence on the wave overtopping. It can also be affected by the reference water levels, strong sea winds and climate change.

4.2 Factors of Influence

The profiles of dikes are quite different from each other, as well as the wave conditions in different cases. In order to consider all these effects on wave overtopping, several parameters will be introduced to make better predictions of wave overtopping.

4.2.1 Various slopes (tanα)

In reality a dike slope in normally consists of several sections with different slope angles. Considering that the wave overtopping requires a characteristic slope in the breaker parameter, the definition of average slope is applied here to replace various slope sections. The representative slope is iteratively calculated as the average slope between still water line $-1.5 \cdot H_{m0}$ and still water line $+z_{2\%}$. (any berm present is not include for calculation of average slope).

4.2.2 Shallow foreshore (h_m/H_{m0}) and breaking parameter (ξ_0)

The waves will break due to limit water depth when they approach to a shallow foreshore, which will consequently decrease the wave overtopping discharge. In addition, the wave height distribution will also be changed due to this effect. In relatively deep water ($h_m/H_{m0} > 3\ to\ 4$), wave heights follow as Rayleigh distribution. In shallow foreshore ($h_m/H_{m0} < 3\ to\ 4$), the wave height distribution will deviate from Rayleigh distribution due to breaking effects of higher waves. This shallow foreshore effect is very important and it is necessary coming up with two equations to calculate the wave overtopping under these two different conditions. The criteria of distinguishing these two conditions are based on the breaker parameter ξ_0, which is given by:

$$\xi_0 = \frac{tan\alpha}{\sqrt{s_0}}$$

Where:

ξ_0 – breaker parameter [-].
α – angle of slope [°].
s_0 – wave steepness [-]

$$s_0 = 2\pi \cdot H_{m0}/(g \cdot T_{m-1,0}^2)$$

Where:

$T_{m-1,0}$ – spectral wave period=m_{-1}/m_0 [s].
m_0 – zero moment of spectrum [m^2].
m_{-1} – first negative moment of spectrum [m^2].

4.2.3 Incident wave angle (γ_β)

The incident wave angle is defined as the angle between propagation direction of waves and the perpendicular direction to long axis of the dike. In real site situation, the incident waves come from various directions and each of them has individual contribution of wave overtopping. In calculation of deterministic approach, it's impossible to do calculation for each wave, so the consideration of evaluating contributions of different incident wave angles is necessary.

Influence factor for this effect is given by γ_β (β indicates incident wave angle, $\beta = 0$ means perpendicular wave attack). The influence factor γ_β is plotted against the angel of wave attack, β (Technical Report Wave Run-up and Wave Overtopping at Dikes, Technical Advisory Committee on Flood Defence) (Dr J.W Van De Meer, 2002). For wave overtopping, the influence factor decrease linearly from 1 to 0.7 when β increase from 0 to 80. It keeps at 0.7 when β is between 80 and 90. Figure 4.1 presents the relation between the influence factor γ_β and the angle of attack β.

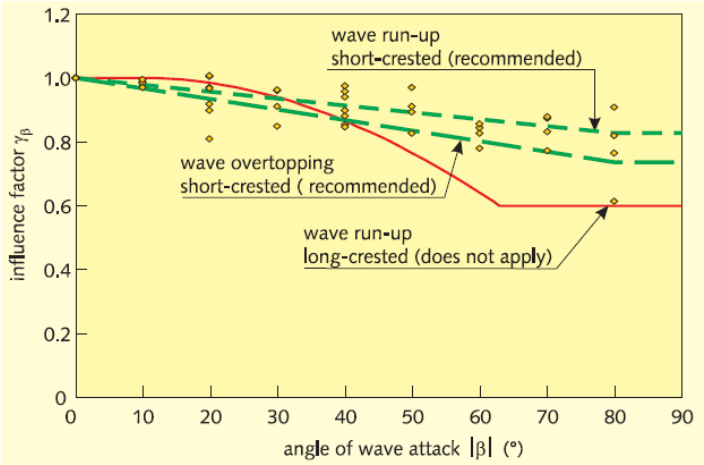

Figure 4.1. Relation between influence factor and angle of wave attack. Source: T. Pullen (2007)

It can be described as following formulae for wave overtopping:

$$\gamma_\beta = 1 - 0.0033|\beta| \quad (0° < |\beta| < 80°)$$

$$\gamma_\beta = 1 - 0.0033 \cdot 80° \quad (|\beta| > 80°)$$

4.2.4 Berms (γ_b)

A berm is defined as part of the dike profile in which the slope varies between horizontal and 1:15. Both the width and the depth of berm are given in Figure 4.2.

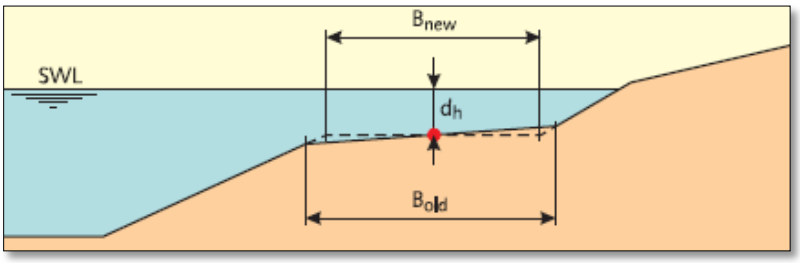

Figure 4.2. Scheme with berm definition. Source:(T. Pullen, 2007)

Normally, it is required that the slope should be gentler than 1:15 and the width should be less than one quarter of the wavelength. If the berm doesn't satisfy with the requirement, then the wave overtopping must be determined by interpolation between the steepest berm (1:15) and a gentle slope (1:8). For calculations of wave overtopping, the inclined berm is drawn to a horizontal berm which is shown in figure as B_{new}. The berm depth is shown as d_h. The influence of berm can be considered as two parts: one is influence of the width of berm,r_B, and one is berm depth,r_{dh}.

For estimation of influence of berm, the following equation is applied:

$$\gamma_b = 1 - r_B \cdot (1 - r_{dh})$$

Where $0.6 \leq \gamma_b \leq 1.0$, $r_{dh} = 0$ relates to condition of $d_h = 0$ and $0 \leq r_B \leq 1$

Based on the information of Pullen et al (2007), the influence of berm width can be calculated by the equation as follows:

$$r_B = 1 - \frac{2 \cdot H_{m0}/L_{berm}}{2 \cdot H_{m0}/(L_{berm} - B)} = \frac{B}{L_{berm}}$$

The corresponding parameters are drawn in Figure 4.3.

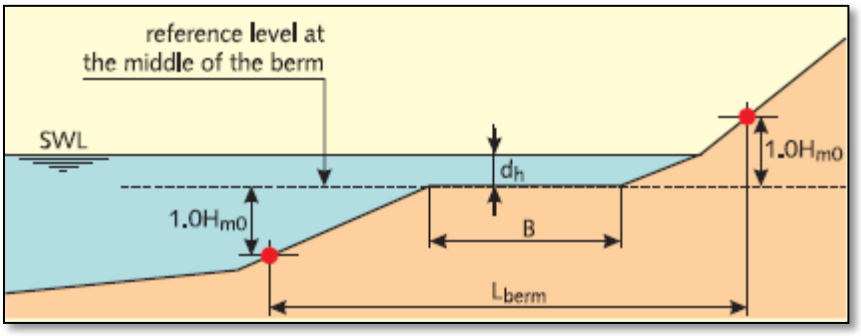

Figure 4.3. Parameters required to define berm influence. Source: T. Pullen (2007)

Also the influence of berm depth can be evaluated by the following formula:

$$r_{dh} = 0.5 - 0.5 \cdot \cos\left(\pi \frac{d_h}{x}\right)$$

Where

x $= z_{2\%}$ if $0 < -d_h < z_{2\%}$ (berm above still water line)
x $= 2 \cdot H_{m0}$ if $0 \leq d_h < 2 \cdot H_{m0}$ (berm below still water line)
$r_{dh} = 1$ if $-d_h \geq z_{2\%}$ or $d_h \geq 2 \cdot H_{m0}$ (outside influence area)

The influence of berm depth described above can only be used over the space between $2 \cdot H_{m0}$ below sea water level up to $z_{2\%}$ in the lower slope. Influence of berm position will disappear when it lies more than $2 \cdot H_{m0}$ under still water level.

In the end, the full expression of influence of berm can be written as:

$$\gamma_b = 1 - \frac{B}{L_{berm}} \cdot \left(0.5 + 0.5 \cdot cos\left(\pi \frac{d_h}{x}\right)\right)$$

Where

$0.6 \leq \gamma_b \leq 1.0$

It can be easily seen that influence of berm position become maximum for $d_h = 0$ which results to $\gamma_b = 1 - \frac{B}{L_{berm}}$.

4.2.5 Roughness of elements (γ_f)

Influence of roughness elements on wave overtopping is measured by factor γ_f. Data of influence factors for various single roughness elements can be found in the Russian study with regular eaves from 1950s. The determination of γ_f is dependent on the various features of dike. More details can be found in (Technical Report Wave Run-up and Wave Overtopping at Dikes, Technical Advisory Committee on Flood Defence).The end result as a table showing a complete overall view of influence factors can be found in Technical Report Wave Run-up and Wave Overtopping at Dikes, Dr J.W. van der Meer, (2007). Some values of several specific roughness elements are shown as follows:

Reference type	γ_f
Concrete	1.0
Asphalt	1.0
Closed concrete block	1.0
Grass	1.0
Vilvoorden stone	0.85
Basalt	0.90
Haringman	0.90
Fixtone - open stone asphalt	0.90
Armorflex	0.90
Small blocks over 1/25 of surface	0.85
Small blocks over 1/9 of surface	0.80
¼ of block revetment 10 cm higher	0.90
Ribs (optimum dimensions)	0.75
Armour rock - two layers thick	0.55
Armour rock - single layer	0.70

Figure 4.4 influence factors of roughness elements, Dr J.W. van der Meer, (2007)

4.2.6 Vertical wall on slope (γ_v)

The influence factor of vertical wall on slope is given by factor γ_v. In some cases, there a vertical wall placed on top of slope to reduce wave overtopping. The wave overtopping for a vertical wall on slope is smaller than for a 1:1 slope on top of dike profile. The influence factor for a vertical wall on a slope is $\gamma_v = 0.65$. For a 1:1 slope, $\gamma_v = 1$. Interpolation should be done for a wall that is between vertical and 1:1.

$$\gamma_v = 1.35 - 0.0078 \cdot \alpha_{wall}$$

Where α_{wall} is steep slope on top of dike ($0^\circ < \alpha_{wall} < 90^\circ$)

4.2.7 Slope with composite roughness elements (γ_f)

Weighting of various roughness factors is exerted by including the lengths of appropriate sections of the slope (between SWL$-0.25 \cdot z_{2\%,smooth}$ and SWL$+0.25 \cdot z_{2\%,smooth}$). Any roughness elements located beyond this limit are considered as no effect on the wave overtopping. If we consider a condition with three roughness elements within this area, and they are in lengths of L_1, L_2 and L_3, and with influence factor of $\gamma_{f,1}$, $\gamma_{f,2}$ and $\gamma_{f,3}$, respectively. Then the weighted influence factor can be written as:

$$\gamma_f = \frac{\gamma_{f,1} \cdot L_1 + \gamma_{f,2} \cdot L_2 + \gamma_{f,3} \cdot L_3}{L_1 + L_2 + L_3}$$

4.3 Mean overtopping discharge

The wave overtopping formulae are exponential functions with the general form:

$$\mathrm{q} = \mathrm{a} \cdot \exp(\mathrm{b} \cdot R_c)$$

The coefficient a and b are functions of the wave height, slope angle, break parameter and the influence factors described previously.

Wave overtopping is usually given as an average discharge per linear meter of width, q (m3/s per m or in l/s per m). Because the wave overtopping increases for increasing breaker parameter ξ_0, It can be described in two formulae: one for breaking waves, ($\xi_0 \leq 5$) and one for the maximum that is achieved for non-breaking waves ($\xi_0 > 7$). In the area in between ($5 < \xi_0 < 7$), the logarithm of q is linearly interpolated.

For $\xi_0 \leq 5$, the calculation of wave overtopping is described as:

$$\frac{q}{\sqrt{gH_{m0}^3}} = \frac{0.067}{\sqrt{tan\alpha}}\gamma_b \cdot \xi_0 \cdot \exp\left(-4.3\frac{R_c}{H_{m0}}\frac{1}{\xi_0 \cdot \gamma_b \cdot \gamma_f \cdot \gamma_\beta \cdot \gamma_v}\right)$$

With a maximum of:

$$\frac{q}{\sqrt{gH_{m0}^3}} = 0.2 \cdot \exp\left(-2.3\frac{R_c}{H_{m0}}\frac{1}{\gamma_f \cdot \gamma_\beta}\right)$$

For $\xi_0 > 7$, the calculation of wave overtopping is described as:

$$\frac{q}{\sqrt{gH_{m0}^3}} = 0.21 \cdot \exp\left(-\frac{R_c}{\gamma_f \cdot \gamma_\beta \cdot H_{m0} \cdot (0.33 + 0.022 \cdot \xi_0)}\right)$$

4.4 Maximum over topping volume

In order to estimate the hazard on buildings and infrastructure caused by wave overtopping, not only mean overtopping discharge is an important factor, but also maximum overtopping volume should be taken into consideration. The maximum volume of wave overtopping during certain is uncertain, but depends on the duration of the storm event. The maximum overtopping volume by one wave during an event depends on the actual number of overtopping waves, N_{ow}, and is given by:

$$V_{max} = a \cdot [\ln(N_{ow})]^{4/3}$$

Where

$\mathrm{a} = 0.84 \cdot \mathrm{q} \cdot \mathrm{t}/N_{ow}$
N_{ow} – number of overtopping waves.
q – mean wave overtopping discharge.
t – storm duration

4.5 Overtopping flow velocity and flow depth

Average wave overtopping discharge and maximum wave overtopping volume are not appropriate for describing the interaction between overtopping flow and failure mechanism.

In contract, the overtopping flow velocity and flow depth is more related to the analysis of erosion of dike inner slope and impact on infrastructure.

4.5.1 On seaward slope

Before calculating the overtopping flow depth and flow velocity, the wave run up velocities and related flow depth are required first. The flow on seaward slope is drawn in Figure 4.4.

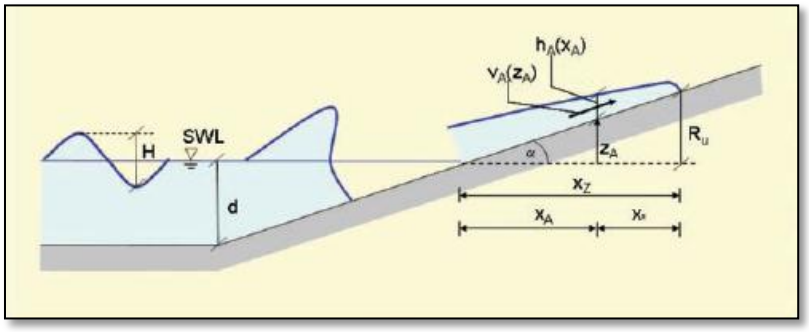

Figure 4.4. Wave run up characteristics. Source: Pullen et al (2007)

The flow depth of wave run up on the seaward slope is a function of horizontal projection x_z of wave run-up height $R_{u2\%.}$, the horizontal coordinate of the dike x_A and a dimensionless coefficient c_2. The calculation formula is under assumption of linear decrease of the lay thickness h_A from SWL to the highest point of wave run-up and it is given as follows:

$$h_A(\mathrm{x}_*) = c_2(x_z - x_A) = c_2 \cdot \mathrm{x}_*$$

Where:

x_* – remaining run-up length($\mathrm{x}_* = x_z - x_A$) and $x_z = R_{u2\%.}/tan\alpha$.

The coefficient can be selected based on different exceedance levels by Table 4.1.

Table 4.1 characteristic values for parameter c_2 (TMA-spectra)

Parameter	c_2	σ'
$h_{A,50\%}$	0.028	0.15
$h_{A,10\%}$	0.042	0.18
$h_{A,2\%}$	0.055	0.22

Source: Pullen et al (2007)

The run-up velocities are defined as the maximum velocity at any position of seaward slope during wave run-up. The equation of wave run-up velocity is given by:

$$v_A = k^* \cdot \sqrt{2g(R_{u2\%.} - z_A)}$$

Where:

v_A – wave run-up velocity at point z_A above SWL.

$R_{u2\%.}$ – wave run-up height exceeded by 2% of the incoming waves.

k^* – dimensionless coefficient.

The dimensionless form is:

$$\frac{v_A}{\sqrt{gH_s}} = a_0^* \sqrt{\frac{R_{u2\%.} - z_A}{H_s}}$$

Where:

H_s – significant wave height.

The values of a_0^* are given in Table 4.2.

Table 4.2 characteristic Values for Parameter a_0^* (TMA-spectra). Source: Pullen et al (2007)

Parameter	a_0^*	σ'
$v_{A,50\%}$	1.03	0.23
$v_{A,10\%}$	1.37	0.18
$v_{A,2\%}$	1.55	0.15

4.5.2 On crest of dike

The overtopping flow on the dike crest is sketched in Figure 4.5.

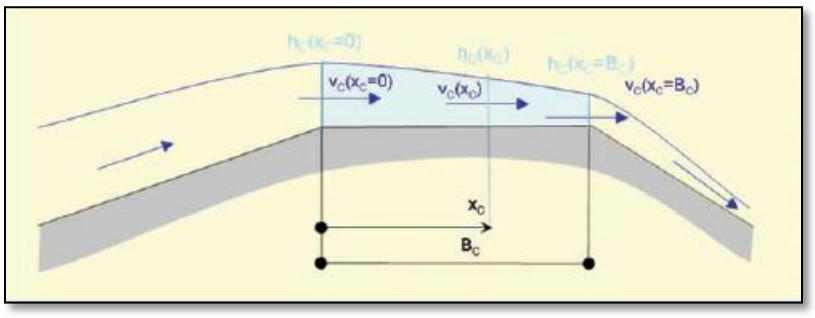

Figure 4.5. Overtopping flow on dike crest. Source: Pullen et al (2007)

The flow depth is given as a function of the width of crest B_c and the coordinate on the crest x_c :

$$\frac{h_c(x_c)}{h_c(x_c=0)} = \frac{c_2(x_c)}{c_2(x_c=0)} = exp\left(-c_3\frac{x_c}{B_c}\right)$$

Where:

c_3 – dimensional coefficient; 0.89 for TMA spectra and 1.11 for natural wave spectra.
B_c – width of dike crest.

The flow velocity is given by simplified Navier-Stokes-equation under several assumptions:

- Dike crest is horizontal.
- Vertical flow velocity to the dike slope can be neglected.
- Pressure term is constant over dike crest.
- Viscous effects in flow direction are small and bottom friction is constant over dike crest.

$$v_c = v_{c(x_c=0)} exp\left(-\frac{x_c \cdot f}{2 \cdot h_c}\right)$$

Where:

v_c – overtopping flow velocity.
f – friction coefficient.
x_c – coordinate on crest.
h_c – flow depth at x_c.

4.5.3 On the landward slope

Overtopping flow velocity and overtopping flow depth [Pullen et al (2007)].

When the overtopping flow runs up the seaside of the dike and crosses the dike crest, it will reach the landward slope of the dike.

An analytical function was developed which describes overtopping flow velocities and overtopping low depths on the landward slope as a function of the overtopping flow velocity at the end of the dike crest ($v_{b,0} = v_C(x_C = B)$), the slope angle . Of the landward side and the position s_B on the landward side with sB = 0 at the intersection between dike crest and landward slope. A definition sketch is given in Figure 4.6 below.

The following assumptions were made to derive an analytical function from the Navier-Stokes-equations:

1. Velocities vertical to the dike slope can be neglected;
2. The pressure term is almost constant over the dike crest; and the viscous effects in flow direction are small.

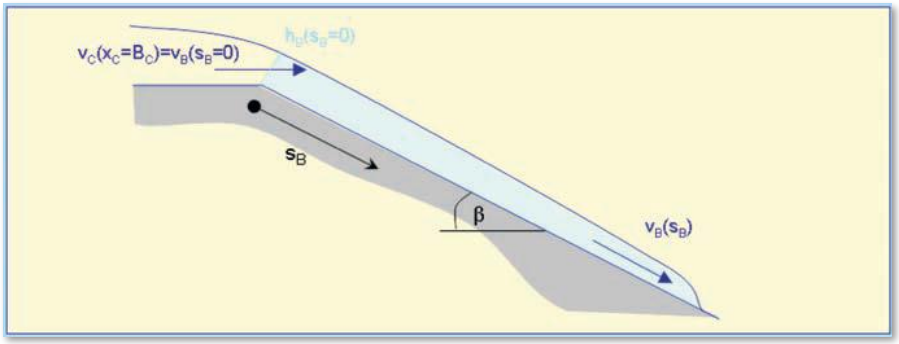

Figure 4.6. Definition of overtopping flow parameter on the landward slope. Source: Pullen et al (2007)

This results in the following formula for overtopping flow velocities:

$$v_b = \frac{v_{b,0} + \frac{k_1 h_b}{f}\tanh\left(\frac{k_1 t}{2}\right)}{1 + \frac{f v_{b,0}}{h_b 1}\tanh\left(\frac{k_1 t}{2}\right)}$$

With:

$$t \approx -\frac{v_{b,0}}{g\sin\beta} + \sqrt{\frac{v_b^2}{g^2\sin\beta^2} + \frac{2s_b}{g\sin\beta}} \quad \text{and} \quad k_1 = \sqrt{\frac{2f\sin\beta}{h_b}}$$

Equation mentioned here needs an iterative solution since the overtopping flow depth h_b and the overtopping flow velocity v_b on the landward slope are unknown. The overtopping flow depth h_b can be replaced in a first step by:

$$h_b = \frac{v_{b,0} \cdot v_{b,0}}{v_b}$$

With $v_{b,0}$ the overtopping flow velocity at the beginning of the landward slope($v_{b,0} = v_B(s_B = 0)$); and $h_{b,0}$ the overtopping flow depth at the beginning of the landward slope ($h_{b,0} = h_B$ ($s_B = 0$)).

The second important factor influencing the overtopping flow on the landward slope is the bottom friction coefficient f which has to be determined experimentally. The overtopping low on the landward slope tends towards an asymptote for $s_b \to \infty$ which is given by:

$$v_b = \sqrt{\frac{2ghsin(\beta)}{t}}$$

4.5.4 Spatial distribution of the overtopping water

Landward ground level

It can be expected that the spatial distribution of the overtopping water depends on the landward ground level, h_{meas}. The trajectory of overtopping volume is in a parabolic type, therefore, we can estimate that if the overtopping volume is dropped into

$$v = \sqrt{\frac{2(y+0)}{g}}m$$

at h_{meas}=0 m, then it will fall into

$$v = \sqrt{\frac{2(y+0.1)}{g}}m$$

at h_{meas}=0.1minstead. Fig 4.7 shows the effect of landward ground level on landward spatial distribution of overtopping water as a function of relative landward distance. The positive h_{means} stands for the ground level lower than the structure crest and negative hmeas represents the ground level higher than the structure crest. It is interesting to observe that for the same wave conditions and structural geometry the proportion of wave overtopping volume passing x increases with landward ground level, hmeas. The overtopping water even reaches to a distance up to three times bigger than significant wave height for hmeas=0.2 m, while it only splashes own in the area of half the significant wave height from structures for hmeas=−0.05 m. However, the computed proportion of wave overtopping water passing a landward location is smaller than predictions by $F(x,y) = \exp\left(\frac{-1.3}{H_{m0}}\left\{\max\left(\frac{x}{\cos\beta} - 2.7ys_{op}^{0.15}, o\right)\right\}\right)$ in EurOtop (2008), in accord with more overtopping water falling into the area just behind the structure. This is mainly due to a nappe (in hydro-engineering refers to the sheet of water over-topping) clinging to the landward face of the weir with very low water heads.

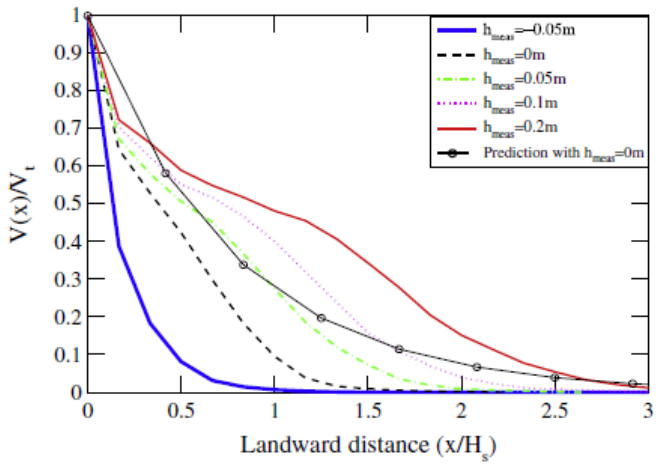

Figure 4.7. Effect of landward ground level, hmeas, on computed landward spatial distribution of overtopping water. Prediction is given by Eq. (6.17) in EurOtop (2008) with h_{meas}=0. The positive hmeas stands for the ground level lower than the structure crest. Hs=0.12 m, Tm=1.6 s, h=0.7 m, Rc=0.1 m, tan(α)=1:2 and B=0.3 m.

Source: Spatial distribution of wave overtopping water behind coastal structures Coastal Engineering, 58 (2011) 489-498. doi:10.1016/j.coastaleng.2011.01.010

Structure porosity

Structure porosity will affect spatial distribution of overtopping water through wave run-up and velocities on the crest as suggested by $x(y_c) = u_{A,50\%}\sqrt{\frac{2(y_c+h_{means})}{g}}$ $0 < y_c < h_A$, in which, $u_{A,50\%}$ =the horizontal velocity at the landward end of the crest (x=0m)

In this study, four types of coastal structures have been employed and shown in Figure 4.8, including a caisson breakwater with concrete protection; caisson breakwater with gravel protection (porosity=0.49); caisson breakwater with rubble protection (porosity=0.53) and rubble mound breakwater. The present model investigates the porous media in a similar way as Liu et al. (1999) by averaging the flow equations over a length scale. This length scale is larger than the characteristic pore size and is much smaller than the scale of the spatial variation of the physical variables in the flow domain. Therefore, the fluid variables can be decomposed into two parts, spatially averaged and spatially fluctuated quantities.

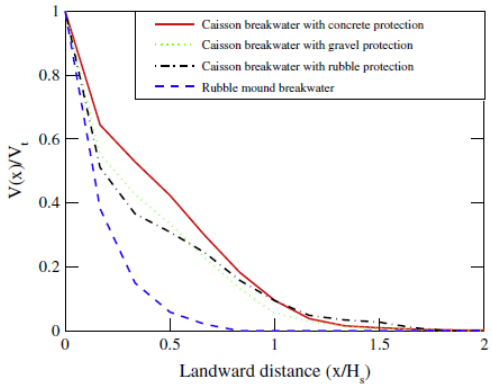

Fig. 11. Effect of structure porosity on landward spatial distribution of wave overtopping water. $H_s = 0.12$ m, $T_m = 1.6$ s, $h = 0.7$ m, $h_{meas} = 0$ m, $R_c = 0.1$ m and $B = 0.3$ m.

Figure 4.8. Effect of structure porosity on landward spatial distribution of wave overtopping water. Source: Spatial distribution of wave overtopping water behind coastal structuresCoastal Engineering, 58 (2011) 489-498. doi:10.1016/j.coastaleng.2011.01.010

Figure 4.8 shows the spatial distribution of wave overtopping water for various structure porosity at the ground level hmeas=0 m. With the same incident wave conditions (Hs=0.12 m, T_p=1.6 s) and the same geometry, the proportion of wave overtopping volume passing x decreases with structure porosity. This is because the employment of permeable protection leads to effective energy dissipation and reduces the overtopping discharge (Liu et al., 1999). In addition, large porosity, equivalent to large roughness or surface friction, leads to large dissipation and deductions of velocity and layer thickness on the structure crest. The proportion of wave overtopping volume passing a landward location for rubble mound breakwater is significantly smaller than that for caisson breakwater with rubble protection (Fig. 11). The structure crest is hydraulically rough for the former case but hydraulically smooth for the latter, although these two layouts have the same structure porosity. Therefore, rubble mound breakwater has smaller velocity of the overtopping water on the crest. As can be seen in $x(y_c) = u_{A,50\%}\sqrt{\frac{2(y_c+h_{means})}{g}}$, small velocity and layer thickness result in small travel distance of the overtopping water. This finding is consistent with the recommendation by EurOtop (2007) that roughness elements located above the still water level minus a quarter of wave run-up on a smooth slope, has a significant effect on the wave overtopping discharge.

Erosion of the inner slope

A tested inner slope of a dike, covered with grass on clay, never failed by erosion due to overtopping for a mean overtopping discharge of **30 l/s** per m or less. Only one section failed at 50 l/s per m; some at 75 l/s per m, but part of the sections did not fail, even not for 75 l/s per m.

It seems that the large erosion resistance of the inner slope of a dike is determined by the combination of grass and clay.

- The grass cover or mattress seems stronger (Boonweg, Figure 4.9) if it grows on a sandy clay. Such a grass cover may resist even up to 75 l/s per m, but if significant damage occurs, the clay layer is not very erosion resistant (Figures 4.10 and 4.11).



Figure 4.9 Source: Guidance on erosion resistance of inner slopes of dikes from three years of testing with the Wave Overtopping Simulator



Figure4.10 Source: Guidance on erosion resistance of inner slopes of dikes from three years of testing with the Wave Overtopping Simulator



Figure 4.11 Source: Guidance on erosion resistance of inner slopes of dikes from three years of testing with the Wave Overtopping Simulator

- On the other hand, good quality clay does not produce a very strong grass cover (it is difficult for roots to penetrate into the clay) and the grass may rip off for overtopping discharges around 30 l/s per m (Figures 4.12 and 4.13). But in that case the remaining good quality clay layer, still reinforced with some roots, has a large erosion resistance against overtopping waves (Figure 4.12).Van der Meer, Schrijver, Hardeman, Van Hoven, Verheij and Steendam 11



Figure 4.12 Afsluitdijk. Grass toe， Source:Guidance on erosion resistance of inner slopes of dikes from three years of testing with the Wave Overtopping Simulator



Figure 4.13 Afsluitdijk.Staircase with fence, before and after testing Source:Guidance on erosion resistance of inner slopes of dikes from three years of testing with the Wave Overtopping Simulator

- This leads to the conclusion that a good grass cover on sandy clay and a worse grass cover on good clay show different failure mechanisms, but they show more or less similar strength against wave overtopping. The variability of the grass sod may, therefore, have less influence on the total strength than previously anticipated.
- This could lead to the conclusion that the way of maintenance of the grass has only minor effect on the strength of the inner slope. The test at St Philipsland may show that the bad grass coverage (small open areas without grass) on sandy clay may show less resistance (Figure 4.14).



Figure 4.14 Final result St Philipsland, Zeeland. Source:Guidance on erosion resistance of inner slopes of dikes from three years of testing with the Wave Overtopping Simulator

Transitions from slope to horizontal are probably the most critical locations for initial and increasing damage.

- During the tests this was often the transition from the inner slope to the toe of the dike, with or without a maintenance road. The tests in 2009 were focused on these kinds of transitions. Damage was initiated by a mean discharge of 10 l/s per m or more. As the damage occurred at the lowest part of the inner slope it will take time for damage to extend to the crest level and subsequently cause a dike breach. Transition higher on the inner slope (cycle paths, stability or piping berms with or without maintenance road, tracks of tractors, roads crossing the dike), which have not yet been investigated, might be more critical. Further investigation may give more confirmative conclusions.
- A hole in the layer of clay, which reaches the under laying sand core and created at a large mean overtopping discharge of **50 l/s** per m or more, will give a very quick ongoing erosion. This has not been observed for smaller overtopping discharges, for the simple reason that these smaller discharges never created significant damage to the inner slope.
- But the test with the parking place of bricks (Figure 4.15) showed that sand erosion with **30 l/s** per m, and even with **10 l/s** per m, goes fairly quickly. It must be noted that although the test was stopped for 30 l/s per m due to fast ongoing damage to the parking area, the dike itself was not in danger at all.



Figure 4.19 Afsluitdijk. Parking area, section 2. Source: Guidance on erosion resistance of inner slopes of dikes from three years of testing with the Wave Overtopping Simulator

- **Small obstacles like poles did not show any erosion**. Small holes from mice and moles did not initiate damage to the grass cover layer. Also a fence (Figure 4.13) and a little bigger pole (0.15 m by 0.15 m) showed no initiation of erosion. The grass around a fence at the toe of the dike had some influence on initiation of erosion, probably due to larger forces in this area. An obstacle like a concrete staircase on the inner slope was totally destroyed at a stage with 75 l/s per m overtopping (Figures 4.13 and 4.20). It should be noted, however, that also here the dike itself was not in danger, due to the large erosion resistance of the clay. Still, further research may give more final conclusions on other large obstacles.



Figure 4.20 Afsluitdijk. Concrete staircase, section 3. Source: Guidance on erosion resistance of inner slopes of dikes from three years of testing with the Wave Overtopping Simulator

5 OVERTOPPING FLOW ENCOUNTERING OBSTACLES

When the flow overtops the dike crest, it flows through the inner slope toward the landside. This landward flow from overtopping is difficult to model due to the complexity of the flow pattern and paths. In addition, when this flow encountered an obstacle, different hydraulic response of the flow and amount of energy dissipation will happen This depends a lot on the flow condition such as the flow speed, approach angle and also on the geometry, surface roughness and porosity of the obstacle.

Currently, there is no literature providing a simple approximation on calculating the flow distribution from overtopping flow when it encounters an obstacle. However, there are many literatures providing equivalent information on the effect of flood wave encountering obstacles which are on a much larger scale e.g. in flood routing simulation. Using this information especially on the flow pattern when encountering obstacle, attempt can be made to carry up conservative approximation on the flow distribution. The amount of the overtopping flow that is (a) reflected by the obstacle and (b) diverted to the sides of the obstacle. In order to determine this flow distribution, how an obstacle affects the flow will first need to be understood.

5.1 Effect of Obstacle on Flow

Syme (2008) review on the methods to account for building's response to the flood wave for 2D modeling. Although his review of the obstacle is strictly on building, it provides an idea on how the type of the obstacle affects the flow so as to correctly account it in a 2D model. These methods are:

1. Increase roughness: increase bed resistance will result in increasing energy dissipation of water flowing through and around the obstacle e.g. buildings. This work well for 2D element with coarse resolution. However, the difficulty is to obtain the appropriate roughness value to represent the flow.
2. Blocking out of Element: This is done provided that the element size for the obstacle is sufficiently fine. However, most of the time, the obstacle is large and in certain case such as building will "adsorb" some of the water.
3. Using energy loss coefficient: Specify form loss coefficient to represent the fine-scale energy dissipation within and around the obstacle. Though it is theoretically more correct to account for the obstacle as energy is loss when the flow passes through or around the obstacle, it is difficult as there is also currently no literature to provide this type of information.
4. Modeling Buildings' Exterior wall: This method is good since it account for the possible deflection of the water and also storage effect for water through building. However, this method required some prior knowledge of the flow direction.
5. Modeling Buildings as "porous": 2D element sides of building are partially blocked to represent certain amount of blockage by external wall. TUFLOW software is used to model partial blockages.

Syme then carried out a numerical simulation using TUFLOW to show the effect on the building response to flow when different methods were applied. Figure 5.1 shows the hypothetical building model layout. Table 5.1 presents a comparison between different building test scenarios. Figure 5.2 presents a comparison between different water surface profiles along the model centreline.

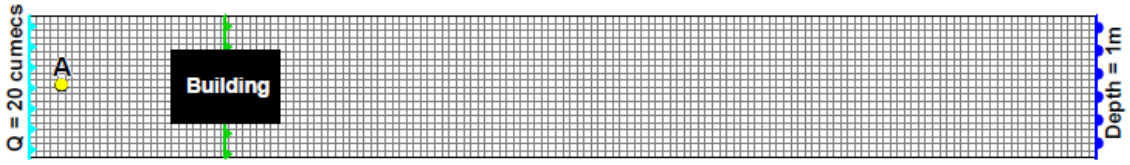

Figure 5.1: Hypothetical Building Model Layout. Source: Syme (2008)

Table 5.1. Comparison of building test scenarios

Scenario	Water Level (m)		Flow Distribution (%)		Average Velocity (m/s)	
	Point A	Increase	Building	Garden	Building	Garden
No Building	1.118	0.000	50%	50%	0.91	0.91
Blocked Out	1.255	0.137	0%	100%	n/a	1.90
High Roughness	1.240	0.122	21%	79%	0.38	1.41
Add Form Loss	1.195	0.077	31%	69%	0.55	1.23
Ext Walls, Open D/S	1.250	0.132	0%	100%	0.00	1.92
Ext Walls, Open U/S	1.263	0.145	0%	100%	0.00	1.93
Porous	1.170	0.052	9%	91%	1.87	1.80
Porous + Form Loss	1.225	0.107	7%	93%	1.28	1.78

Source: Syme (2008)

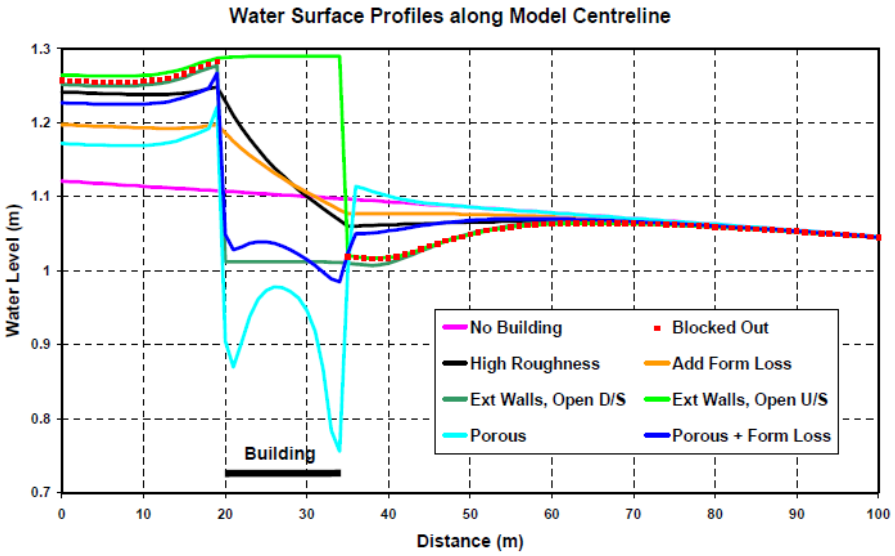

Figure 5.2. Comparison of Water Level Profiles along Model Centerline. Source: Syme (2008)

Figure 5.1 shows the hypothetical building model layout with the results shown on Table 5.1 and Figure 5.2 from the by Syme (Syme 2008). The change in the water level can be seems as it (a) reaches, (b) through and (c) over the obstacle. When the flow reaches that the obstacle, there is a slight increase in the water level. Depending on the type of obstacle, the water level decreases significantly when the flow passes through the obstacle. After passing the obstacle, the reduced water level continues to reduce gradually as it travels further landward.

Referring to study by Michal Szydlowski [Szydlowski (2011)] on his numerical simulation and laboratory experiment on open channel flow between bridge priers, we can have addition insight on the effect of geometry of obstacle to flow.

Figure 5.3 shows that the water depth increases (i.e. hydraulic jump) in front of pier (obstacle) and sudden lowering directly after passing the pier. Local flow circulation just behind pier can also be seemed. Even for an obstacle that has a smooth rounded surface such as a pier, the resulting surface wave merged after encountering the obstacle has a complex structure with turbulence eddies, diffraction and interference due to the abrupt swelling and depression of the water level shown in Figure 5.4.

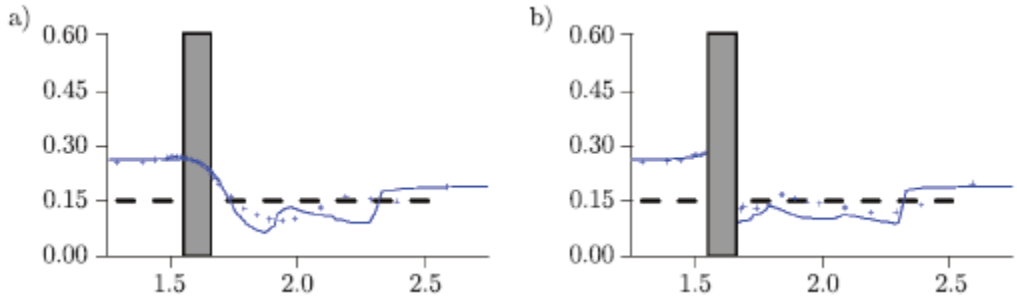

Figure 5.3. Measured (+ + +) and calculated (——) water surface profile for the second experiment together with the critical depth line (– –): a) along the channel axis, b) along the pier axis (dimensions in metres). Source: Szydlowski (2011)

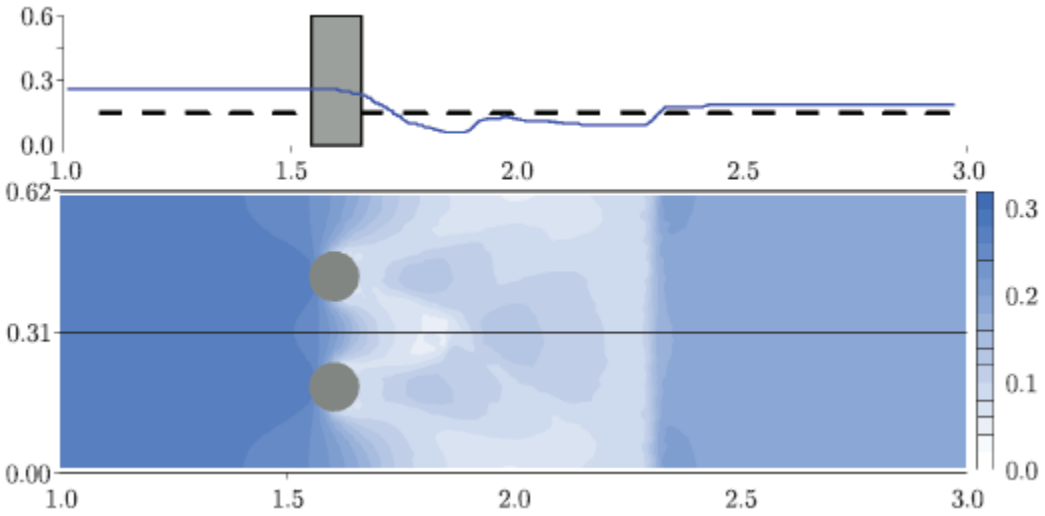

Figure 5.4. Surface profile and horizontal distribution of the computed water depth (dimensions in metres). Source: Szydlowski (2011)

Figure 5.5 and 5.6 shows the spatial distribution of the velocity and Froude number, provide additional information on the velocity flow and flow condition.

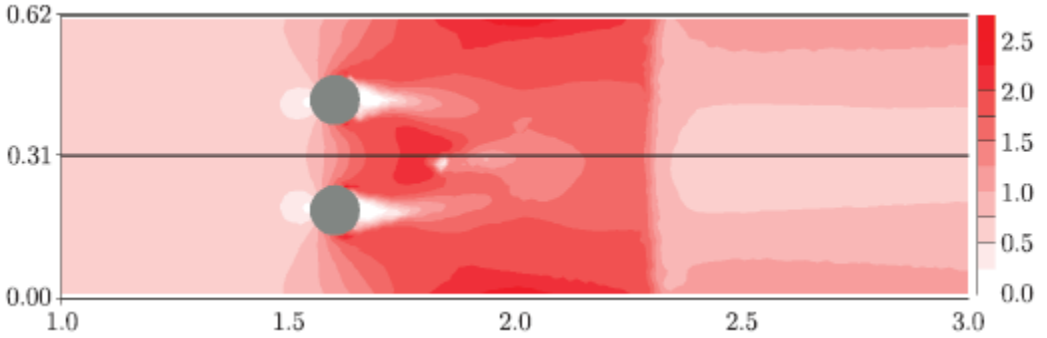

Figure 5.5. Distribution of flow velocity (m/s) (dimensions in metres). Source: Szydlowski (2011)

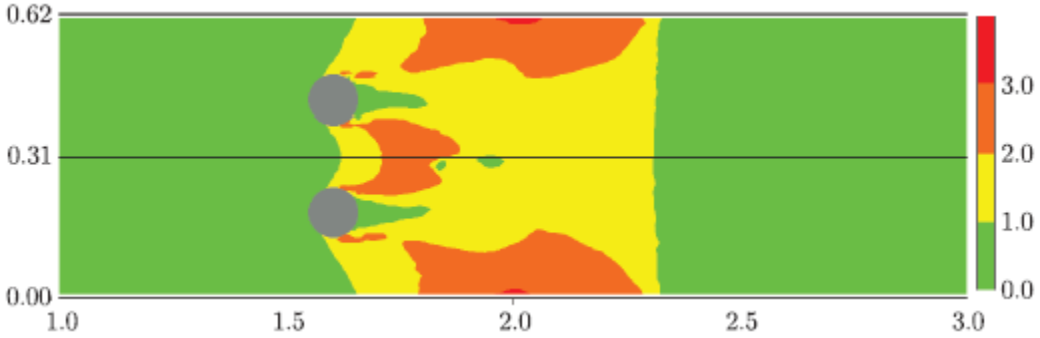

Figure 5.6: Spatial distribution of the Froude number (dimensions in metres). Source: Szydlowski (2011)

Hence, these methods, conclude that the surface roughness, geometry and porosity of the obstacle will affect the amount of energy dissipation by the flow and the flow movement.

5.2 Effect of Flow when encountering obstacle

Knowing that the different types of obstacles will affect the hydraulic response of the flow, the hydraulic response of the flow such as its flow pattern when encountering an obstacle will now be look into. In the paper by Hyung (Kim, Lee et al. 2012), the laboratory experiment was performed to study the variation in flood intensity due to structure. Numerical model was then used to verify the measured water depth from the laboratory experiment.

Figure 5.7 shows that laboratory setup of the experiment in plan and side view. The different placement of the block/s to simulate obstacle for flow shown on Figure 5.8. The experiment conditions for the flood wave propagation on Table 5.2. The location of the observation pointswith wave height gauges on the inundation area shown on Figure 5.9.

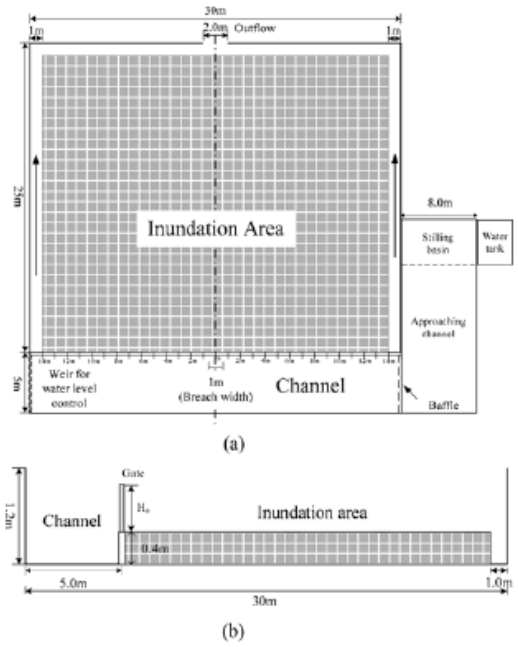

Figure 5.7: Schematic of the Flood Wave Experimental Channel: (a) Plan View, (b) Side View. Source: Kim et al (2012)

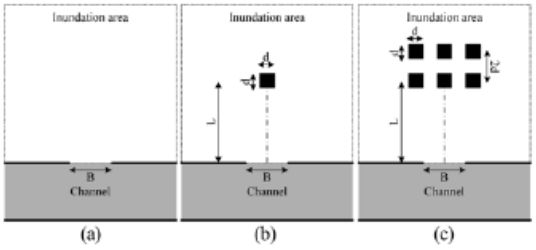

Figure 5.8: Schematic of Structure Layouts for Experiments: (a) Case1: None-structure, (b) Case 2: Single Structure, (c) Case 3: Group Structure. Source: Kim et al (2012)

Breach width B (m)	Overflow depth H0 (m)	Initial flow velocity (m/s)	Structure layout
1.0	0.55	2.3	None Single Group
	0.50	2.2	
	0.45	2.1	
	0.40	2.0	
	0.35	1.9	

Table 5.2: Experimental Conditions for Flood Wave Propagation. Source: Kim et al (2012)

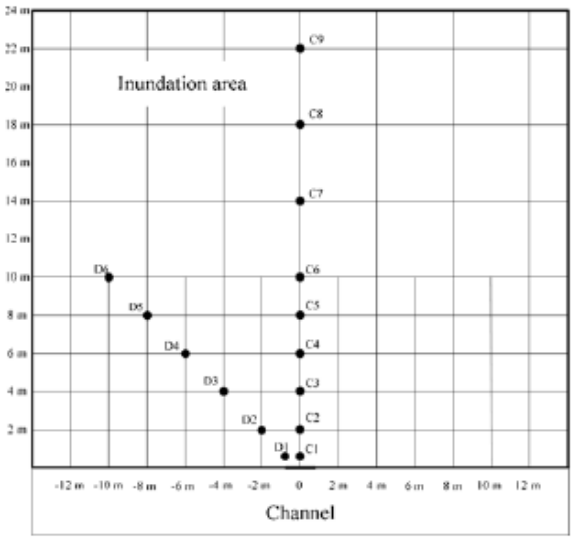

Figure 5.9: Experimental Observation Points with Wave Height Gauges. Source: Kim et al (2012)

The wave height measured in the (a) normal and (b) diagonal direction for the three cases were shown on Figure 5.10, 5.11 and 5.12, respectively.

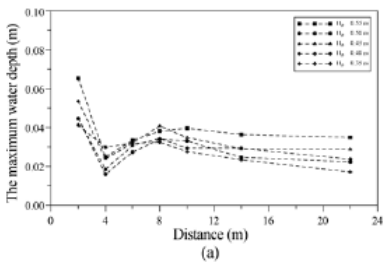

Figure 5.10: Observed Maximum Water Depth in Case 1: (a) Normal Direction, (b) Diagonal Direction. Kim et al (2012)

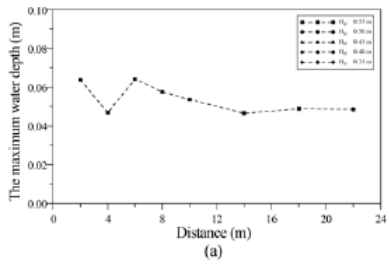

Figure 5.11: Observed Maximum Water Depth in Case 2: (a) Normal Direction, (b) Diagonal Direction. Kim et al (2012)

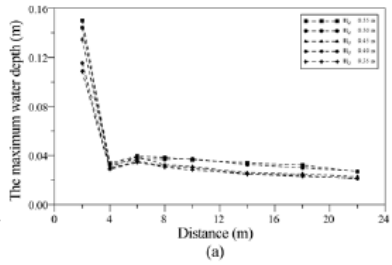

Figure 5.12: Observed Maximum Water Depth in Case 3: (a) Normal Direction, (b) Diagonal Direction. Kim et al (2012)

From these Figure, Hyung obtained the following observations:

1. When the water was released by overflow from the channel to the inundation area, its water depth was at maximum at x = 2m. This maximum water depth increase with the increase of the overflow height.
2. This maximum water depth decreases rapidly, as the flood wave velocity increase rapidly until x = 4 m.
3. After distance x = 4 m, maximum water depth increase as bottom rough cause velocity to decrease slightly.
4. If there is a obstacle, there will be water depth increase between the structure and the source of the flood wave. The water depth increase will be more for Case 3 than Case 2.
5. For flow encountering obstacle in Case 2 and 3, there were also water height increase for observation in the diagonal direction than the normal direction. This means that some of the flow instead of being reflected by the obstacle have been diverted to the sides of the obstacle.
6. Water depth is also slightly greater immediately behind the structure due to the superpositioning of the flood wave.
7. After x = 8 m, for all cases, the maximium water depth decrease as distance increase.

Figure 5.8 showns the maximum flood intensity distribution generated by the numerical model which the water depth has been verified by the experiment results.

As there are many ways of determining flood intensity, the Swiss method (OFEE et al., 1977) was adopted by the Hyung . The Swiss method defined flood intensity in term of the maximum water depth generated throughout the event and the product of the maximum velocity multiplied by the maximum depth. The flood intensity produced a quantity similar flow rate per unit wide when we consider the amount of overtopping rate.

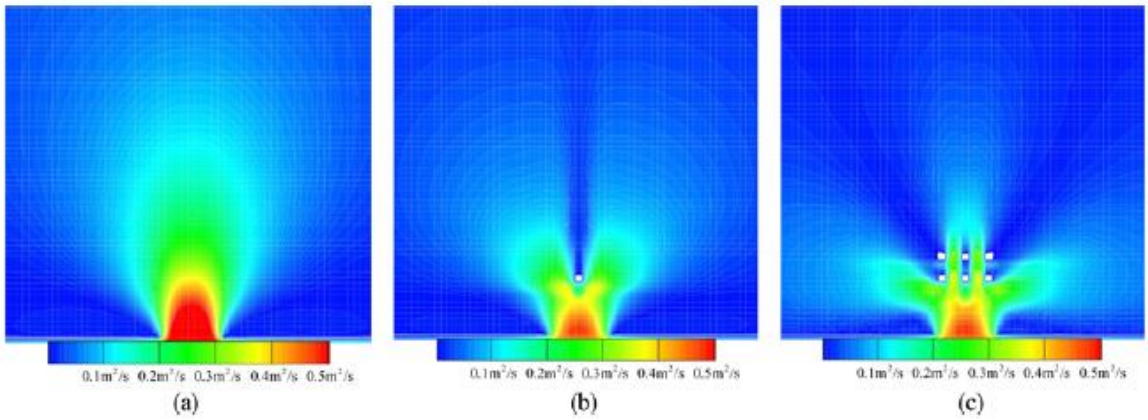

Figure 5.13: Maximum Flood Intensity Distributions: (a) None-structure, (b) Single Structure, (c) Group Structures. Source: OFFE et al (1977)

The numerical result shown was in line with the observations made from the laboratory results and it provide a more hoslistic and overview on the intensity of the flow when encountering obstacle/s. Figure 13 shows that the flood intensity was maximum when it was initially released from the opening. Without an obstacle in Figure 13(a), the flood wave will propagate, spread and reduce in its intensity as it traveled furtehr away from the source. In Figure 13(b) and 13(c), when encountering an obstacle, the flood intensity changes at the front and sides regions of the obstacle. Funneling effect also causes the increase of flood intensity at the gaps between the structures.

In addition, to analyze changes in flood intensity due to obstruction, the ratios of the maximum flood intensity increase are calculated by taking dividing the calculated flood intensity for Case 2 and 3 to that of Case 1.

Figure 5.14 shows that there is a significant increase in flood intensity in the diagonal direction. It shows that as the water depth increase, the obstacle divert more of the the wave propagation to the diagonal direction. Thus, the flood intensity behind the obstacle decreases more.

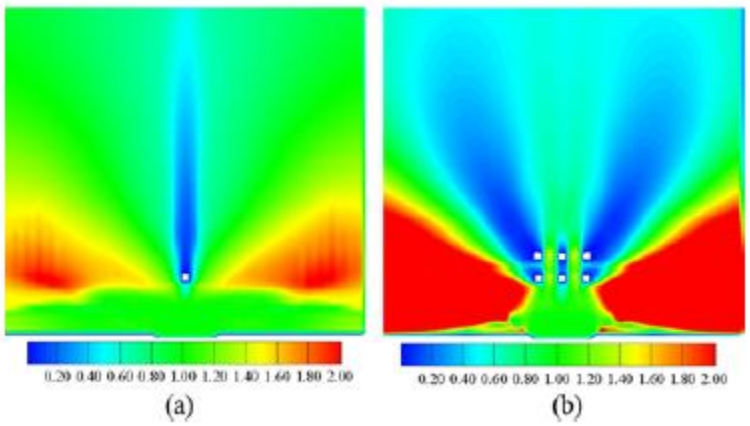

Figure 5.14: Increase Ratio of Maximum Flood Intensity: (a) Single Structure, (b) Group Structures. Source: OFFE et al (1977)

Hence, through the laboratory experiment and numerical model by Hyung (Kim, Lee et al. 2012), a better idea on the effect on flow when it encountered obstacle can be obtained.

A similar type of laboratory experiment was also done by Guido Testa (Testa, Zuccalà et al. 2007), the experimental results on the behavior of the flow when encountering obstacle/s were similar to that done by Hyung (Kim, Lee et al. 2012) as described earlier. Guido's experiment result provided an added dimension to the understanding on flow encountering obstacle.

Guido described that that the flow pattern as almost standing with a strong hydraulic jump occurred when the flow encountered the obstacle's front. This hydraulic jump propagates very slowly in the upstream direction until its intensity diminishes with time according to the inflow discharge. He added that the intensity of this hydraulic jump does not depend on any obstacles behind it. Thus the shock from the impact is equally strong whether there is any other obstacle behind it or not. This can be seen also from the results by Hyung.

Guido also mentioned that for a block layout similar to Case 3, if the spacing of the blocks is very close, this can make the obstacles to appear as a compact obstacle to the main flow.

6 REFERENCES

- CIRIA, CUR, CETMEF (2007), 'The Rock Manual. The Use of Rock in Hydraulic Engineering' . 2nd edition, C683, CIRIA, London.
- Eijgenraam, C., Brekelmans, R., den Hertog, D., Roos, K. (2010), 'Safe Dike Heights at Minimal costs: The Homogeneous Case'. Submitted to Management Science. Available on http://www.tilburguniversity.edu/research/institutes-and-research-groups/center/ graduate-school/chp/opmaast/dike1.pdf
- Inspectie Verkeer en Waterstaat (2006), 'Assessment of Primary Flood Defences in The Netherlands, National Report on 2006'. Available on http://www.safecoast.nl/editor/databank/File/Assessment%20primary%20flood%20defences%20in%20NL.pdf
- Jonkman, S., Jongejan, R., Maaskant, B., Vrijling, H. (2010), 'New Safety Standards for Coastal Flood Defences in The Netherlands'. 32nd International Conference on Coastal Engineering, ICCE 2010, June 30 – July 5 2010, Shanghai, China.
- Kim, H., Lee, J. et al (2012). 'Numerical Analysis of Flood Risk Change Due to Obstruction'. KSCE Journal of Civil Engineering 16 (2). 207-214.
- OFFE, OFAT and OFEFP (1997), 'Prise en compte des dangers dus aux dans le cadre des activities del'amenagement du territoire'. Bienne, 1997, Office Federal de l'Economie des Aux (OFFE), Office Federal de l'Amenagement du Territoire (OFAT), Office Federal de l'Environnent, Desforets, et du Paysage (OFEFP).
- Pullen, T., Allsop, N. W. H., Bruce, T., Kortenhaus, A., Schüttrumpf, H., Van der Meer, J. W. (2007), 'EurOtop – Wave Overtopping of Sea Defences and Related Structures: Assessment Manual'. Environment Agency, UK, Expertise Netwerk Waterkeren, NL and Kuratorium für Forshung im Küsteningenieurwessen, DE.
- Roos, A., Riedstra, D. (2010), 'Safety Standards in The Netherlands'. Rijkswaterstaat Centre for Water Management. Presentation of March 17th, 2010.
- Syme, W. (2008), 'Flooding in Urban Areas – 2D Modelling Approaches for Buildings and Fences'. 9th National Conference on Hydraulics in Water Engineering. Engineers Australia. Darwin Convention Centre, Australia.
- Szydlowski, M. (2011), 'Numerical Simulation of Open Channel Flow Between Bridge Piers'. TASK Quarterly 15 (3-4). 271-282.
- Testa, G., Zuccala, D. et al (2007), 'Flash Flood Flow Experiment in a Simplified Urban District'. Journal of Hydraulic Research 45 (supl. 1). 37-44.
- Lin, P.Z., Liu, P.L.F., 1999. Internal wave-maker for Navier-Stokes equations models. Journal of Waterway Port Coastal and Ocean Engineering 125 (4), 207‐215.
- Guidance on erosion resistance of inner slopes of dikes from three years of testing with the Wave Overtopping Simulator, Van der Meer, Schrijver, Hardeman, Van Hoven, Verheij and SteendamW. Allsop, MICE, T. Bruce, J. Pearson BEng and P. Besley 'Wave overtopping at vertical and steep seawalls'. Maritime Engineering 158 September 2005 Issue MA3,103–114
- Dr J.W. van der Meer (2002), 'Technical Report Wave Run-up and Wave Overtopping at Dikes', Technical Advisory Committee on Flood Defence

TU DELFT – MULTIDISCIPLINARY PROJECT CIE4061

Afsluitdijk Project
"The Monument" Location

Literature Review

Sien Liu, Jun Huang, Sebastian Rayo, Tai Yan Lim

21/12/2012



CONTENTS

1 Introduction 2
1.1 Background 2
1.2 Problem Description 2
1.3 Document Scope 2
2 Interaction Between Waves and Structures 3
2.1 Definitions 3
2.2 Types of Overtopping 3
3 Safety Standards 5
3.1 Hazards 5
3.2 Existing Criteria 5
3.2.1 Return Period 5
3.2.2 Tolerable Discharges 7
3.2.3 Overtopping Velocities 8
4 Overtopping Modelling 9
4.1 Description 9
4.2 Factors of Influence 9
4.2.1 Various slopes ($\tan\alpha$) 9
4.2.2 Shallow foreshore (h_m/H_{m0}) and breaking parameter (ξ_0) 9
4.2.3 Incident wave angle (γ_β) 10
4.2.4 Berms (γb) 10
4.2.5 Roughness of elements (γf) 12
4.2.6 Vertical wall on slope (γv) 12
4.2.7 Slope with composite roughness elements (γf) 12
4.3 Mean overtopping discharge 13
4.4 Maximum over topping volume 13
4.5 Overtopping flow velocity and flow depth 13
4.5.1 On seaward slope 14
4.5.2 On crest of dike 15
4.5.3 On the landward slope 16
4.5.4 Spatial distribution of the overtopping water 17
5 Overtopping Flow Encountering Obstacles 24
5.1 Effect of Obstacle on Flow 24
5.2 Effect of Flow when encountering obstacle 27
6 References 32

1 INTRODUCTION

1.1 Background

The Afsluitdijk (Enclosure Dam) is a main dam that forms the fundamental part of the larger Zuiderzee Works that separates the Zuiderzee, a salt water inlet of the North Sea, and turning it into the fresh water lake of the IJsselmeer. It protects the central Netherlands from the effects of the North Sea. It was constructed between 1927 and 1933, and runs from Den Oever on Wieringen to the village of Zurich in Friesland. It is 32 km long and 90 meters wide, rising to 7.25 meters above sea-level, with an incline of 25% on each side.

At the location along the Afsluitdijk where the final water passage was closed ('De Vlieter'), a lookout tower known as 'The Monument' was built in 1933. It was presented by the Zuiderzee Works Construction Company and designed by architect W.M. Dudok. The site has a statue of a "Steenzetter", and also marks the inscription 'A living nation builds for its future'. A statue of Cornelis Lely has also been erected near Den Oever on the Barrier Dam itself.

The Afsluitdijk with The Monument are currently managed by the Ministry of Infrastructure and the Environment ("The client"). There is a restaurant at The Monument where the client has sublet it for private operator to manage it.

1.2 Problem Description

With the anticipation of increase storm intensity and sea level rise in the future, the client had previously engaged a consultant to analyze the existing design of Afsluitdijk for a design storm of 1:10,000 years. According to the client, the result of the study concluded that the standard cross-section of Afsluitdijk is not sufficient to withstand the design storm of 1:10,000 years, hence, modifications of it are required. The study also found that during the design storm, there is a significant overtopping over the dike.

The client is concerned about the significant overtopping found from the previous study may have adverse impact on the non-standard cross-section of the dike where The Monument is located. Therefore, the client has requested our design team to look into the dike section at the Monument location.

1.3 Document Scope

The main objectives of this document are:

1. To introduce the typical processes related to the interaction between waves and a hydraulic structure.
2. To establish the state-of-art of safety standards of dikes in the Netherlands.
3. To establish a methodology to model wave overtopping and its characteristics discharge, height and velocity) on top and the rear slope of a dike.
4. To look for research related with 2D distribution of un-steady flow when there are some obstacles in front of it.

2 INTERACTION BETWEEN WAVES AND STRUCTURES

2.1 Definitions

CIRIA et al (2007) defines that the interaction between waves and hydraulic structures (such as dikes) can be classified into: wave run-up (and run down), wave overtopping, wave transmission and wave reflection.

Definitions for each interaction process are:

- Wave conditions are defined by incident wave height (usually significant wave height), the wave period, the angle of incidence and the local depth.
- Wave run-up and run-down are defined as the extreme levels that a wave can reach on a sloping structure.
- Wave overtopping occurs when wave run-up exceeds the crest level.
- Wave transmission occurs when a structure has a permeable core, which permits the transmission of part of the wave energy through the structure.
- Wave reflection is when part of the wave energy returns towards the sea because of the influence of a hydraulic structure.

Figure 2.1 presents schemes of different type of interaction between waves and a dike.

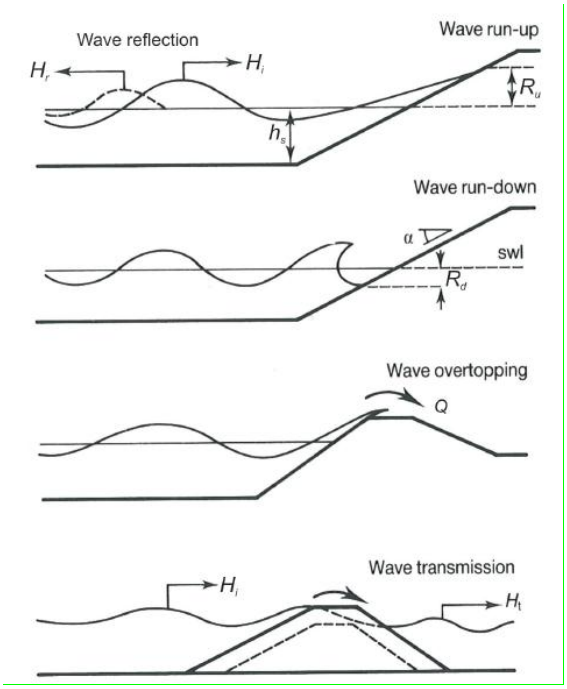

Figure 2.1. Different type of interaction between waves and a dike. Source: CIRIA et al (2007)

2.2 Types of Overtopping

According to Pullen et al (2007), two different types of overtopping are distinguished:

- ‘Green water’, which is related with complete sheets of water that run over the crest of a defence;
- ‘White water’, which is related with waves that break at the seaside, generating an important amount of spray and a non-continuous overtopping flow.

Spray generated by wind can generate some hazards for people and vehicles near the dike, due to lack of visibility. Nevertheless, it is not considered as an overtopping flow like the previous definitions.

3 SAFETY STANDARDS

3.1 Hazards

According to Pullen et al (2007), overtopping effects and its related consequences can be classified within four different categories:

a) *Direct hazard of injury or death to people immediately behind the defence;*
b) *Damage to property, operation and/or infrastructure in the area defended, including loss of economic, environmental or other resource, or disruption to an economic activity or process;*
c) *Damage to defence structure(s), either short-term or longer-term, with the possibility of breaching and flooding;*
d) *Low depth flooding (inconvenient but no dangerous).*

According to Pullen et al (2007), the main responses to these hazards are three:

a) *Move human activities away from the area subject to overtopping and/or flooding hazard, thus modifying the land use category and/or habitat status;*
b) *Accept hazard at a given probability (acceptable risk) by providing for temporary use and/or short-term evacuation with reliable forecast, warning and evacuation systems, and/or use of temporary/demountable defence systems;*
c) *Increase defence standard to reduce risk to (permanently) acceptable levels probably by enhancing the defence and/or reducing loadings.*

3.2 Existing Criteria

3.2.1 Return Period

The return period for which a defence is designed is usually determined in accordance with local and national guidelines, as well as is related with local circumstances, a balance between risk and benefits and the level of overall exposure. Table 3.1 presents some typical values of design life and levels of protection.

Table 3.1. Hazard type

Hazard type and reason	Design life *(years)*	Level of protection *(years)*
Temporary or short term measures	1 – 20	5 – 50
Majority of coast protection or sea defence walls	30 – 70	50 – 100
Flood defences protecting large areas at risk	50 – 100	100 – 10,000
Special structure, high capital cost	200	Up to 10,000
Nuclear power stations, etc.	-	10,000

Source: Pullen et al (2007)

According to Pullen et al (2007), the design life in Netherlands for flood defences is 50 years. However, for special structures with high capital cost, the design life can be extended to 200 years.

Roos and Riesdstra (2010) give more detailed information. In the Netherlands, every ring has a specific safety standard. West and North Netherlands have safety standards of 1:10,000 and 1:4,000, respectively. Figure 3.1 shows details of safety standard definition in the Netherlands.

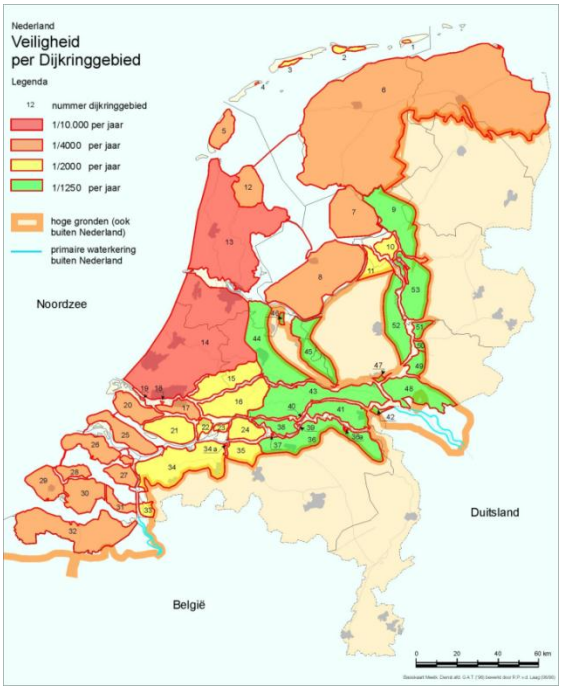

Figure 3.1. Details of safety standards definition in the Netherlands. Source: Roos and Riedstra (2010)

Nevertheless, because of climate change, a discussion started in 2006 with respect to the definition of safety standards, which will be updated in 2017. Figure 2.3 shows a map of the Netherlands with detailed information about safety standard achievement for several locations. Particularly, the Aflsluitdijk does not comply with the standard.



Figure 2.2. Results second safety assessment primary flood defences, 1 January 2006. Source: Inspectie Verkeer en Waterstaat (2006)

Jonkman et al (2010) mention that in the Netherlands, current safety standards are based on cost – benefits analysis, but they do not incorporate casualties in a proper way. Hence, they propose that a research on risk definition should be made, considering both individual (probability of death of a person in one year) and societal risks (probability of occurrence of an event with several fatalities).

Eijgenraam et al (2010) propose a numerical method to determine optimal dike heights, considering a risk analysis definition. They conclude that in the Netherlands there is a need to increase safety standards, which will increase expenses of the Dutch government for the protection against flooding item.

3.2.2 Tolerable Discharges

Information available in Pullen et al (2007) gives several limits of overtopping (flow discharges and volumes) for pedestrians, vehicles and properties behind the defence. Tables 3.2 to 3.4 present that information.

Table 3.2. Limits for overtopping for pedestrians

Hazard type and reason	Mean discharge	Max volume
	q (l/s/m)	V_{max} *(l/m)*
Trained staff, well shod and protected, expecting to get wet, overtopping flows at lower levels only, no falling jet, low danger of fall from walkway.	1 – 10	500 at low level
Aware pedestrian, clear view of the sea, not easily upset or frightened, able to tolerate getting wet, wider walkway.	0.1	20 – 50 at high level or velocity

Source: Pullen et al (2007)

Table 3.3. Limits for overtopping for vehicles

Hazard type and reason	Mean discharge	Max volume
	q (l/s/m)	V_{max} *(l/m)*
Driving at low speed, overtopping by pulsating flows at low flow depths, no falling jets, vehicle not immersed.	10 – 50	100 – 1,000
Driving at moderate or high speed, impulsive overtopping giving falling or high velocity jets.	0.01 – 0.05	5 – 50 at high level or velocity

Source: Pullen et al (2007)

Table 3.4. Limits for overtopping for property behind the defence

Hazard type and reason	Mean discharge	Max volume
	q (l/s/m)	V_{max} *(l/m)*
Significant damage or sinking of larger yachts	50	5,000 – 50,000
Sinking small boats set 5 – 10 m from wall. Damage to larger yachts.	10	1,000 – 10,000
Building structure elements	1	-
Damage to equipment set back 5 – 10 m	0.4	

Source: Pullen et al (2007

Information available in Pullen et al (2007) indicates that the work realized by Goda and other researchers gave some guidelines of setting limits for the defence structures. That information is summarized in Table 3.5.

Table 3.5. Limits for overtopping for damage to the defence crest or rear slope

Hazard type and reason	Mean discharge *q (l/s/m)*
Embankment seawalls / sea dikes	
No damage if crest and rear slope are well protected	50 – 200
No damage to crest and rear face of grass covered embankment of clay	1 – 10
No damage to crest and rear face of embankment if not protected	0.1
Promenade or revetment seawalls	
Damage to paved or armoured promenade behind seawall	200
Damage to grassed or lightly protected promenade or reclamation cover	50

Source: Pullen et al (2007)

Further research was done in Netherlands during year 2007. Wave overtopping tests were developed on existing dikes (both made of clay and covered with grass). Results indicated that the resistance of these dikes is higher than the values defined by Goda. Particularly, the resistance of a dike covered with grass was good enough for overtopping rates up to 50 l/s/m.

3.2.3 Overtopping Velocities

Information available in Pullen et al (2007) indicates that maximum velocities of 5 – 8 m/s can occur for overtopping discharges in the range 10 – 30 l/s/m.

4 OVERTOPPING MODELLING

4.1 Description

The dikes in Netherlands normally consist of a toe structure, a gentle slope with a berm, a crest of a certain width, outer and inner crest lines and inner slope. For some special dikes, transport infrastructure like bicycle lanes and highways may lie behind the inner slope. The configurations of dikes described above all have influence on the wave overtopping. It can also be affected by the reference water levels, strong sea winds and climate change.

4.2 Factors of Influence

The profiles of dikes are quite different from each other, as well as the wave conditions in different cases. In order to consider all these effects on wave overtopping, several parameters will be introduced to make better predictions of wave overtopping.

4.2.1 Various slopes (tanα)

In reality a dike slope in normally consists of several sections with different slope angles. Considering that the wave overtopping requires a characteristic slope in the breaker parameter, the definition of average slope is applied here to replace various slope sections. The representative slope is iteratively calculated as the average slope between still water line $-1.5 \cdot H_{m0}$ and still water line $+z_{2\%}$. (any berm present is not include for calculation of average slope).

4.2.2 Shallow foreshore (h_m/H_{m0}) and breaking parameter (ξ_0)

The waves will break due to limit water depth when they approach to a shallow foreshore, which will consequently decrease the wave overtopping discharge. In addition, the wave height distribution will also be changed due to this effect. In relatively deep water ($h_m/H_{m0} > 3\ to\ 4$), wave heights follow as Rayleigh distribution. In shallow foreshore ($h_m/H_{m0} < 3\ to\ 4$), the wave height distribution will deviate from Rayleigh distribution due to breaking effects of higher waves. This shallow foreshore effect is very important and it is necessary coming up with two equations to calculate the wave overtopping under these two different conditions. The criteria of distinguishing these two conditions are based on the breaker parameter ξ_0, which is given by:

$$\xi_0 = \frac{tan\alpha}{\sqrt{s_0}}$$

Where:

ξ_0 – breaker parameter [-].
α – angle of slope [°].
s_0 – wave steepness [-]

$$s_0 = 2\pi \cdot H_{m0}/(g \cdot T_{m-1,0}^2)$$

Where:

$T_{m-1,0}$ – spectral wave period=m_{-1}/m_0 [s].
m_0 – zero moment of spectrum [m^2].
m_{-1} – first negative moment of spectrum [m^2].

4.2.3 Incident wave angle (γ_β)

The incident wave angle is defined as the angle between propagation direction of waves and the perpendicular direction to long axis of the dike. In real site situation, the incident waves come from various directions and each of them has individual contribution of wave overtopping. In calculation of deterministic approach, it's impossible to do calculation for each wave, so the consideration of evaluating contributions of different incident wave angles is necessary.

Influence factor for this effect is given by γ_β (β indicates incident wave angle, $\beta = 0$ means perpendicular wave attack). The influence factor γ_β is plotted against the angel of wave attack, β (Technical Report Wave Run-up and Wave Overtopping at Dikes, Technical Advisory Committee on Flood Defence) (Dr J.W Van De Meer, 2002). For wave overtopping, the influence factor decrease linearly from 1 to 0.7 when β increase from 0 to 80. It keeps at 0.7 when β is between 80 and 90. Figure 4.1 presents the relation between the influence factor γ_β and the angle of attack β.

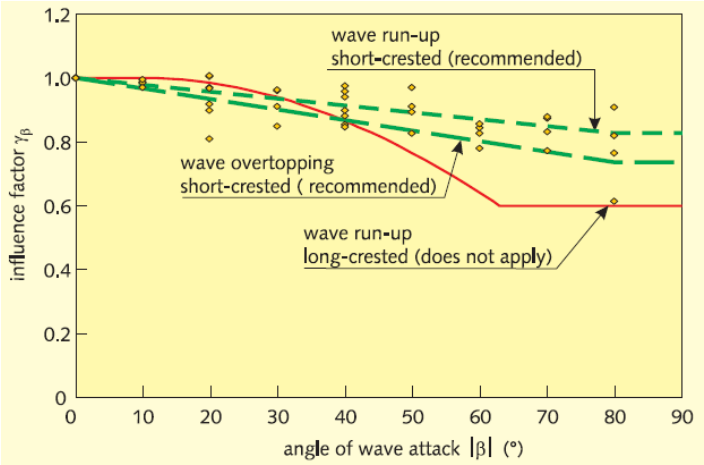

Figure 4.1. Relation between influence factor and angle of wave attack. Source: T. Pullen (2007)

It can be described as following formulae for wave overtopping:

$$\gamma_\beta = 1 - 0.0033|\beta| \quad (0° < |\beta| < 80°)$$

$$\gamma_\beta = 1 - 0.0033 \cdot 80° \quad (|\beta| > 80°)$$

4.2.4 Berms (γ_b)

A berm is defined as part of the dike profile in which the slope varies between horizontal and 1:15. Both the width and the depth of berm are given in Figure 4.2.

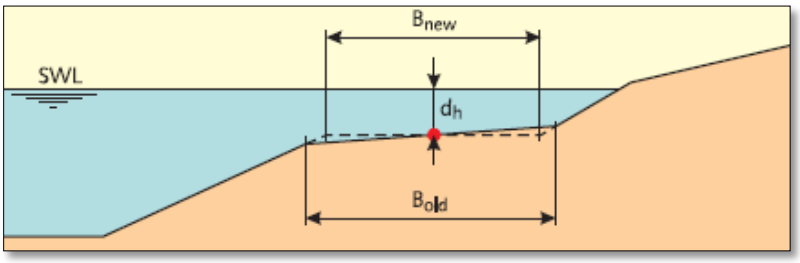

Figure 4.2. Scheme with berm definition. Source:(T. Pullen, 2007)

Normally, it is required that the slope should be gentler than 1:15 and the width should be less than one quarter of the wavelength. If the berm doesn't satisfy with the requirement, then the wave overtopping must be determined by interpolation between the steepest berm (1:15) and a gentle slope (1:8). For calculations of wave overtopping, the inclined berm is drawn to a horizontal berm which is shown in figure as B_{new}. The berm depth is shown as d_h. The influence of berm can be considered as two parts: one is influence of the width of berm,r_B, and one is berm depth,r_{dh}.

For estimation of influence of berm, the following equation is applied:

$$\gamma_b = 1 - r_B \cdot (1 - r_{dh})$$

Where $0.6 \leq \gamma_b \leq 1.0$, $r_{dh} = 0$ relates to condition of $d_h = 0$ and $0 \leq r_B \leq 1$

Based on the information of Pullen et al (2007), the influence of berm width can be calculated by the equation as follows:

$$r_B = 1 - \frac{2 \cdot H_{m0}/L_{berm}}{2 \cdot H_{m0}/(L_{berm} - B)} = \frac{B}{L_{berm}}$$

The corresponding parameters are drawn in Figure 4.3.

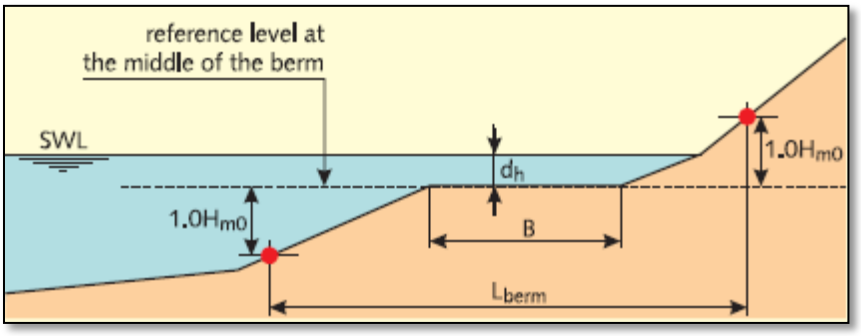

Figure 4.3. Parameters required to define berm influence. Source: T. Pullen (2007)

Also the influence of berm depth can be evaluated by the following formula:

$$r_{dh} = 0.5 - 0.5 \cdot \cos\left(\pi \frac{d_h}{x}\right)$$

Where

x $= z_{2\%}$ if $0 < -d_h < z_{2\%}$ (berm above still water line)
x $= 2 \cdot H_{m0}$ if $0 \leq d_h < 2 \cdot H_{m0}$ (berm below still water line)
$r_{dh} = 1$ if $-d_h \geq z_{2\%}$ or $d_h \geq 2 \cdot H_{m0}$ (outside influence area)

The influence of berm depth described above can only be used over the space between $2 \cdot H_{m0}$ below sea water level up to $z_{2\%}$ in the lower slope. Influence of berm position will disappear when it lies more than $2 \cdot H_{m0}$ under still water level.

In the end, the full expression of influence of berm can be written as:

$$\gamma_b = 1 - \frac{B}{L_{berm}} \cdot \left(0.5 + 0.5 \cdot cos\left(\pi \frac{d_h}{x}\right)\right)$$

Where

$0.6 \leq \gamma_b \leq 1.0$

It can be easily seen that influence of berm position become maximum for $d_h = 0$ which results to $\gamma_b = 1 - \frac{B}{L_{berm}}$.

4.2.5 Roughness of elements (γ_f)

Influence of roughness elements on wave overtopping is measured by factor γ_f. Data of influence factors for various single roughness elements can be found in the Russian study with regular eaves from 1950s. The determination of γ_f is dependent on the various features of dike. More details can be found in (Technical Report Wave Run-up and Wave Overtopping at Dikes, Technical Advisory Committee on Flood Defence).The end result as a table showing a complete overall view of influence factors can be found in Technical Report Wave Run-up and Wave Overtopping at Dikes, Dr J.W. van der Meer, (2007). Some values of several specific roughness elements are shown as follows:

Reference type	γ_f
Concrete	1.0
Asphalt	1.0
Closed concrete block	1.0
Grass	1.0
Vilvoorden stone	0.85
Basalt	0.90
Haringman	0.90
Fixtone - open stone asphalt	0.90
Armorflex	0.90
Small blocks over 1/25 of surface	0.85
Small blocks over 1/9 of surface	0.80
¼ of block revetment 10 cm higher	0.90
Ribs (optimum dimensions)	0.75
Armour rock - two layers thick	0.55
Armour rock - single layer	0.70

Figure 4.4 influence factors of roughness elements, Dr J.W. van der Meer, (2007)

4.2.6 Vertical wall on slope (γ_v)

The influence factor of vertical wall on slope is given by factor γ_v. In some cases, there a vertical wall placed on top of slope to reduce wave overtopping. The wave overtopping for a vertical wall on slope is smaller than for a 1:1 slope on top of dike profile. The influence factor for a vertical wall on a slope is $\gamma_v = 0.65$. For a 1:1 slope, $\gamma_v = 1$. Interpolation should be done for a wall that is between vertical and 1:1.

$$\gamma_v = 1.35 - 0.0078 \cdot \alpha_{wall}$$

Where α_{wall} is steep slope on top of dike ($0^\circ < \alpha_{wall} < 90^\circ$)

4.2.7 Slope with composite roughness elements (γ_f)

Weighting of various roughness factors is exerted by including the lengths of appropriate sections of the slope (between SWL$-0.25 \cdot z_{2\%,smooth}$ and SWL$+0.25 \cdot z_{2\%,smooth}$). Any roughness elements located beyond this limit are considered as no effect on the wave overtopping. If we consider a condition with three roughness elements within this area, and they are in lengths of L_1, L_2 and L_3, and with influence factor of $\gamma_{f,1}$, $\gamma_{f,2}$ and $\gamma_{f,3}$, respectively. Then the weighted influence factor can be written as:

$$\gamma_f = \frac{\gamma_{f,1} \cdot L_1 + \gamma_{f,2} \cdot L_2 + \gamma_{f,3} \cdot L_3}{L_1 + L_2 + L_3}$$

4.3 Mean overtopping discharge

The wave overtopping formulae are exponential functions with the general form:

$$\mathrm{q} = \mathrm{a} \cdot \exp(\mathrm{b} \cdot R_c)$$

The coefficient a and b are functions of the wave height, slope angle, break parameter and the influence factors described previously.

Wave overtopping is usually given as an average discharge per linear meter of width, q (m3/s per m or in l/s per m). Because the wave overtopping increases for increasing breaker parameter ξ_0, It can be described in two formulae: one for breaking waves, ($\xi_0 \leq 5$) and one for the maximum that is achieved for non-breaking waves ($\xi_0 > 7$). In the area in between ($5 < \xi_0 < 7$), the logarithm of q is linearly interpolated.

For $\xi_0 \leq 5$, the calculation of wave overtopping is described as:

$$\frac{q}{\sqrt{gH_{m0}^3}} = \frac{0.067}{\sqrt{tan\alpha}}\gamma_b \cdot \xi_0 \cdot \exp\left(-4.3\frac{R_c}{H_{m0}}\frac{1}{\xi_0 \cdot \gamma_b \cdot \gamma_f \cdot \gamma_\beta \cdot \gamma_v}\right)$$

With a maximum of:

$$\frac{q}{\sqrt{gH_{m0}^3}} = 0.2 \cdot \exp\left(-2.3\frac{R_c}{H_{m0}}\frac{1}{\gamma_f \cdot \gamma_\beta}\right)$$

For $\xi_0 > 7$, the calculation of wave overtopping is described as:

$$\frac{q}{\sqrt{gH_{m0}^3}} = 0.21 \cdot \exp\left(-\frac{R_c}{\gamma_f \cdot \gamma_\beta \cdot H_{m0} \cdot (0.33 + 0.022 \cdot \xi_0)}\right)$$

4.4 Maximum over topping volume

In order to estimate the hazard on buildings and infrastructure caused by wave overtopping, not only mean overtopping discharge is an important factor, but also maximum overtopping volume should be taken into consideration. The maximum volume of wave overtopping during certain is uncertain, but depends on the duration of the storm event. The maximum overtopping volume by one wave during an event depends on the actual number of overtopping waves, N_{ow}, and is given by:

$$V_{max} = a \cdot [\ln(N_{ow})]^{4/3}$$

Where

$\mathrm{a} = 0.84 \cdot \mathrm{q} \cdot \mathrm{t}/N_{ow}$
N_{ow} – number of overtopping waves.
q – mean wave overtopping discharge.
t – storm duration

4.5 Overtopping flow velocity and flow depth

Average wave overtopping discharge and maximum wave overtopping volume are not appropriate for describing the interaction between overtopping flow and failure mechanism.

In contract, the overtopping flow velocity and flow depth is more related to the analysis of erosion of dike inner slope and impact on infrastructure.

4.5.1 On seaward slope

Before calculating the overtopping flow depth and flow velocity, the wave run up velocities and related flow depth are required first. The flow on seaward slope is drawn in Figure 4.4.

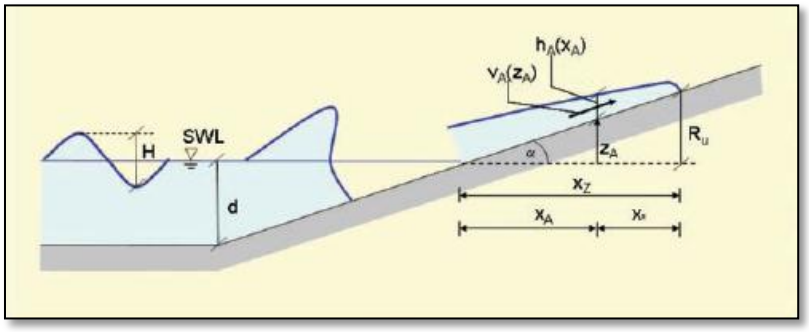

Figure 4.4. Wave run up characteristics. Source: Pullen et al (2007)

The flow depth of wave run up on the seaward slope is a function of horizontal projection x_z of wave run-up height $R_{u2\%.}$, the horizontal coordinate of the dike x_A and a dimensionless coefficient c_2. The calculation formula is under assumption of linear decrease of the lay thickness h_A from SWL to the highest point of wave run-up and it is given as follows:

$$h_A(\mathrm{x}_*) = c_2(x_z - x_A) = c_2 \cdot \mathrm{x}_*$$

Where:

x_* – remaining run-up length($\mathrm{x}_* = x_z - x_A$) and $x_z = R_{u2\%.}/tan\alpha$.

The coefficient can be selected based on different exceedance levels by Table 4.1.

Table 4.1 characteristic values for parameter c_2 (TMA-spectra)

Parameter	c_2	σ'
$h_{A,50\%}$	0.028	0.15
$h_{A,10\%}$	0.042	0.18
$h_{A,2\%}$	0.055	0.22

Source: Pullen et al (2007)

The run-up velocities are defined as the maximum velocity at any position of seaward slope during wave run-up. The equation of wave run-up velocity is given by:

$$v_A = k^* \cdot \sqrt{2g(R_{u2\%.} - z_A)}$$

Where:

v_A – wave run-up velocity at point z_A above SWL.

$R_{u2\%.}$ – wave run-up height exceeded by 2% of the incoming waves.

k^* – dimensionless coefficient.

The dimensionless form is:

$$\frac{v_A}{\sqrt{gH_s}} = a_0^* \sqrt{\frac{R_{u2\%.} - z_A}{H_s}}$$

Where:

H_s – significant wave height.

The values of a_0^* are given in Table 4.2.

Table 4.2 characteristic Values for Parameter a_0^* (TMA-spectra). Source: Pullen et al (2007)

Parameter	a_0^*	σ'
$v_{A,50\%}$	1.03	0.23
$v_{A,10\%}$	1.37	0.18
$v_{A,2\%}$	1.55	0.15

4.5.2 On crest of dike

The overtopping flow on the dike crest is sketched in Figure 4.5.

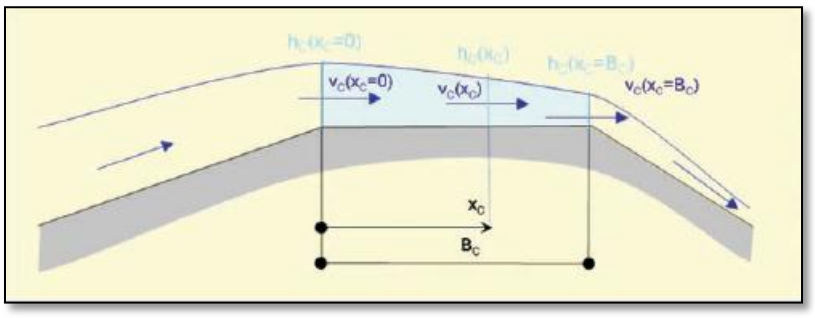

Figure 4.5. Overtopping flow on dike crest. Source: Pullen et al (2007)

The flow depth is given as a function of the width of crest B_c and the coordinate on the crest x_c :

$$\frac{h_c(x_c)}{h_c(x_c=0)} = \frac{c_2(x_c)}{c_2(x_c=0)} = exp\left(-c_3\frac{x_c}{B_c}\right)$$

Where:

c_3 – dimensional coefficient; 0.89 for TMA spectra and 1.11 for natural wave spectra.
B_c – width of dike crest.

The flow velocity is given by simplified Navier-Stokes-equation under several assumptions:

- Dike crest is horizontal.
- Vertical flow velocity to the dike slope can be neglected.
- Pressure term is constant over dike crest.
- Viscous effects in flow direction are small and bottom friction is constant over dike crest.

$$v_c = v_{c(x_c=0)} exp\left(-\frac{x_c \cdot f}{2 \cdot h_c}\right)$$

Where:

v_c – overtopping flow velocity.
f – friction coefficient.
x_c – coordinate on crest.
h_c – flow depth at x_c.

4.5.3 On the landward slope

Overtopping flow velocity and overtopping flow depth [Pullen et al (2007)].

When the overtopping flow runs up the seaside of the dike and crosses the dike crest, it will reach the landward slope of the dike.

An analytical function was developed which describes overtopping flow velocities and overtopping low depths on the landward slope as a function of the overtopping flow velocity at the end of the dike crest ($v_{b,0} = v_C(x_C = B)$), the slope angle . Of the landward side and the position s_B on the landward side with sB = 0 at the intersection between dike crest and landward slope. A definition sketch is given in Figure 4.6 below.

The following assumptions were made to derive an analytical function from the Navier-Stokes-equations:

1. Velocities vertical to the dike slope can be neglected;
2. The pressure term is almost constant over the dike crest; and the viscous effects in flow direction are small.

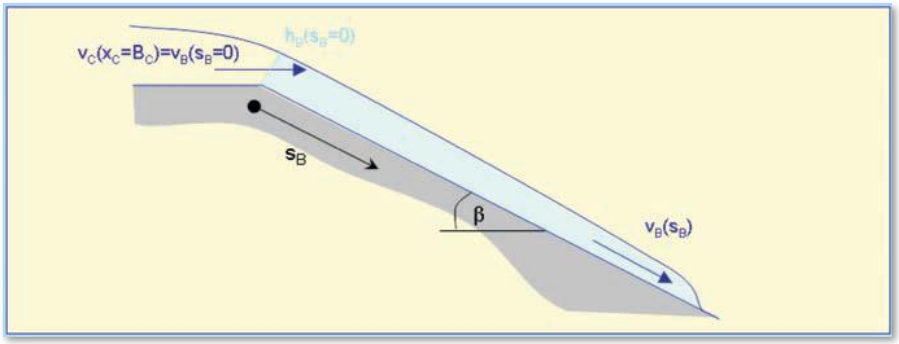

Figure 4.6. Definition of overtopping flow parameter on the landward slope. Source: Pullen et al (2007)

This results in the following formula for overtopping flow velocities:

$$v_b = \frac{v_{b,0} + \frac{k_1 h_b}{f}\tanh\left(\frac{k_1 t}{2}\right)}{1 + \frac{f v_{b,0}}{h_b 1}\tanh\left(\frac{k_1 t}{2}\right)}$$

With:

$$t \approx -\frac{v_{b,0}}{g\sin\beta} + \sqrt{\frac{v_b^2}{g^2\sin\beta^2} + \frac{2s_b}{g\sin\beta}} \quad \text{and} \quad k_1 = \sqrt{\frac{2f\sin\beta}{h_b}}$$

Equation mentioned here needs an iterative solution since the overtopping flow depth h_b and the overtopping flow velocity v_b on the landward slope are unknown. The overtopping flow depth h_b can be replaced in a first step by:

$$h_b = \frac{v_{b,0} \cdot v_{b,0}}{v_b}$$

With $v_{b,0}$ the overtopping flow velocity at the beginning of the landward slope($v_{b,0} = v_B(s_B = 0)$); and $h_{b,0}$ the overtopping flow depth at the beginning of the landward slope ($h_{b,0} = h_B$ ($s_B = 0$)).

The second important factor influencing the overtopping flow on the landward slope is the bottom friction coefficient f which has to be determined experimentally. The overtopping low on the landward slope tends towards an asymptote for $s_b \to \infty$ which is given by:

$$v_b = \sqrt{\frac{2ghsin(\beta)}{t}}$$

4.5.4 Spatial distribution of the overtopping water

Landward ground level

It can be expected that the spatial distribution of the overtopping water depends on the landward ground level, h_{meas}. The trajectory of overtopping volume is in a parabolic type, therefore, we can estimate that if the overtopping volume is dropped into

$$v = \sqrt{\frac{2(y+0)}{g}}m$$

at h_{meas}=0 m, then it will fall into

$$v = \sqrt{\frac{2(y+0.1)}{g}}m$$

at h_{meas}=0.1minstead. Fig 4.7 shows the effect of landward ground level on landward spatial distribution of overtopping water as a function of relative landward distance. The positive h_{means} stands for the ground level lower than the structure crest and negative hmeas represents the ground level higher than the structure crest. It is interesting to observe that for the same wave conditions and structural geometry the proportion of wave overtopping volume passing x increases with landward ground level, hmeas. The overtopping water even reaches to a distance up to three times bigger than significant wave height for hmeas=0.2 m, while it only splashes own in the area of half the significant wave height from structures for hmeas=−0.05 m. However, the computed proportion of wave overtopping water passing a landward location is smaller than predictions by $F(x,y) = \exp\left(\frac{-1.3}{H_{m0}}\left\{\max\left(\frac{x}{\cos\beta} - 2.7ys_{op}^{0.15}, o\right)\right\}\right)$ in EurOtop (2008), in accord with more overtopping water falling into the area just behind the structure. This is mainly due to a nappe (in hydro-engineering refers to the sheet of water over-topping) clinging to the landward face of the weir with very low water heads.

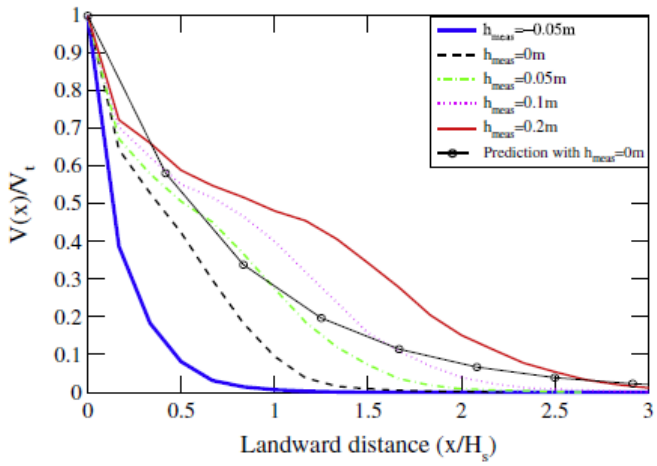

Figure 4.7. Effect of landward ground level, hmeas, on computed landward spatial distribution of overtopping water. Prediction is given by Eq. (6.17) in EurOtop (2008) with h_{meas}=0. The positive hmeas stands for the ground level lower than the structure crest. Hs=0.12 m, Tm=1.6 s, h=0.7 m, Rc=0.1 m, tan(α)=1:2 and B=0.3 m.

Source: Spatial distribution of wave overtopping water behind coastal structures Coastal Engineering, 58 (2011) 489-498. doi:10.1016/j.coastaleng.2011.01.010

Structure porosity

Structure porosity will affect spatial distribution of overtopping water through wave run-up and velocities on the crest as suggested by $x(y_c) = u_{A,50\%}\sqrt{\frac{2(y_c+h_{means})}{g}}$ $0 < y_c < h_A$, in which, $u_{A,50\%}$ =the horizontal velocity at the landward end of the crest (x=0m)

In this study, four types of coastal structures have been employed and shown in Figure 4.8, including a caisson breakwater with concrete protection; caisson breakwater with gravel protection (porosity=0.49); caisson breakwater with rubble protection (porosity=0.53) and rubble mound breakwater. The present model investigates the porous media in a similar way as Liu et al. (1999) by averaging the flow equations over a length scale. This length scale is larger than the characteristic pore size and is much smaller than the scale of the spatial variation of the physical variables in the flow domain. Therefore, the fluid variables can be decomposed into two parts, spatially averaged and spatially fluctuated quantities.

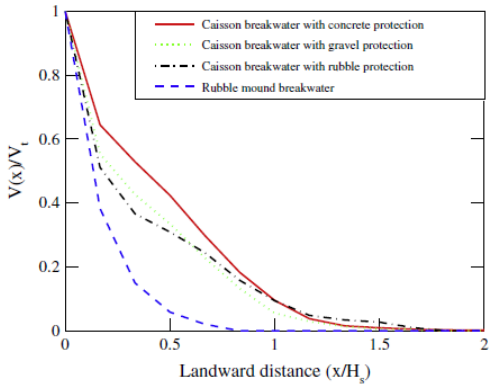

Fig. 11. Effect of structure porosity on landward spatial distribution of wave overtopping water. $H_s = 0.12$ m, $T_m = 1.6$ s, $h = 0.7$ m, $h_{meas} = 0$ m, $R_c = 0.1$ m and $B = 0.3$ m.

Figure 4.8. Effect of structure porosity on landward spatial distribution of wave overtopping water. Source: Spatial distribution of wave overtopping water behind coastal structuresCoastal Engineering, 58 (2011) 489-498. doi:10.1016/j.coastaleng.2011.01.010

Figure 4.8 shows the spatial distribution of wave overtopping water for various structure porosity at the ground level hmeas=0 m. With the same incident wave conditions (Hs=0.12 m, T_p=1.6 s) and the same geometry, the proportion of wave overtopping volume passing x decreases with structure porosity. This is because the employment of permeable protection leads to effective energy dissipation and reduces the overtopping discharge (Liu et al., 1999). In addition, large porosity, equivalent to large roughness or surface friction, leads to large dissipation and deductions of velocity and layer thickness on the structure crest. The proportion of wave overtopping volume passing a landward location for rubble mound breakwater is significantly smaller than that for caisson breakwater with rubble protection (Fig. 11). The structure crest is hydraulically rough for the former case but hydraulically smooth for the latter, although these two layouts have the same structure porosity. Therefore, rubble mound breakwater has smaller velocity of the overtopping water on the crest. As can be seen in $x(y_c) = u_{A,50\%}\sqrt{\frac{2(y_c+h_{means})}{g}}$, small velocity and layer thickness result in small travel distance of the overtopping water. This finding is consistent with the recommendation by EurOtop (2007) that roughness elements located above the still water level minus a quarter of wave run-up on a smooth slope, has a significant effect on the wave overtopping discharge.

Erosion of the inner slope

A tested inner slope of a dike, covered with grass on clay, never failed by erosion due to overtopping for a mean overtopping discharge of **30 l/s** per m or less. Only one section failed at 50 l/s per m; some at 75 l/s per m, but part of the sections did not fail, even not for 75 l/s per m.

It seems that the large erosion resistance of the inner slope of a dike is determined by the combination of grass and clay.

- The grass cover or mattress seems stronger (Boonweg, Figure 4.9) if it grows on a sandy clay. Such a grass cover may resist even up to 75 l/s per m, but if significant damage occurs, the clay layer is not very erosion resistant (Figures 4.10 and 4.11).



Figure 4.9 Source: Guidance on erosion resistance of inner slopes of dikes from three years of testing with the Wave Overtopping Simulator



Figure4.10 Source: Guidance on erosion resistance of inner slopes of dikes from three years of testing with the Wave Overtopping Simulator



Figure 4.11 Source: Guidance on erosion resistance of inner slopes of dikes from three years of testing with the Wave Overtopping Simulator

- On the other hand, good quality clay does not produce a very strong grass cover (it is difficult for roots to penetrate into the clay) and the grass may rip off for overtopping discharges around 30 l/s per m (Figures 4.12 and 4.13). But in that case the remaining good quality clay layer, still reinforced with some roots, has a large erosion resistance against overtopping waves (Figure 4.12).Van der Meer, Schrijver, Hardeman, Van Hoven, Verheij and Steendam 11



Figure 4.12 Afsluitdijk. Grass toe， Source:Guidance on erosion resistance of inner slopes of dikes from three years of testing with the Wave Overtopping Simulator



Figure 4.13 Afsluitdijk.Staircase with fence, before and after testing Source:Guidance on erosion resistance of inner slopes of dikes from three years of testing with the Wave Overtopping Simulator

- This leads to the conclusion that a good grass cover on sandy clay and a worse grass cover on good clay show different failure mechanisms, but they show more or less similar strength against wave overtopping. The variability of the grass sod may, therefore, have less influence on the total strength than previously anticipated.
- This could lead to the conclusion that the way of maintenance of the grass has only minor effect on the strength of the inner slope. The test at St Philipsland may show that the bad grass coverage (small open areas without grass) on sandy clay may show less resistance (Figure 4.14).



Figure 4.14 Final result St Philipsland, Zeeland. Source:Guidance on erosion resistance of inner slopes of dikes from three years of testing with the Wave Overtopping Simulator

Transitions from slope to horizontal are probably the most critical locations for initial and increasing damage.

- During the tests this was often the transition from the inner slope to the toe of the dike, with or without a maintenance road. The tests in 2009 were focused on these kinds of transitions. Damage was initiated by a mean discharge of 10 l/s per m or more. As the damage occurred at the lowest part of the inner slope it will take time for damage to extend to the crest level and subsequently cause a dike breach. Transition higher on the inner slope (cycle paths, stability or piping berms with or without maintenance road, tracks of tractors, roads crossing the dike), which have not yet been investigated, might be more critical. Further investigation may give more confirmative conclusions.
- A hole in the layer of clay, which reaches the under laying sand core and created at a large mean overtopping discharge of **50 l/s** per m or more, will give a very quick ongoing erosion. This has not been observed for smaller overtopping discharges, for the simple reason that these smaller discharges never created significant damage to the inner slope.
- But the test with the parking place of bricks (Figure 4.15) showed that sand erosion with **30 l/s** per m, and even with **10 l/s** per m, goes fairly quickly. It must be noted that although the test was stopped for 30 l/s per m due to fast ongoing damage to the parking area, the dike itself was not in danger at all.



Figure 4.19 Afsluitdijk. Parking area, section 2. Source: Guidance on erosion resistance of inner slopes of dikes from three years of testing with the Wave Overtopping Simulator

- **Small obstacles like poles did not show any erosion**. Small holes from mice and moles did not initiate damage to the grass cover layer. Also a fence (Figure 4.13) and a little bigger pole (0.15 m by 0.15 m) showed no initiation of erosion. The grass around a fence at the toe of the dike had some influence on initiation of erosion, probably due to larger forces in this area. An obstacle like a concrete staircase on the inner slope was totally destroyed at a stage with 75 l/s per m overtopping (Figures 4.13 and 4.20). It should be noted, however, that also here the dike itself was not in danger, due to the large erosion resistance of the clay. Still, further research may give more final conclusions on other large obstacles.



Figure 4.20 Afsluitdijk. Concrete staircase, section 3. Source: Guidance on erosion resistance of inner slopes of dikes from three years of testing with the Wave Overtopping Simulator

5 OVERTOPPING FLOW ENCOUNTERING OBSTACLES

When the flow overtops the dike crest, it flows through the inner slope toward the landside. This landward flow from overtopping is difficult to model due to the complexity of the flow pattern and paths. In addition, when this flow encountered an obstacle, different hydraulic response of the flow and amount of energy dissipation will happen This depends a lot on the flow condition such as the flow speed, approach angle and also on the geometry, surface roughness and porosity of the obstacle.

Currently, there is no literature providing a simple approximation on calculating the flow distribution from overtopping flow when it encounters an obstacle. However, there are many literatures providing equivalent information on the effect of flood wave encountering obstacles which are on a much larger scale e.g. in flood routing simulation. Using this information especially on the flow pattern when encountering obstacle, attempt can be made to carry up conservative approximation on the flow distribution. The amount of the overtopping flow that is (a) reflected by the obstacle and (b) diverted to the sides of the obstacle. In order to determine this flow distribution, how an obstacle affects the flow will first need to be understood.

5.1 Effect of Obstacle on Flow

Syme (2008) review on the methods to account for building's response to the flood wave for 2D modeling. Although his review of the obstacle is strictly on building, it provides an idea on how the type of the obstacle affects the flow so as to correctly account it in a 2D model. These methods are:

1. Increase roughness: increase bed resistance will result in increasing energy dissipation of water flowing through and around the obstacle e.g. buildings. This work well for 2D element with coarse resolution. However, the difficulty is to obtain the appropriate roughness value to represent the flow.
2. Blocking out of Element: This is done provided that the element size for the obstacle is sufficiently fine. However, most of the time, the obstacle is large and in certain case such as building will "adsorb" some of the water.
3. Using energy loss coefficient: Specify form loss coefficient to represent the fine-scale energy dissipation within and around the obstacle. Though it is theoretically more correct to account for the obstacle as energy is loss when the flow passes through or around the obstacle, it is difficult as there is also currently no literature to provide this type of information.
4. Modeling Buildings' Exterior wall: This method is good since it account for the possible deflection of the water and also storage effect for water through building. However, this method required some prior knowledge of the flow direction.
5. Modeling Buildings as "porous": 2D element sides of building are partially blocked to represent certain amount of blockage by external wall. TUFLOW software is used to model partial blockages.

Syme then carried out a numerical simulation using TUFLOW to show the effect on the building response to flow when different methods were applied. Figure 5.1 shows the hypothetical building model layout. Table 5.1 presents a comparison between different building test scenarios. Figure 5.2 presents a comparison between different water surface profiles along the model centreline.

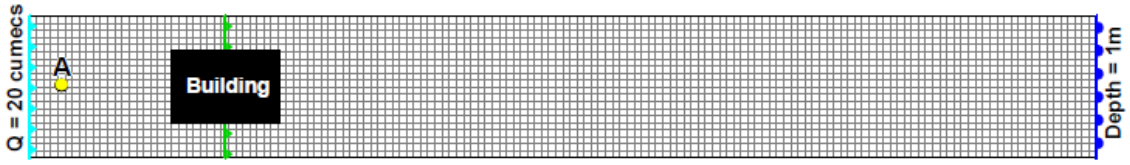

Figure 5.1: Hypothetical Building Model Layout. Source: Syme (2008)

Table 5.1. Comparison of building test scenarios

Scenario	Water Level (m)		Flow Distribution (%)		Average Velocity (m/s)	
	Point A	Increase	Building	Garden	Building	Garden
No Building	1.118	0.000	50%	50%	0.91	0.91
Blocked Out	1.255	0.137	0%	100%	n/a	1.90
High Roughness	1.240	0.122	21%	79%	0.38	1.41
Add Form Loss	1.195	0.077	31%	69%	0.55	1.23
Ext Walls, Open D/S	1.250	0.132	0%	100%	0.00	1.92
Ext Walls, Open U/S	1.263	0.145	0%	100%	0.00	1.93
Porous	1.170	0.052	9%	91%	1.87	1.80
Porous + Form Loss	1.225	0.107	7%	93%	1.28	1.78

Source: Syme (2008)

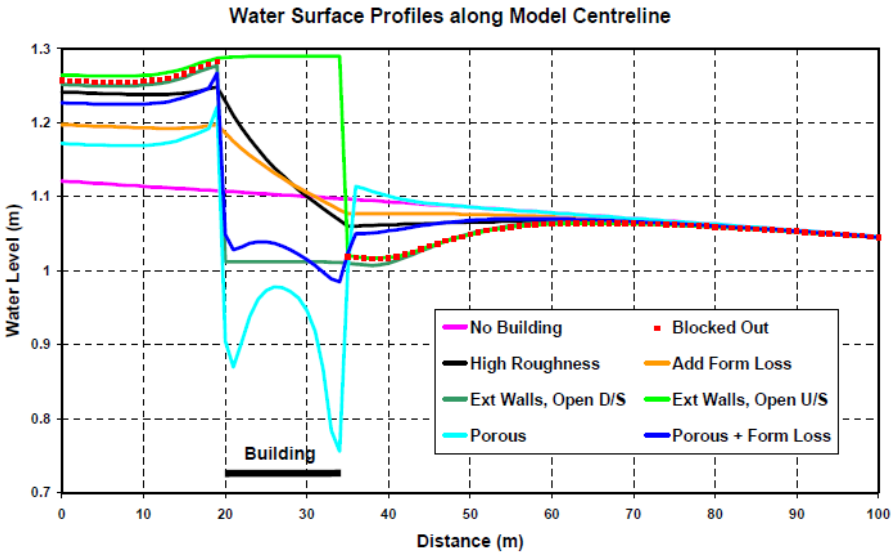

Figure 5.2. Comparison of Water Level Profiles along Model Centerline. Source: Syme (2008)

Figure 5.1 shows the hypothetical building model layout with the results shown on Table 5.1 and Figure 5.2 from the by Syme (Syme 2008). The change in the water level can be seems as it (a) reaches, (b) through and (c) over the obstacle. When the flow reaches that the obstacle, there is a slight increase in the water level. Depending on the type of obstacle, the water level decreases significantly when the flow passes through the obstacle. After passing the obstacle, the reduced water level continues to reduce gradually as it travels further landward.

Referring to study by Michal Szydlowski [Szydlowski (2011)] on his numerical simulation and laboratory experiment on open channel flow between bridge priers, we can have addition insight on the effect of geometry of obstacle to flow.

Figure 5.3 shows that the water depth increases (i.e. hydraulic jump) in front of pier (obstacle) and sudden lowering directly after passing the pier. Local flow circulation just behind pier can also be seemed. Even for an obstacle that has a smooth rounded surface such as a pier, the resulting surface wave merged after encountering the obstacle has a complex structure with turbulence eddies, diffraction and interference due to the abrupt swelling and depression of the water level shown in Figure 5.4.

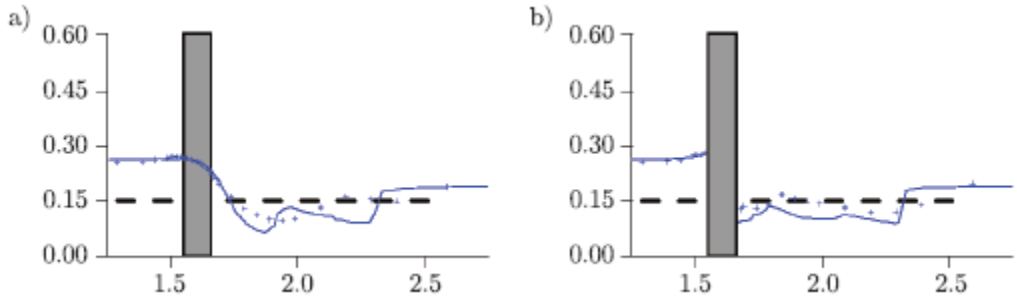

Figure 5.3. Measured (+ + +) and calculated (——) water surface profile for the second experiment together with the critical depth line (– –): a) along the channel axis, b) along the pier axis (dimensions in metres). Source: Szydlowski (2011)

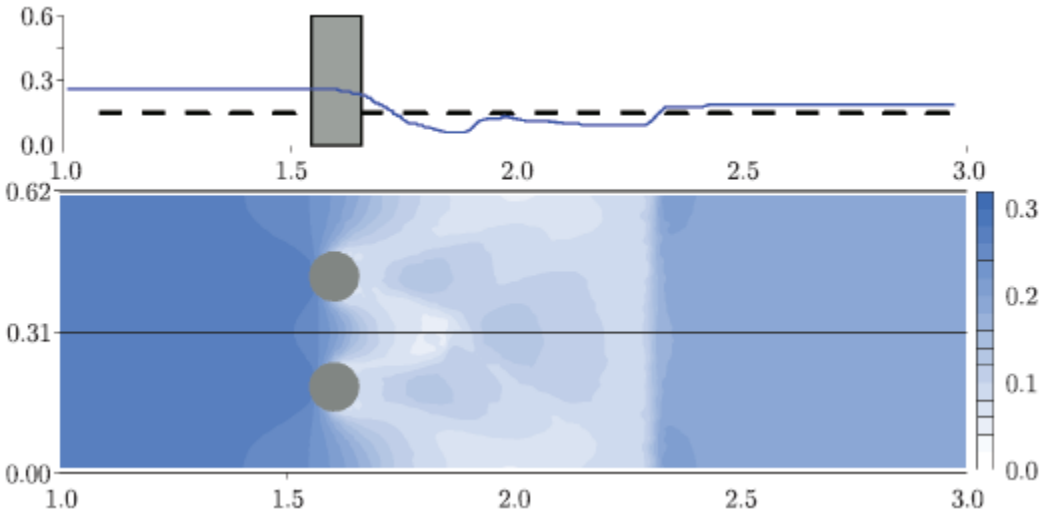

Figure 5.4. Surface profile and horizontal distribution of the computed water depth (dimensions in metres). Source: Szydlowski (2011)

Figure 5.5 and 5.6 shows the spatial distribution of the velocity and Froude number, provide additional information on the velocity flow and flow condition.

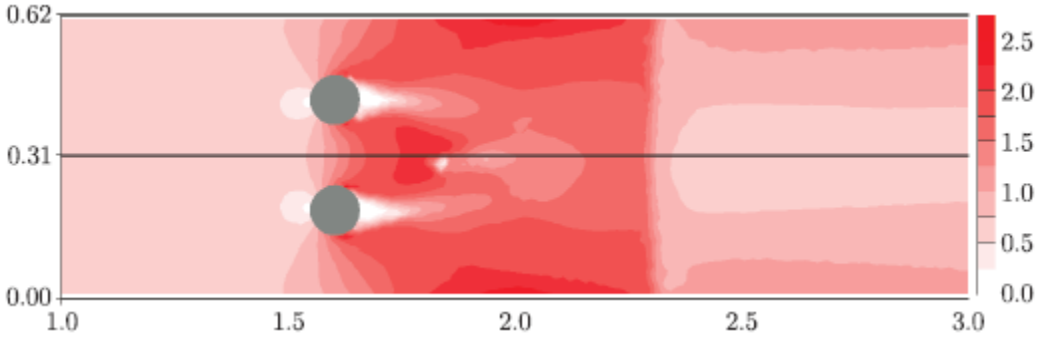

Figure 5.5. Distribution of flow velocity (m/s) (dimensions in metres). Source: Szydlowski (2011)

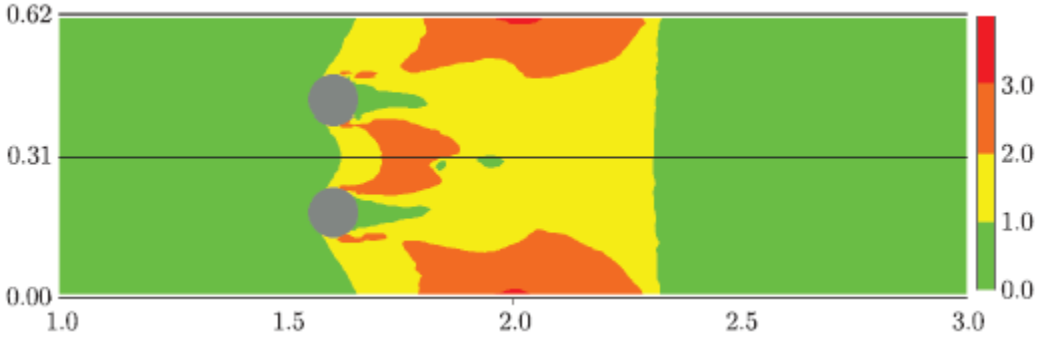

Figure 5.6: Spatial distribution of the Froude number (dimensions in metres). Source: Szydlowski (2011)

Hence, these methods, conclude that the surface roughness, geometry and porosity of the obstacle will affect the amount of energy dissipation by the flow and the flow movement.

5.2 Effect of Flow when encountering obstacle

Knowing that the different types of obstacles will affect the hydraulic response of the flow, the hydraulic response of the flow such as its flow pattern when encountering an obstacle will now be look into. In the paper by Hyung (Kim, Lee et al. 2012), the laboratory experiment was performed to study the variation in flood intensity due to structure. Numerical model was then used to verify the measured water depth from the laboratory experiment.

Figure 5.7 shows that laboratory setup of the experiment in plan and side view. The different placement of the block/s to simulate obstacle for flow shown on Figure 5.8. The experiment conditions for the flood wave propagation on Table 5.2. The location of the observation pointswith wave height gauges on the inundation area shown on Figure 5.9.

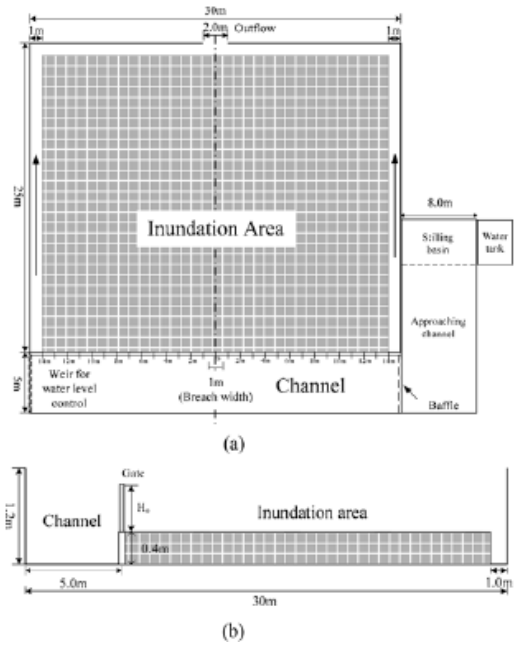

Figure 5.7: Schematic of the Flood Wave Experimental Channel: (a) Plan View, (b) Side View. Source: Kim et al (2012)

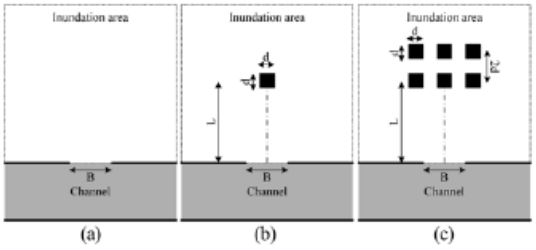

Figure 5.8: Schematic of Structure Layouts for Experiments: (a) Case1: None-structure, (b) Case 2: Single Structure, (c) Case 3: Group Structure. Source: Kim et al (2012)

Breach width B (m)	Overflow depth H0 (m)	Initial flow velocity (m/s)	Structure layout
1.0	0.55	2.3	None Single Group
	0.50	2.2	
	0.45	2.1	
	0.40	2.0	
	0.35	1.9	

Table 5.2: Experimental Conditions for Flood Wave Propagation. Source: Kim et al (2012)

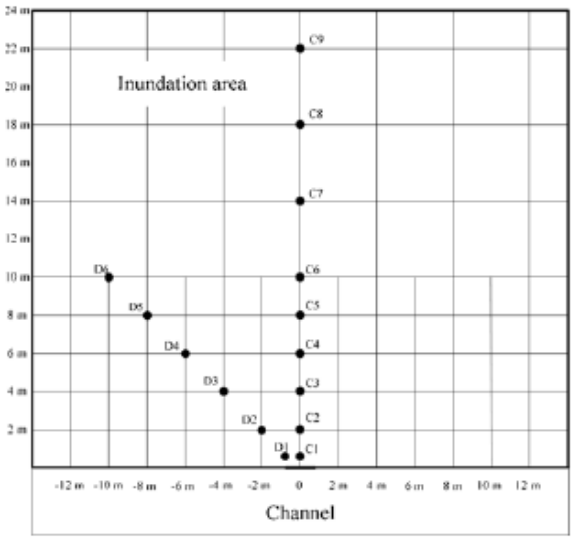

Figure 5.9: Experimental Observation Points with Wave Height Gauges. Source: Kim et al (2012)

The wave height measured in the (a) normal and (b) diagonal direction for the three cases were shown on Figure 5.10, 5.11 and 5.12, respectively.

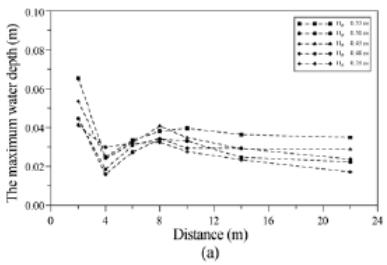

Figure 5.10: Observed Maximum Water Depth in Case 1: (a) Normal Direction, (b) Diagonal Direction. Kim et al (2012)

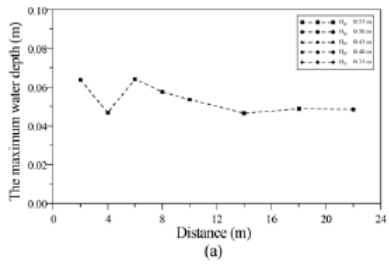

Figure 5.11: Observed Maximum Water Depth in Case 2: (a) Normal Direction, (b) Diagonal Direction. Kim et al (2012)

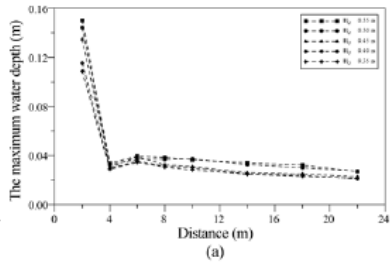

Figure 5.12: Observed Maximum Water Depth in Case 3: (a) Normal Direction, (b) Diagonal Direction. Kim et al (2012)

From these Figure, Hyung obtained the following observations:

1. When the water was released by overflow from the channel to the inundation area, its water depth was at maximum at x = 2m. This maximum water depth increase with the increase of the overflow height.
2. This maximum water depth decreases rapidly, as the flood wave velocity increase rapidly until x = 4 m.
3. After distance x = 4 m, maximum water depth increase as bottom rough cause velocity to decrease slightly.
4. If there is a obstacle, there will be water depth increase between the structure and the source of the flood wave. The water depth increase will be more for Case 3 than Case 2.
5. For flow encountering obstacle in Case 2 and 3, there were also water height increase for observation in the diagonal direction than the normal direction. This means that some of the flow instead of being reflected by the obstacle have been diverted to the sides of the obstacle.
6. Water depth is also slightly greater immediately behind the structure due to the superpositioning of the flood wave.
7. After x = 8 m, for all cases, the maximium water depth decrease as distance increase.

Figure 5.8 showns the maximum flood intensity distribution generated by the numerical model which the water depth has been verified by the experiment results.

As there are many ways of determining flood intensity, the Swiss method (OFEE et al., 1977) was adopted by the Hyung . The Swiss method defined flood intensity in term of the maximum water depth generated throughout the event and the product of the maximum velocity multiplied by the maximum depth. The flood intensity produced a quantity similar flow rate per unit wide when we consider the amount of overtopping rate.

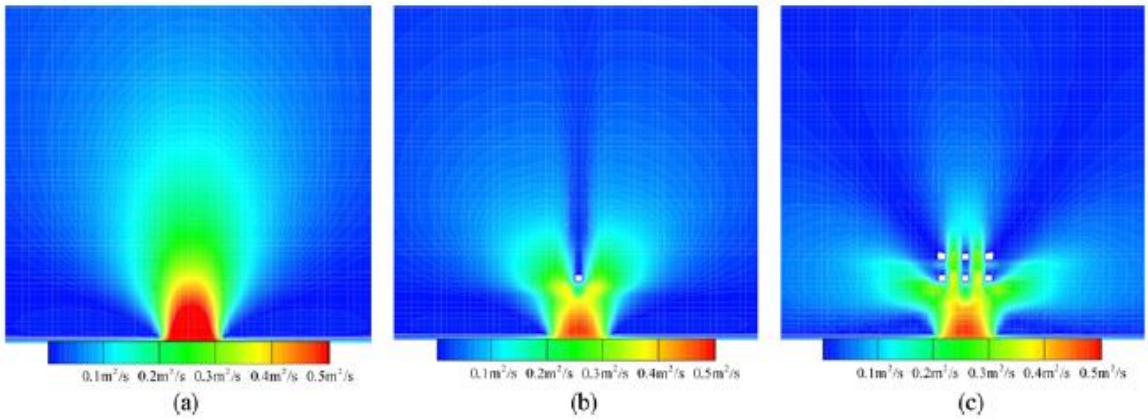

Figure 5.13: Maximum Flood Intensity Distributions: (a) None-structure, (b) Single Structure, (c) Group Structures. Source: OFFE et al (1977)

The numerical result shown was in line with the observations made from the laboratory results and it provide a more hoslistic and overview on the intensity of the flow when encountering obstacle/s. Figure 13 shows that the flood intensity was maximum when it was initially released from the opening. Without an obstacle in Figure 13(a), the flood wave will propagate, spread and reduce in its intensity as it traveled furtehr away from the source. In Figure 13(b) and 13(c), when encountering an obstacle, the flood intensity changes at the front and sides regions of the obstacle. Funneling effect also causes the increase of flood intensity at the gaps between the structures.

In addition, to analyze changes in flood intensity due to obstruction, the ratios of the maximum flood intensity increase are calculated by taking dividing the calculated flood intensity for Case 2 and 3 to that of Case 1.

Figure 5.14 shows that there is a significant increase in flood intensity in the diagonal direction. It shows that as the water depth increase, the obstacle divert more of the the wave propagation to the diagonal direction. Thus, the flood intensity behind the obstacle decreases more.

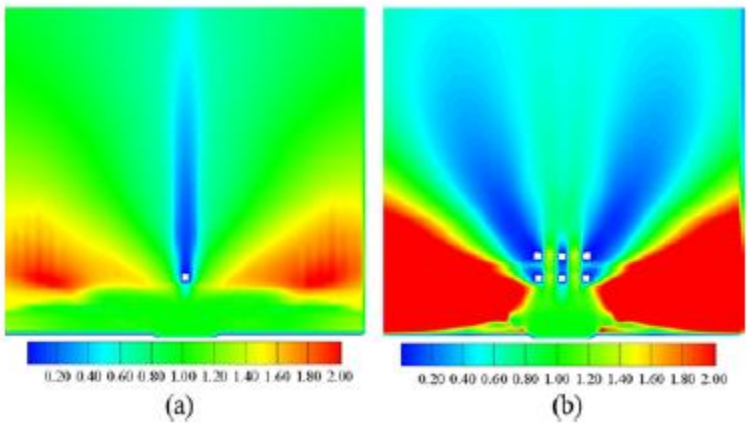

Figure 5.14: Increase Ratio of Maximum Flood Intensity: (a) Single Structure, (b) Group Structures. Source: OFFE et al (1977)

Hence, through the laboratory experiment and numerical model by Hyung (Kim, Lee et al. 2012), a better idea on the effect on flow when it encountered obstacle can be obtained.

A similar type of laboratory experiment was also done by Guido Testa (Testa, Zuccalà et al. 2007), the experimental results on the behavior of the flow when encountering obstacle/s were similar to that done by Hyung (Kim, Lee et al. 2012) as described earlier. Guido's experiment result provided an added dimension to the understanding on flow encountering obstacle.

Guido described that that the flow pattern as almost standing with a strong hydraulic jump occurred when the flow encountered the obstacle's front. This hydraulic jump propagates very slowly in the upstream direction until its intensity diminishes with time according to the inflow discharge. He added that the intensity of this hydraulic jump does not depend on any obstacles behind it. Thus the shock from the impact is equally strong whether there is any other obstacle behind it or not. This can be seen also from the results by Hyung.

Guido also mentioned that for a block layout similar to Case 3, if the spacing of the blocks is very close, this can make the obstacles to appear as a compact obstacle to the main flow.

6 REFERENCES

- CIRIA, CUR, CETMEF (2007), 'The Rock Manual. The Use of Rock in Hydraulic Engineering' . 2nd edition, C683, CIRIA, London.
- Eijgenraam, C., Brekelmans, R., den Hertog, D., Roos, K. (2010), 'Safe Dike Heights at Minimal costs: The Homogeneous Case'. Submitted to Management Science. Available on http://www.tilburguniversity.edu/research/institutes-and-research-groups/center/ graduate-school/chp/opmaast/dike1.pdf
- Inspectie Verkeer en Waterstaat (2006), 'Assessment of Primary Flood Defences in The Netherlands, National Report on 2006'. Available on http://www.safecoast.nl/editor/databank/File/Assessment%20primary%20flood%20defences%20in%20NL.pdf
- Jonkman, S., Jongejan, R., Maaskant, B., Vrijling, H. (2010), 'New Safety Standards for Coastal Flood Defences in The Netherlands'. 32nd International Conference on Coastal Engineering, ICCE 2010, June 30 – July 5 2010, Shanghai, China.
- Kim, H., Lee, J. et al (2012). 'Numerical Analysis of Flood Risk Change Due to Obstruction'. KSCE Journal of Civil Engineering 16 (2). 207-214.
- OFFE, OFAT and OFEFP (1997), 'Prise en compte des dangers dus aux dans le cadre des activities del'amenagement du territoire'. Bienne, 1997, Office Federal de l'Economie des Aux (OFFE), Office Federal de l'Amenagement du Territoire (OFAT), Office Federal de l'Environnent, Desforets, et du Paysage (OFEFP).
- Pullen, T., Allsop, N. W. H., Bruce, T., Kortenhaus, A., Schüttrumpf, H., Van der Meer, J. W. (2007), 'EurOtop – Wave Overtopping of Sea Defences and Related Structures: Assessment Manual'. Environment Agency, UK, Expertise Netwerk Waterkeren, NL and Kuratorium für Forshung im Küsteningenieurwessen, DE.
- Roos, A., Riedstra, D. (2010), 'Safety Standards in The Netherlands'. Rijkswaterstaat Centre for Water Management. Presentation of March 17th, 2010.
- Syme, W. (2008), 'Flooding in Urban Areas – 2D Modelling Approaches for Buildings and Fences'. 9th National Conference on Hydraulics in Water Engineering. Engineers Australia. Darwin Convention Centre, Australia.
- Szydlowski, M. (2011), 'Numerical Simulation of Open Channel Flow Between Bridge Piers'. TASK Quarterly 15 (3-4). 271-282.
- Testa, G., Zuccala, D. et al (2007), 'Flash Flood Flow Experiment in a Simplified Urban District'. Journal of Hydraulic Research 45 (supl. 1). 37-44.
- Lin, P.Z., Liu, P.L.F., 1999. Internal wave-maker for Navier-Stokes equations models. Journal of Waterway Port Coastal and Ocean Engineering 125 (4), 207‐215.
- Guidance on erosion resistance of inner slopes of dikes from three years of testing with the Wave Overtopping Simulator, Van der Meer, Schrijver, Hardeman, Van Hoven, Verheij and SteendamW. Allsop, MICE, T. Bruce, J. Pearson BEng and P. Besley 'Wave overtopping at vertical and steep seawalls'. Maritime Engineering 158 September 2005 Issue MA3,103–114
- Dr J.W. van der Meer (2002), 'Technical Report Wave Run-up and Wave Overtopping at Dikes', Technical Advisory Committee on Flood Defence

TU DELFT – MULTIDISCIPLINARY PROJECT CIE4061

Afsluitdijk Project
"The Monument" Location

Literature Review

Sien Liu, Jun Huang, Sebastian Rayo, Tai Yan Lim

21/12/2012



CONTENTS

1 Introduction 2
1.1 Background 2
1.2 Problem Description 2
1.3 Document Scope 2
2 Interaction Between Waves and Structures 3
2.1 Definitions 3
2.2 Types of Overtopping 3
3 Safety Standards 5
3.1 Hazards 5
3.2 Existing Criteria 5
3.2.1 Return Period 5
3.2.2 Tolerable Discharges 7
3.2.3 Overtopping Velocities 8
4 Overtopping Modelling 9
4.1 Description 9
4.2 Factors of Influence 9
4.2.1 Various slopes ($\tan\alpha$) 9
4.2.2 Shallow foreshore (h_m/H_{m0}) and breaking parameter (ξ_0) 9
4.2.3 Incident wave angle (γ_β) 10
4.2.4 Berms (γb) 10
4.2.5 Roughness of elements (γf) 12
4.2.6 Vertical wall on slope (γv) 12
4.2.7 Slope with composite roughness elements (γf) 12
4.3 Mean overtopping discharge 13
4.4 Maximum over topping volume 13
4.5 Overtopping flow velocity and flow depth 13
4.5.1 On seaward slope 14
4.5.2 On crest of dike 15
4.5.3 On the landward slope 16
4.5.4 Spatial distribution of the overtopping water 17
5 Overtopping Flow Encountering Obstacles 24
5.1 Effect of Obstacle on Flow 24
5.2 Effect of Flow when encountering obstacle 27
6 References 32

1 INTRODUCTION

1.1 Background

The Afsluitdijk (Enclosure Dam) is a main dam that forms the fundamental part of the larger Zuiderzee Works that separates the Zuiderzee, a salt water inlet of the North Sea, and turning it into the fresh water lake of the IJsselmeer. It protects the central Netherlands from the effects of the North Sea. It was constructed between 1927 and 1933, and runs from Den Oever on Wieringen to the village of Zurich in Friesland. It is 32 km long and 90 meters wide, rising to 7.25 meters above sea-level, with an incline of 25% on each side.

At the location along the Afsluitdijk where the final water passage was closed ('De Vlieter'), a lookout tower known as 'The Monument' was built in 1933. It was presented by the Zuiderzee Works Construction Company and designed by architect W.M. Dudok. The site has a statue of a "Steenzetter", and also marks the inscription 'A living nation builds for its future'. A statue of Cornelis Lely has also been erected near Den Oever on the Barrier Dam itself.

The Afsluitdijk with The Monument are currently managed by the Ministry of Infrastructure and the Environment ("The client"). There is a restaurant at The Monument where the client has sublet it for private operator to manage it.

1.2 Problem Description

With the anticipation of increase storm intensity and sea level rise in the future, the client had previously engaged a consultant to analyze the existing design of Afsluitdijk for a design storm of 1:10,000 years. According to the client, the result of the study concluded that the standard cross-section of Afsluitdijk is not sufficient to withstand the design storm of 1:10,000 years, hence, modifications of it are required. The study also found that during the design storm, there is a significant overtopping over the dike.

The client is concerned about the significant overtopping found from the previous study may have adverse impact on the non-standard cross-section of the dike where The Monument is located. Therefore, the client has requested our design team to look into the dike section at the Monument location.

1.3 Document Scope

The main objectives of this document are:

1. To introduce the typical processes related to the interaction between waves and a hydraulic structure.
2. To establish the state-of-art of safety standards of dikes in the Netherlands.
3. To establish a methodology to model wave overtopping and its characteristics discharge, height and velocity) on top and the rear slope of a dike.
4. To look for research related with 2D distribution of un-steady flow when there are some obstacles in front of it.

2 INTERACTION BETWEEN WAVES AND STRUCTURES

2.1 Definitions

CIRIA et al (2007) defines that the interaction between waves and hydraulic structures (such as dikes) can be classified into: wave run-up (and run down), wave overtopping, wave transmission and wave reflection.

Definitions for each interaction process are:

- Wave conditions are defined by incident wave height (usually significant wave height), the wave period, the angle of incidence and the local depth.
- Wave run-up and run-down are defined as the extreme levels that a wave can reach on a sloping structure.
- Wave overtopping occurs when wave run-up exceeds the crest level.
- Wave transmission occurs when a structure has a permeable core, which permits the transmission of part of the wave energy through the structure.
- Wave reflection is when part of the wave energy returns towards the sea because of the influence of a hydraulic structure.

Figure 2.1 presents schemes of different type of interaction between waves and a dike.

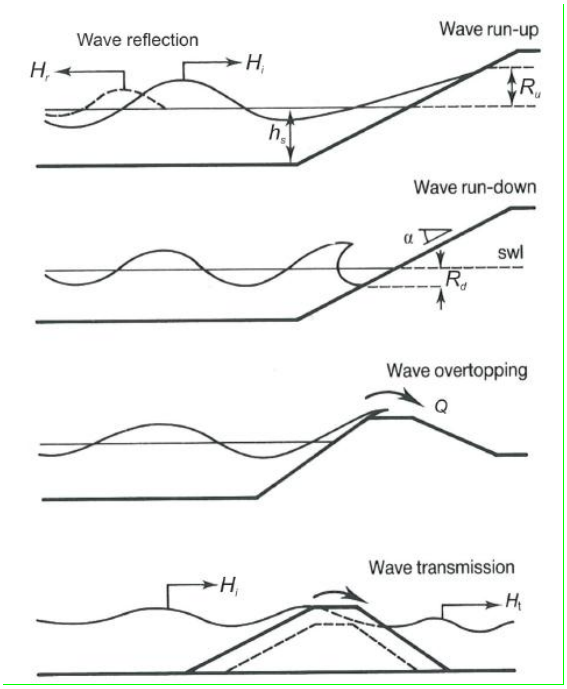

Figure 2.1. Different type of interaction between waves and a dike. Source: CIRIA et al (2007)

2.2 Types of Overtopping

According to Pullen et al (2007), two different types of overtopping are distinguished:

- ‘Green water’, which is related with complete sheets of water that run over the crest of a defence;
- ‘White water’, which is related with waves that break at the seaside, generating an important amount of spray and a non-continuous overtopping flow.

Spray generated by wind can generate some hazards for people and vehicles near the dike, due to lack of visibility. Nevertheless, it is not considered as an overtopping flow like the previous definitions.

3 SAFETY STANDARDS

3.1 Hazards

According to Pullen et al (2007), overtopping effects and its related consequences can be classified within four different categories:

a) *Direct hazard of injury or death to people immediately behind the defence;*
b) *Damage to property, operation and/or infrastructure in the area defended, including loss of economic, environmental or other resource, or disruption to an economic activity or process;*
c) *Damage to defence structure(s), either short-term or longer-term, with the possibility of breaching and flooding;*
d) *Low depth flooding (inconvenient but no dangerous).*

According to Pullen et al (2007), the main responses to these hazards are three:

a) *Move human activities away from the area subject to overtopping and/or flooding hazard, thus modifying the land use category and/or habitat status;*
b) *Accept hazard at a given probability (acceptable risk) by providing for temporary use and/or short-term evacuation with reliable forecast, warning and evacuation systems, and/or use of temporary/demountable defence systems;*
c) *Increase defence standard to reduce risk to (permanently) acceptable levels probably by enhancing the defence and/or reducing loadings.*

3.2 Existing Criteria

3.2.1 Return Period

The return period for which a defence is designed is usually determined in accordance with local and national guidelines, as well as is related with local circumstances, a balance between risk and benefits and the level of overall exposure. Table 3.1 presents some typical values of design life and levels of protection.

Table 3.1. Hazard type

Hazard type and reason	Design life *(years)*	Level of protection *(years)*
Temporary or short term measures	1 – 20	5 – 50
Majority of coast protection or sea defence walls	30 – 70	50 – 100
Flood defences protecting large areas at risk	50 – 100	100 – 10,000
Special structure, high capital cost	200	Up to 10,000
Nuclear power stations, etc.	-	10,000

Source: Pullen et al (2007)

According to Pullen et al (2007), the design life in Netherlands for flood defences is 50 years. However, for special structures with high capital cost, the design life can be extended to 200 years.

Roos and Riesdstra (2010) give more detailed information. In the Netherlands, every ring has a specific safety standard. West and North Netherlands have safety standards of 1:10,000 and 1:4,000, respectively. Figure 3.1 shows details of safety standard definition in the Netherlands.

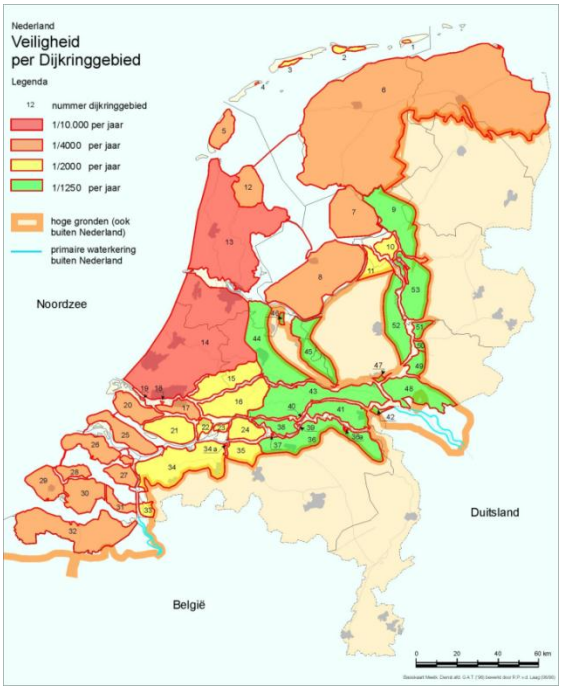

Figure 3.1. Details of safety standards definition in the Netherlands. Source: Roos and Riedstra (2010)

Nevertheless, because of climate change, a discussion started in 2006 with respect to the definition of safety standards, which will be updated in 2017. Figure 2.3 shows a map of the Netherlands with detailed information about safety standard achievement for several locations. Particularly, the Aflsluitdijk does not comply with the standard.



Figure 2.2. Results second safety assessment primary flood defences, 1 January 2006. Source: Inspectie Verkeer en Waterstaat (2006)

Jonkman et al (2010) mention that in the Netherlands, current safety standards are based on cost – benefits analysis, but they do not incorporate casualties in a proper way. Hence, they propose that a research on risk definition should be made, considering both individual (probability of death of a person in one year) and societal risks (probability of occurrence of an event with several fatalities).

Eijgenraam et al (2010) propose a numerical method to determine optimal dike heights, considering a risk analysis definition. They conclude that in the Netherlands there is a need to increase safety standards, which will increase expenses of the Dutch government for the protection against flooding item.

3.2.2 Tolerable Discharges

Information available in Pullen et al (2007) gives several limits of overtopping (flow discharges and volumes) for pedestrians, vehicles and properties behind the defence. Tables 3.2 to 3.4 present that information.

Table 3.2. Limits for overtopping for pedestrians

Hazard type and reason	Mean discharge	Max volume
	q (l/s/m)	*V_{max} (l/m)*
Trained staff, well shod and protected, expecting to get wet, overtopping flows at lower levels only, no falling jet, low danger of fall from walkway.	1 – 10	500 at low level
Aware pedestrian, clear view of the sea, not easily upset or frightened, able to tolerate getting wet, wider walkway.	0.1	20 – 50 at high level or velocity

Source: Pullen et al (2007)

Table 3.3. Limits for overtopping for vehicles

Hazard type and reason	Mean discharge	Max volume
	q (l/s/m)	*V_{max} (l/m)*
Driving at low speed, overtopping by pulsating flows at low flow depths, no falling jets, vehicle not immersed.	10 – 50	100 – 1,000
Driving at moderate or high speed, impulsive overtopping giving falling or high velocity jets.	0.01 – 0.05	5 – 50 at high level or velocity

Source: Pullen et al (2007)

Table 3.4. Limits for overtopping for property behind the defence

Hazard type and reason	Mean discharge	Max volume
	q (l/s/m)	*V_{max} (l/m)*
Significant damage or sinking of larger yachts	50	5,000 – 50,000
Sinking small boats set 5 – 10 m from wall. Damage to larger yachts.	10	1,000 – 10,000
Building structure elements	1	-
Damage to equipment set back 5 – 10 m	0.4	

Source: Pullen et al (2007

Information available in Pullen et al (2007) indicates that the work realized by Goda and other researchers gave some guidelines of setting limits for the defence structures. That information is summarized in Table 3.5.

Table 3.5. Limits for overtopping for damage to the defence crest or rear slope

Hazard type and reason	Mean discharge *q (l/s/m)*
Embankment seawalls / sea dikes	
No damage if crest and rear slope are well protected	50 – 200
No damage to crest and rear face of grass covered embankment of clay	1 – 10
No damage to crest and rear face of embankment if not protected	0.1
Promenade or revetment seawalls	
Damage to paved or armoured promenade behind seawall	200
Damage to grassed or lightly protected promenade or reclamation cover	50

Source: Pullen et al (2007)

Further research was done in Netherlands during year 2007. Wave overtopping tests were developed on existing dikes (both made of clay and covered with grass). Results indicated that the resistance of these dikes is higher than the values defined by Goda. Particularly, the resistance of a dike covered with grass was good enough for overtopping rates up to 50 l/s/m.

3.2.3 Overtopping Velocities

Information available in Pullen et al (2007) indicates that maximum velocities of 5 – 8 m/s can occur for overtopping discharges in the range 10 – 30 l/s/m.

4 OVERTOPPING MODELLING

4.1 Description

The dikes in Netherlands normally consist of a toe structure, a gentle slope with a berm, a crest of a certain width, outer and inner crest lines and inner slope. For some special dikes, transport infrastructure like bicycle lanes and highways may lie behind the inner slope. The configurations of dikes described above all have influence on the wave overtopping. It can also be affected by the reference water levels, strong sea winds and climate change.

4.2 Factors of Influence

The profiles of dikes are quite different from each other, as well as the wave conditions in different cases. In order to consider all these effects on wave overtopping, several parameters will be introduced to make better predictions of wave overtopping.

4.2.1 Various slopes (tanα)

In reality a dike slope in normally consists of several sections with different slope angles. Considering that the wave overtopping requires a characteristic slope in the breaker parameter, the definition of average slope is applied here to replace various slope sections. The representative slope is iteratively calculated as the average slope between still water line $-1.5 \cdot H_{m0}$ and still water line $+z_{2\%}$. (any berm present is not include for calculation of average slope).

4.2.2 Shallow foreshore (h_m/H_{m0}) and breaking parameter (ξ_0)

The waves will break due to limit water depth when they approach to a shallow foreshore, which will consequently decrease the wave overtopping discharge. In addition, the wave height distribution will also be changed due to this effect. In relatively deep water ($h_m/H_{m0} > 3\ to\ 4$), wave heights follow as Rayleigh distribution. In shallow foreshore ($h_m/H_{m0} < 3\ to\ 4$), the wave height distribution will deviate from Rayleigh distribution due to breaking effects of higher waves. This shallow foreshore effect is very important and it is necessary coming up with two equations to calculate the wave overtopping under these two different conditions. The criteria of distinguishing these two conditions are based on the breaker parameter ξ_0, which is given by:

$$\xi_0 = \frac{tan\alpha}{\sqrt{s_0}}$$

Where:

ξ_0 – breaker parameter [-].
α – angle of slope [°].
s_0 – wave steepness [-]

$$s_0 = 2\pi \cdot H_{m0}/(g \cdot T_{m-1,0}^2)$$

Where:

$T_{m-1,0}$ – spectral wave period=m_{-1}/m_0 [s].
m_0 – zero moment of spectrum [m^2].
m_{-1} – first negative moment of spectrum [m^2].

4.2.3 Incident wave angle (γ_β)

The incident wave angle is defined as the angle between propagation direction of waves and the perpendicular direction to long axis of the dike. In real site situation, the incident waves come from various directions and each of them has individual contribution of wave overtopping. In calculation of deterministic approach, it's impossible to do calculation for each wave, so the consideration of evaluating contributions of different incident wave angles is necessary.

Influence factor for this effect is given by γ_β (β indicates incident wave angle, $\beta = 0$ means perpendicular wave attack). The influence factor γ_β is plotted against the angel of wave attack, β (Technical Report Wave Run-up and Wave Overtopping at Dikes, Technical Advisory Committee on Flood Defence) (Dr J.W Van De Meer, 2002). For wave overtopping, the influence factor decrease linearly from 1 to 0.7 when β increase from 0 to 80. It keeps at 0.7 when β is between 80 and 90. Figure 4.1 presents the relation between the influence factor γ_β and the angle of attack β.

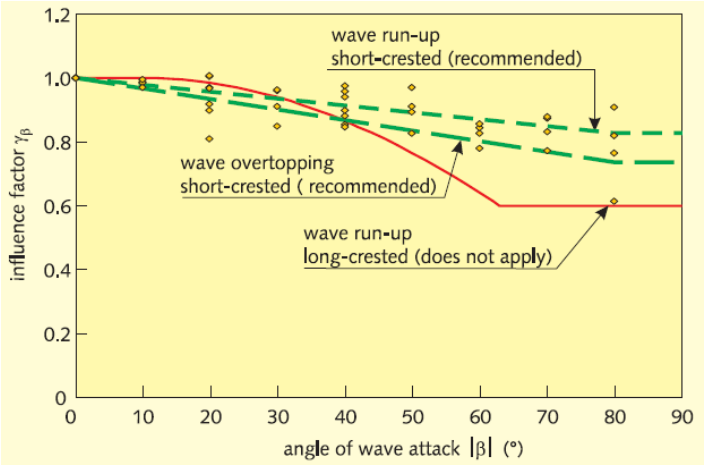

Figure 4.1. Relation between influence factor and angle of wave attack. Source: T. Pullen (2007)

It can be described as following formulae for wave overtopping:

$$\gamma_\beta = 1 - 0.0033|\beta| \quad (0° < |\beta| < 80°)$$

$$\gamma_\beta = 1 - 0.0033 \cdot 80° \quad (|\beta| > 80°)$$

4.2.4 Berms (γ_b)

A berm is defined as part of the dike profile in which the slope varies between horizontal and 1:15. Both the width and the depth of berm are given in Figure 4.2.

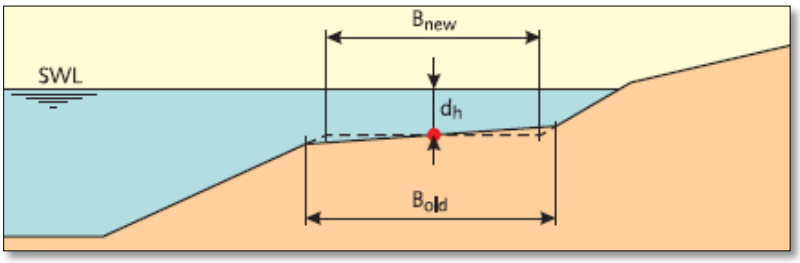

Figure 4.2. Scheme with berm definition. Source:(T. Pullen, 2007)

Normally, it is required that the slope should be gentler than 1:15 and the width should be less than one quarter of the wavelength. If the berm doesn't satisfy with the requirement, then the wave overtopping must be determined by interpolation between the steepest berm (1:15) and a gentle slope (1:8). For calculations of wave overtopping, the inclined berm is drawn to a horizontal berm which is shown in figure as B_{new}. The berm depth is shown as d_h. The influence of berm can be considered as two parts: one is influence of the width of berm,r_B, and one is berm depth,r_{dh}.

For estimation of influence of berm, the following equation is applied:

$$\gamma_b = 1 - r_B \cdot (1 - r_{dh})$$

Where $0.6 \leq \gamma_b \leq 1.0$, $r_{dh} = 0$ relates to condition of $d_h = 0$ and $0 \leq r_B \leq 1$

Based on the information of Pullen et al (2007), the influence of berm width can be calculated by the equation as follows:

$$r_B = 1 - \frac{2 \cdot H_{m0}/L_{berm}}{2 \cdot H_{m0}/(L_{berm} - B)} = \frac{B}{L_{berm}}$$

The corresponding parameters are drawn in Figure 4.3.

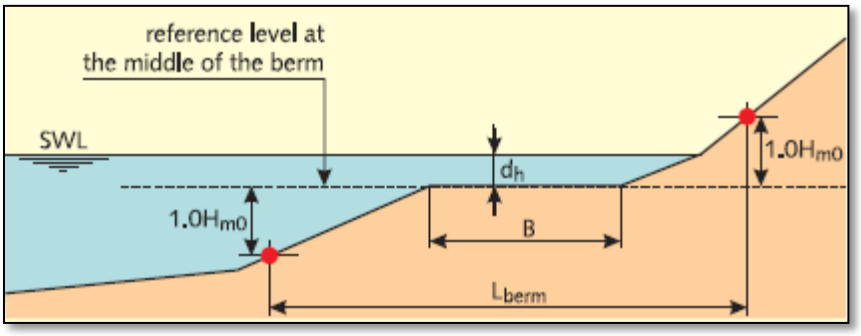

Figure 4.3. Parameters required to define berm influence. Source: T. Pullen (2007)

Also the influence of berm depth can be evaluated by the following formula:

$$r_{dh} = 0.5 - 0.5 \cdot \cos\left(\pi \frac{d_h}{x}\right)$$

Where

x $= z_{2\%}$ if $0 < -d_h < z_{2\%}$ (berm above still water line)
x $= 2 \cdot H_{m0}$ if $0 \leq d_h < 2 \cdot H_{m0}$ (berm below still water line)
$r_{dh} = 1$ if $-d_h \geq z_{2\%}$ or $d_h \geq 2 \cdot H_{m0}$ (outside influence area)

The influence of berm depth described above can only be used over the space between $2 \cdot H_{m0}$ below sea water level up to $z_{2\%}$ in the lower slope. Influence of berm position will disappear when it lies more than $2 \cdot H_{m0}$ under still water level.

In the end, the full expression of influence of berm can be written as:

$$\gamma_b = 1 - \frac{B}{L_{berm}} \cdot \left(0.5 + 0.5 \cdot cos\left(\pi \frac{d_h}{x}\right)\right)$$

Where

$0.6 \leq \gamma_b \leq 1.0$

It can be easily seen that influence of berm position become maximum for $d_h = 0$ which results to $\gamma_b = 1 - \frac{B}{L_{berm}}$.

4.2.5 Roughness of elements (γ_f)

Influence of roughness elements on wave overtopping is measured by factor γ_f. Data of influence factors for various single roughness elements can be found in the Russian study with regular eaves from 1950s. The determination of γ_f is dependent on the various features of dike. More details can be found in (Technical Report Wave Run-up and Wave Overtopping at Dikes, Technical Advisory Committee on Flood Defence).The end result as a table showing a complete overall view of influence factors can be found in Technical Report Wave Run-up and Wave Overtopping at Dikes, Dr J.W. van der Meer, (2007). Some values of several specific roughness elements are shown as follows:

Reference type	γ_f
Concrete	1.0
Asphalt	1.0
Closed concrete block	1.0
Grass	1.0
Vilvoorden stone	0.85
Basalt	0.90
Haringman	0.90
Fixtone - open stone asphalt	0.90
Armorflex	0.90
Small blocks over 1/25 of surface	0.85
Small blocks over 1/9 of surface	0.80
¼ of block revetment 10 cm higher	0.90
Ribs (optimum dimensions)	0.75
Armour rock - two layers thick	0.55
Armour rock - single layer	0.70

Figure 4.4 influence factors of roughness elements, Dr J.W. van der Meer, (2007)

4.2.6 Vertical wall on slope (γ_v)

The influence factor of vertical wall on slope is given by factor γ_v. In some cases, there a vertical wall placed on top of slope to reduce wave overtopping. The wave overtopping for a vertical wall on slope is smaller than for a 1:1 slope on top of dike profile. The influence factor for a vertical wall on a slope is $\gamma_v = 0.65$. For a 1:1 slope, $\gamma_v = 1$. Interpolation should be done for a wall that is between vertical and 1:1.

$$\gamma_v = 1.35 - 0.0078 \cdot \alpha_{wall}$$

Where α_{wall} is steep slope on top of dike ($0^\circ < \alpha_{wall} < 90^\circ$)

4.2.7 Slope with composite roughness elements (γ_f)

Weighting of various roughness factors is exerted by including the lengths of appropriate sections of the slope (between SWL$-0.25 \cdot z_{2\%,smooth}$ and SWL$+0.25 \cdot z_{2\%,smooth}$). Any roughness elements located beyond this limit are considered as no effect on the wave overtopping. If we consider a condition with three roughness elements within this area, and they are in lengths of L_1, L_2 and L_3, and with influence factor of $\gamma_{f,1}$, $\gamma_{f,2}$ and $\gamma_{f,3}$, respectively. Then the weighted influence factor can be written as:

$$\gamma_f = \frac{\gamma_{f,1} \cdot L_1 + \gamma_{f,2} \cdot L_2 + \gamma_{f,3} \cdot L_3}{L_1 + L_2 + L_3}$$

4.3 Mean overtopping discharge

The wave overtopping formulae are exponential functions with the general form:

$$\mathrm{q} = \mathrm{a} \cdot \exp(\mathrm{b} \cdot R_c)$$

The coefficient a and b are functions of the wave height, slope angle, break parameter and the influence factors described previously.

Wave overtopping is usually given as an average discharge per linear meter of width, q (m3/s per m or in l/s per m). Because the wave overtopping increases for increasing breaker parameter ξ_0, It can be described in two formulae: one for breaking waves, ($\xi_0 \leq 5$) and one for the maximum that is achieved for non-breaking waves ($\xi_0 > 7$). In the area in between ($5 < \xi_0 < 7$), the logarithm of q is linearly interpolated.

For $\xi_0 \leq 5$, the calculation of wave overtopping is described as:

$$\frac{q}{\sqrt{gH_{m0}^3}} = \frac{0.067}{\sqrt{tan\alpha}}\gamma_b \cdot \xi_0 \cdot \exp\left(-4.3\frac{R_c}{H_{m0}}\frac{1}{\xi_0 \cdot \gamma_b \cdot \gamma_f \cdot \gamma_\beta \cdot \gamma_v}\right)$$

With a maximum of:

$$\frac{q}{\sqrt{gH_{m0}^3}} = 0.2 \cdot \exp\left(-2.3\frac{R_c}{H_{m0}}\frac{1}{\gamma_f \cdot \gamma_\beta}\right)$$

For $\xi_0 > 7$, the calculation of wave overtopping is described as:

$$\frac{q}{\sqrt{gH_{m0}^3}} = 0.21 \cdot \exp\left(-\frac{R_c}{\gamma_f \cdot \gamma_\beta \cdot H_{m0} \cdot (0.33 + 0.022 \cdot \xi_0)}\right)$$

4.4 Maximum over topping volume

In order to estimate the hazard on buildings and infrastructure caused by wave overtopping, not only mean overtopping discharge is an important factor, but also maximum overtopping volume should be taken into consideration. The maximum volume of wave overtopping during certain is uncertain, but depends on the duration of the storm event. The maximum overtopping volume by one wave during an event depends on the actual number of overtopping waves, N_{ow}, and is given by:

$$V_{max} = a \cdot [\ln(N_{ow})]^{4/3}$$

Where

$\mathrm{a} = 0.84 \cdot \mathrm{q} \cdot \mathrm{t}/N_{ow}$
N_{ow} – number of overtopping waves.
q – mean wave overtopping discharge.
t – storm duration

4.5 Overtopping flow velocity and flow depth

Average wave overtopping discharge and maximum wave overtopping volume are not appropriate for describing the interaction between overtopping flow and failure mechanism.

In contract, the overtopping flow velocity and flow depth is more related to the analysis of erosion of dike inner slope and impact on infrastructure.

4.5.1 On seaward slope

Before calculating the overtopping flow depth and flow velocity, the wave run up velocities and related flow depth are required first. The flow on seaward slope is drawn in Figure 4.4.

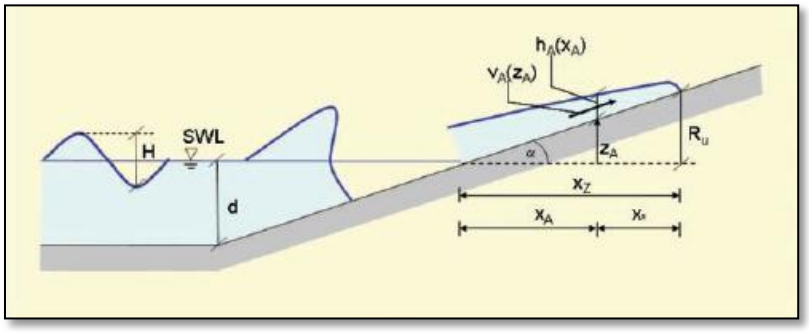

Figure 4.4. Wave run up characteristics. Source: Pullen et al (2007)

The flow depth of wave run up on the seaward slope is a function of horizontal projection x_z of wave run-up height $R_{u2\%.}$, the horizontal coordinate of the dike x_A and a dimensionless coefficient c_2. The calculation formula is under assumption of linear decrease of the lay thickness h_A from SWL to the highest point of wave run-up and it is given as follows:

$$h_A(\mathrm{x}_*) = c_2(x_z - x_A) = c_2 \cdot \mathrm{x}_*$$

Where:

x_* – remaining run-up length($\mathrm{x}_* = x_z - x_A$) and $x_z = R_{u2\%.}/tan\alpha$.

The coefficient can be selected based on different exceedance levels by Table 4.1.

Table 4.1 characteristic values for parameter c_2 (TMA-spectra)

Parameter	c_2	σ'
$h_{A,50\%}$	0.028	0.15
$h_{A,10\%}$	0.042	0.18
$h_{A,2\%}$	0.055	0.22

Source: Pullen et al (2007)

The run-up velocities are defined as the maximum velocity at any position of seaward slope during wave run-up. The equation of wave run-up velocity is given by:

$$v_A = k^* \cdot \sqrt{2g(R_{u2\%.} - z_A)}$$

Where:

v_A – wave run-up velocity at point z_A above SWL.

$R_{u2\%.}$ – wave run-up height exceeded by 2% of the incoming waves.

k^* – dimensionless coefficient.

The dimensionless form is:

$$\frac{v_A}{\sqrt{gH_s}} = a_0^* \sqrt{\frac{R_{u2\%.} - z_A}{H_s}}$$

Where:

H_s – significant wave height.

The values of a_0^* are given in Table 4.2.

Table 4.2 characteristic Values for Parameter a_0^* (TMA-spectra). Source: Pullen et al (2007)

Parameter	a_0^*	σ'
$v_{A,50\%}$	1.03	0.23
$v_{A,10\%}$	1.37	0.18
$v_{A,2\%}$	1.55	0.15

4.5.2 On crest of dike

The overtopping flow on the dike crest is sketched in Figure 4.5.

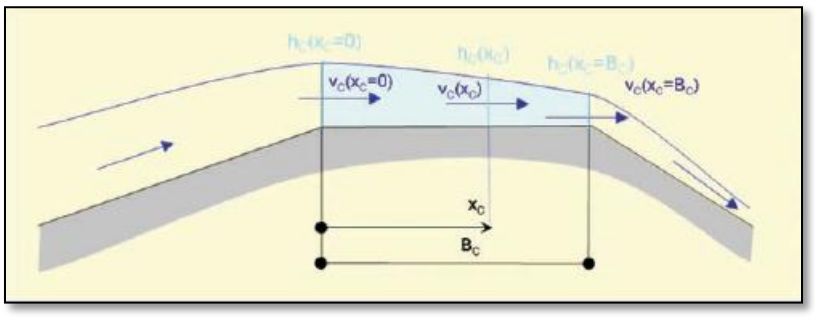

Figure 4.5. Overtopping flow on dike crest. Source: Pullen et al (2007)

The flow depth is given as a function of the width of crest B_c and the coordinate on the crest x_c :

$$\frac{h_c(x_c)}{h_c(x_c=0)} = \frac{c_2(x_c)}{c_2(x_c=0)} = exp\left(-c_3\frac{x_c}{B_c}\right)$$

Where:

c_3 – dimensional coefficient; 0.89 for TMA spectra and 1.11 for natural wave spectra.
B_c – width of dike crest.

The flow velocity is given by simplified Navier-Stokes-equation under several assumptions:

- Dike crest is horizontal.
- Vertical flow velocity to the dike slope can be neglected.
- Pressure term is constant over dike crest.
- Viscous effects in flow direction are small and bottom friction is constant over dike crest.

$$v_c = v_{c(x_c=0)} exp\left(-\frac{x_c \cdot f}{2 \cdot h_c}\right)$$

Where:

v_c – overtopping flow velocity.
f – friction coefficient.
x_c – coordinate on crest.
h_c – flow depth at x_c.

4.5.3 On the landward slope

Overtopping flow velocity and overtopping flow depth [Pullen et al (2007)].

When the overtopping flow runs up the seaside of the dike and crosses the dike crest, it will reach the landward slope of the dike.

An analytical function was developed which describes overtopping flow velocities and overtopping low depths on the landward slope as a function of the overtopping flow velocity at the end of the dike crest ($v_{b,0} = v_C(x_C = B)$), the slope angle . Of the landward side and the position s_B on the landward side with sB = 0 at the intersection between dike crest and landward slope. A definition sketch is given in Figure 4.6 below.

The following assumptions were made to derive an analytical function from the Navier-Stokes-equations:

1. Velocities vertical to the dike slope can be neglected;
2. The pressure term is almost constant over the dike crest; and the viscous effects in flow direction are small.

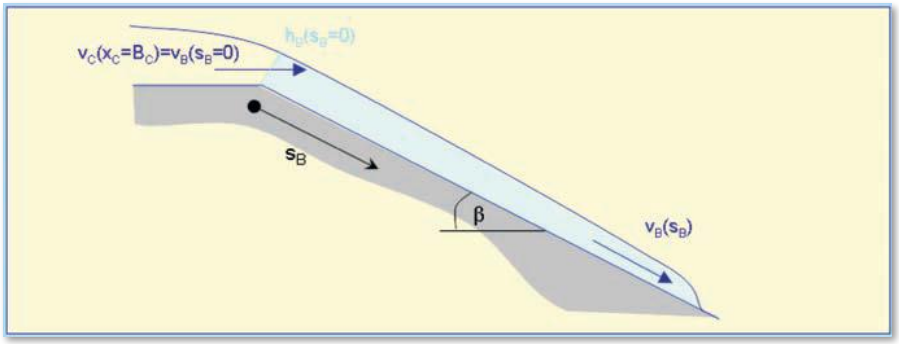

Figure 4.6. Definition of overtopping flow parameter on the landward slope. Source: Pullen et al (2007)

This results in the following formula for overtopping flow velocities:

$$v_b = \frac{v_{b,0} + \frac{k_1 h_b}{f}\tanh\left(\frac{k_1 t}{2}\right)}{1 + \frac{f v_{b,0}}{h_b 1}\tanh\left(\frac{k_1 t}{2}\right)}$$

With:

$$t \approx -\frac{v_{b,0}}{g\sin\beta} + \sqrt{\frac{v_b^2}{g^2\sin\beta^2} + \frac{2s_b}{g\sin\beta}} \quad \text{and} \quad k_1 = \sqrt{\frac{2f\sin\beta}{h_b}}$$

Equation mentioned here needs an iterative solution since the overtopping flow depth h_b and the overtopping flow velocity v_b on the landward slope are unknown. The overtopping flow depth h_b can be replaced in a first step by:

$$h_b = \frac{v_{b,0} \cdot v_{b,0}}{v_b}$$

With $v_{b,0}$ the overtopping flow velocity at the beginning of the landward slope($v_{b,0} = v_B(s_B = 0)$); and $h_{b,0}$ the overtopping flow depth at the beginning of the landward slope ($h_{b,0} = h_B$ ($s_B = 0$)).

The second important factor influencing the overtopping flow on the landward slope is the bottom friction coefficient f which has to be determined experimentally. The overtopping low on the landward slope tends towards an asymptote for $s_b \to \infty$ which is given by:

$$v_b = \sqrt{\frac{2ghsin(\beta)}{t}}$$

4.5.4 Spatial distribution of the overtopping water

Landward ground level

It can be expected that the spatial distribution of the overtopping water depends on the landward ground level, h_{meas}. The trajectory of overtopping volume is in a parabolic type, therefore, we can estimate that if the overtopping volume is dropped into

$$v = \sqrt{\frac{2(y+0)}{g}}m$$

at h_{meas}=0 m, then it will fall into

$$v = \sqrt{\frac{2(y+0.1)}{g}}m$$

at h_{meas}=0.1minstead. Fig 4.7 shows the effect of landward ground level on landward spatial distribution of overtopping water as a function of relative landward distance. The positive h_{means} stands for the ground level lower than the structure crest and negative hmeas represents the ground level higher than the structure crest. It is interesting to observe that for the same wave conditions and structural geometry the proportion of wave overtopping volume passing x increases with landward ground level, hmeas. The overtopping water even reaches to a distance up to three times bigger than significant wave height for hmeas=0.2 m, while it only splashes own in the area of half the significant wave height from structures for hmeas=−0.05 m. However, the computed proportion of wave overtopping water passing a landward location is smaller than predictions by $F(x,y) = \exp\left(\frac{-1.3}{H_{m0}}\left\{\max\left(\frac{x}{\cos\beta} - 2.7ys_{op}^{0.15}, o\right)\right\}\right)$ in EurOtop (2008), in accord with more overtopping water falling into the area just behind the structure. This is mainly due to a nappe (in hydro-engineering refers to the sheet of water over-topping) clinging to the landward face of the weir with very low water heads.

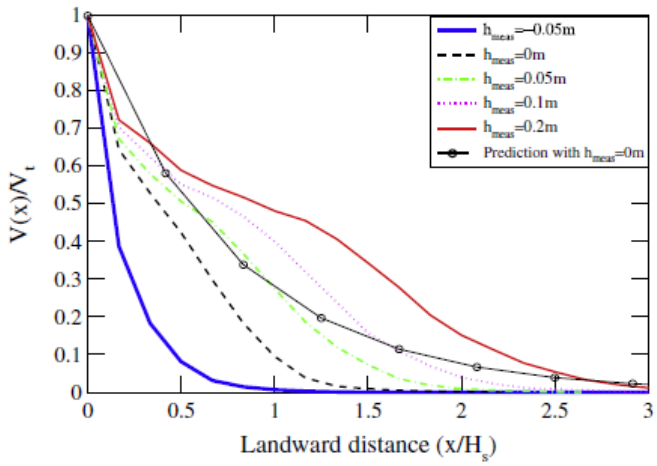

Figure 4.7. Effect of landward ground level, hmeas, on computed landward spatial distribution of overtopping water. Prediction is given by Eq. (6.17) in EurOtop (2008) with h_{meas}=0. The positive hmeas stands for the ground level lower than the structure crest. Hs=0.12 m, Tm=1.6 s, h=0.7 m, Rc=0.1 m, tan(α)=1:2 and B=0.3 m.

Source: Spatial distribution of wave overtopping water behind coastal structures Coastal Engineering, 58 (2011) 489-498. doi:10.1016/j.coastaleng.2011.01.010

Structure porosity

Structure porosity will affect spatial distribution of overtopping water through wave run-up and velocities on the crest as suggested by $x(y_c) = u_{A,50\%}\sqrt{\frac{2(y_c+h_{means})}{g}}$ $0 < y_c < h_A$, in which, $u_{A,50\%}$ =the horizontal velocity at the landward end of the crest (x=0m)

In this study, four types of coastal structures have been employed and shown in Figure 4.8, including a caisson breakwater with concrete protection; caisson breakwater with gravel protection (porosity=0.49); caisson breakwater with rubble protection (porosity=0.53) and rubble mound breakwater. The present model investigates the porous media in a similar way as Liu et al. (1999) by averaging the flow equations over a length scale. This length scale is larger than the characteristic pore size and is much smaller than the scale of the spatial variation of the physical variables in the flow domain. Therefore, the fluid variables can be decomposed into two parts, spatially averaged and spatially fluctuated quantities.

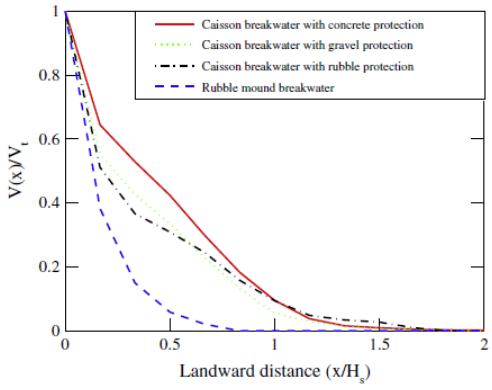

Fig. 11. Effect of structure porosity on landward spatial distribution of wave overtopping water. $H_s = 0.12$ m, $T_m = 1.6$ s, $h = 0.7$ m, $h_{meas} = 0$ m, $R_c = 0.1$ m and $B = 0.3$ m.

Figure 4.8. Effect of structure porosity on landward spatial distribution of wave overtopping water. Source: Spatial distribution of wave overtopping water behind coastal structuresCoastal Engineering, 58 (2011) 489-498. doi:10.1016/j.coastaleng.2011.01.010

Figure 4.8 shows the spatial distribution of wave overtopping water for various structure porosity at the ground level hmeas=0 m. With the same incident wave conditions (Hs=0.12 m, T_p=1.6 s) and the same geometry, the proportion of wave overtopping volume passing x decreases with structure porosity. This is because the employment of permeable protection leads to effective energy dissipation and reduces the overtopping discharge (Liu et al., 1999). In addition, large porosity, equivalent to large roughness or surface friction, leads to large dissipation and deductions of velocity and layer thickness on the structure crest. The proportion of wave overtopping volume passing a landward location for rubble mound breakwater is significantly smaller than that for caisson breakwater with rubble protection (Fig. 11). The structure crest is hydraulically rough for the former case but hydraulically smooth for the latter, although these two layouts have the same structure porosity. Therefore, rubble mound breakwater has smaller velocity of the overtopping water on the crest. As can be seen in $x(y_c) = u_{A,50\%}\sqrt{\frac{2(y_c+h_{means})}{g}}$, small velocity and layer thickness result in small travel distance of the overtopping water. This finding is consistent with the recommendation by EurOtop (2007) that roughness elements located above the still water level minus a quarter of wave run-up on a smooth slope, has a significant effect on the wave overtopping discharge.

Erosion of the inner slope

A tested inner slope of a dike, covered with grass on clay, never failed by erosion due to overtopping for a mean overtopping discharge of **30 l/s** per m or less. Only one section failed at 50 l/s per m; some at 75 l/s per m, but part of the sections did not fail, even not for 75 l/s per m.

It seems that the large erosion resistance of the inner slope of a dike is determined by the combination of grass and clay.

- The grass cover or mattress seems stronger (Boonweg, Figure 4.9) if it grows on a sandy clay. Such a grass cover may resist even up to 75 l/s per m, but if significant damage occurs, the clay layer is not very erosion resistant (Figures 4.10 and 4.11).



Figure 4.9 Source: Guidance on erosion resistance of inner slopes of dikes from three years of testing with the Wave Overtopping Simulator



Figure4.10 Source: Guidance on erosion resistance of inner slopes of dikes from three years of testing with the Wave Overtopping Simulator



Figure 4.11 Source: Guidance on erosion resistance of inner slopes of dikes from three years of testing with the Wave Overtopping Simulator

- On the other hand, good quality clay does not produce a very strong grass cover (it is difficult for roots to penetrate into the clay) and the grass may rip off for overtopping discharges around 30 l/s per m (Figures 4.12 and 4.13). But in that case the remaining good quality clay layer, still reinforced with some roots, has a large erosion resistance against overtopping waves (Figure 4.12).Van der Meer, Schrijver, Hardeman, Van Hoven, Verheij and Steendam 11



Figure 4.12 Afsluitdijk. Grass toe， Source:Guidance on erosion resistance of inner slopes of dikes from three years of testing with the Wave Overtopping Simulator



Figure 4.13 Afsluitdijk.Staircase with fence, before and after testing Source:Guidance on erosion resistance of inner slopes of dikes from three years of testing with the Wave Overtopping Simulator

- This leads to the conclusion that a good grass cover on sandy clay and a worse grass cover on good clay show different failure mechanisms, but they show more or less similar strength against wave overtopping. The variability of the grass sod may, therefore, have less influence on the total strength than previously anticipated.
- This could lead to the conclusion that the way of maintenance of the grass has only minor effect on the strength of the inner slope. The test at St Philipsland may show that the bad grass coverage (small open areas without grass) on sandy clay may show less resistance (Figure 4.14).



Figure 4.14 Final result St Philipsland, Zeeland. Source:Guidance on erosion resistance of inner slopes of dikes from three years of testing with the Wave Overtopping Simulator

Transitions from slope to horizontal are probably the most critical locations for initial and increasing damage.

- During the tests this was often the transition from the inner slope to the toe of the dike, with or without a maintenance road. The tests in 2009 were focused on these kinds of transitions. Damage was initiated by a mean discharge of 10 l/s per m or more. As the damage occurred at the lowest part of the inner slope it will take time for damage to extend to the crest level and subsequently cause a dike breach. Transition higher on the inner slope (cycle paths, stability or piping berms with or without maintenance road, tracks of tractors, roads crossing the dike), which have not yet been investigated, might be more critical. Further investigation may give more confirmative conclusions.
- A hole in the layer of clay, which reaches the under laying sand core and created at a large mean overtopping discharge of **50 l/s** per m or more, will give a very quick ongoing erosion. This has not been observed for smaller overtopping discharges, for the simple reason that these smaller discharges never created significant damage to the inner slope.
- But the test with the parking place of bricks (Figure 4.15) showed that sand erosion with **30 l/s** per m, and even with **10 l/s** per m, goes fairly quickly. It must be noted that although the test was stopped for 30 l/s per m due to fast ongoing damage to the parking area, the dike itself was not in danger at all.



Figure 4.19 Afsluitdijk. Parking area, section 2. Source: Guidance on erosion resistance of inner slopes of dikes from three years of testing with the Wave Overtopping Simulator

- **Small obstacles like poles did not show any erosion**. Small holes from mice and moles did not initiate damage to the grass cover layer. Also a fence (Figure 4.13) and a little bigger pole (0.15 m by 0.15 m) showed no initiation of erosion. The grass around a fence at the toe of the dike had some influence on initiation of erosion, probably due to larger forces in this area. An obstacle like a concrete staircase on the inner slope was totally destroyed at a stage with 75 l/s per m overtopping (Figures 4.13 and 4.20). It should be noted, however, that also here the dike itself was not in danger, due to the large erosion resistance of the clay. Still, further research may give more final conclusions on other large obstacles.



Figure 4.20 Afsluitdijk. Concrete staircase, section 3. Source: Guidance on erosion resistance of inner slopes of dikes from three years of testing with the Wave Overtopping Simulator

5 OVERTOPPING FLOW ENCOUNTERING OBSTACLES

When the flow overtops the dike crest, it flows through the inner slope toward the landside. This landward flow from overtopping is difficult to model due to the complexity of the flow pattern and paths. In addition, when this flow encountered an obstacle, different hydraulic response of the flow and amount of energy dissipation will happen This depends a lot on the flow condition such as the flow speed, approach angle and also on the geometry, surface roughness and porosity of the obstacle.

Currently, there is no literature providing a simple approximation on calculating the flow distribution from overtopping flow when it encounters an obstacle. However, there are many literatures providing equivalent information on the effect of flood wave encountering obstacles which are on a much larger scale e.g. in flood routing simulation. Using this information especially on the flow pattern when encountering obstacle, attempt can be made to carry up conservative approximation on the flow distribution. The amount of the overtopping flow that is (a) reflected by the obstacle and (b) diverted to the sides of the obstacle. In order to determine this flow distribution, how an obstacle affects the flow will first need to be understood.

5.1 Effect of Obstacle on Flow

Syme (2008) review on the methods to account for building's response to the flood wave for 2D modeling. Although his review of the obstacle is strictly on building, it provides an idea on how the type of the obstacle affects the flow so as to correctly account it in a 2D model. These methods are:

1. Increase roughness: increase bed resistance will result in increasing energy dissipation of water flowing through and around the obstacle e.g. buildings. This work well for 2D element with coarse resolution. However, the difficulty is to obtain the appropriate roughness value to represent the flow.
2. Blocking out of Element: This is done provided that the element size for the obstacle is sufficiently fine. However, most of the time, the obstacle is large and in certain case such as building will "adsorb" some of the water.
3. Using energy loss coefficient: Specify form loss coefficient to represent the fine-scale energy dissipation within and around the obstacle. Though it is theoretically more correct to account for the obstacle as energy is loss when the flow passes through or around the obstacle, it is difficult as there is also currently no literature to provide this type of information.
4. Modeling Buildings' Exterior wall: This method is good since it account for the possible deflection of the water and also storage effect for water through building. However, this method required some prior knowledge of the flow direction.
5. Modeling Buildings as "porous": 2D element sides of building are partially blocked to represent certain amount of blockage by external wall. TUFLOW software is used to model partial blockages.

Syme then carried out a numerical simulation using TUFLOW to show the effect on the building response to flow when different methods were applied. Figure 5.1 shows the hypothetical building model layout. Table 5.1 presents a comparison between different building test scenarios. Figure 5.2 presents a comparison between different water surface profiles along the model centreline.

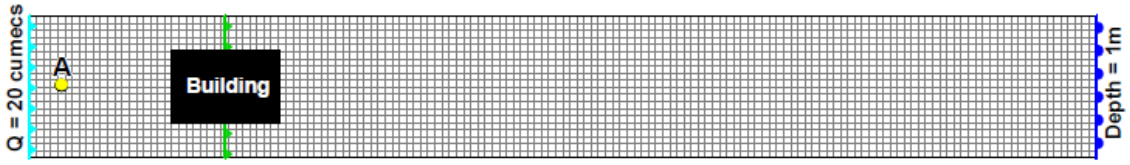

Figure 5.1: Hypothetical Building Model Layout. Source: Syme (2008)

Table 5.1. Comparison of building test scenarios

Scenario	Water Level (m)		Flow Distribution (%)		Average Velocity (m/s)	
	Point A	Increase	Building	Garden	Building	Garden
No Building	1.118	0.000	50%	50%	0.91	0.91
Blocked Out	1.255	0.137	0%	100%	n/a	1.90
High Roughness	1.240	0.122	21%	79%	0.38	1.41
Add Form Loss	1.195	0.077	31%	69%	0.55	1.23
Ext Walls, Open D/S	1.250	0.132	0%	100%	0.00	1.92
Ext Walls, Open U/S	1.263	0.145	0%	100%	0.00	1.93
Porous	1.170	0.052	9%	91%	1.87	1.80
Porous + Form Loss	1.225	0.107	7%	93%	1.28	1.78

Source: Syme (2008)

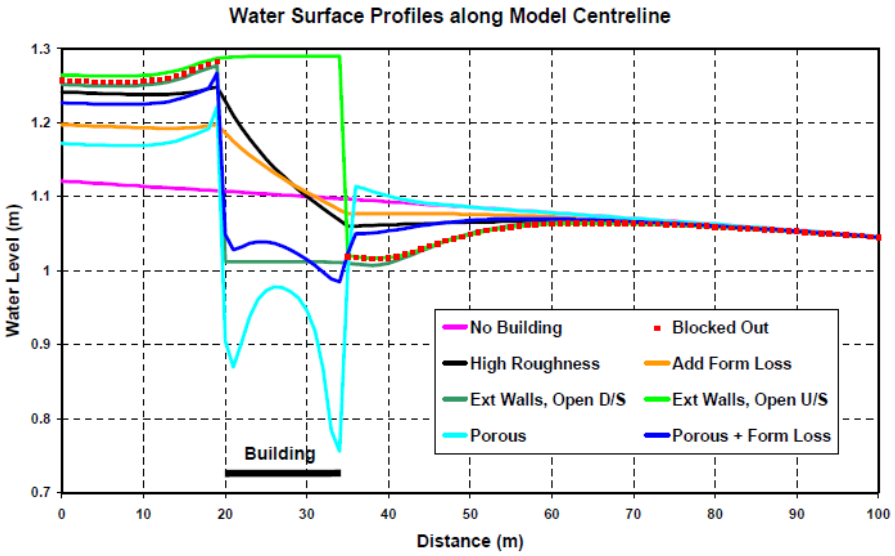

Figure 5.2. Comparison of Water Level Profiles along Model Centerline. Source: Syme (2008)

Figure 5.1 shows the hypothetical building model layout with the results shown on Table 5.1 and Figure 5.2 from the by Syme (Syme 2008). The change in the water level can be seems as it (a) reaches, (b) through and (c) over the obstacle. When the flow reaches that the obstacle, there is a slight increase in the water level. Depending on the type of obstacle, the water level decreases significantly when the flow passes through the obstacle. After passing the obstacle, the reduced water level continues to reduce gradually as it travels further landward.

Referring to study by Michal Szydlowski [Szydlowski (2011)] on his numerical simulation and laboratory experiment on open channel flow between bridge priers, we can have addition insight on the effect of geometry of obstacle to flow.

Figure 5.3 shows that the water depth increases (i.e. hydraulic jump) in front of pier (obstacle) and sudden lowering directly after passing the pier. Local flow circulation just behind pier can also be seemed. Even for an obstacle that has a smooth rounded surface such as a pier, the resulting surface wave merged after encountering the obstacle has a complex structure with turbulence eddies, diffraction and interference due to the abrupt swelling and depression of the water level shown in Figure 5.4.

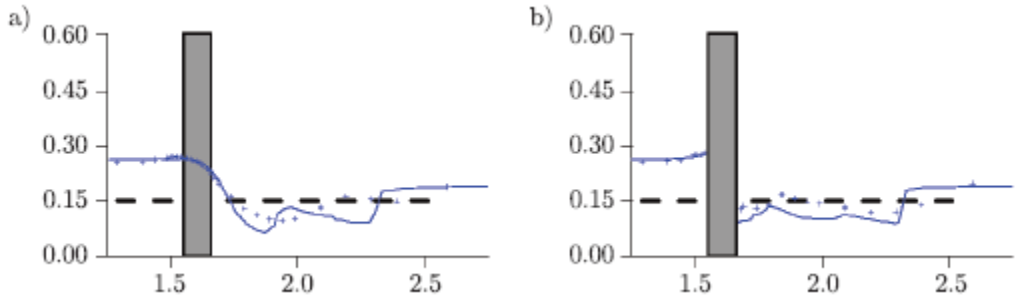

Figure 5.3. Measured (+ + +) and calculated (——) water surface profile for the second experiment together with the critical depth line (– –): a) along the channel axis, b) along the pier axis (dimensions in metres). Source: Szydlowski (2011)

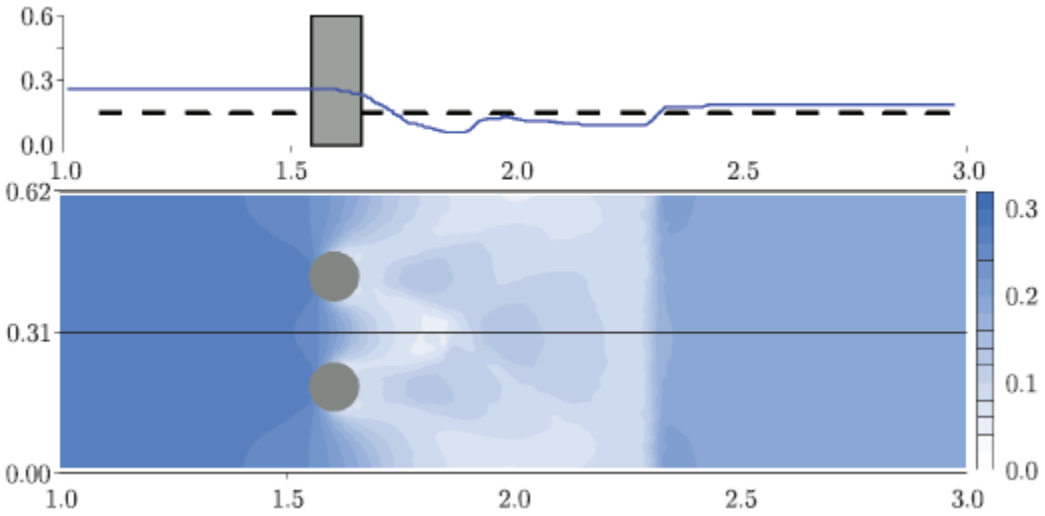

Figure 5.4. Surface profile and horizontal distribution of the computed water depth (dimensions in metres). Source: Szydlowski (2011)

Figure 5.5 and 5.6 shows the spatial distribution of the velocity and Froude number, provide additional information on the velocity flow and flow condition.

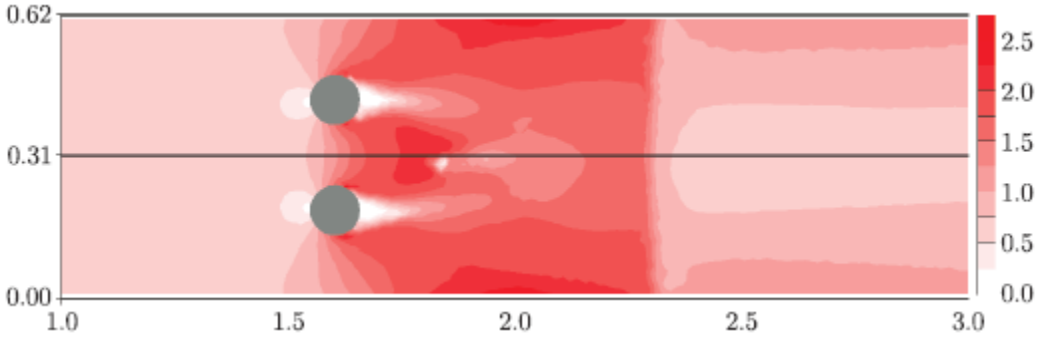

Figure 5.5. Distribution of flow velocity (m/s) (dimensions in metres). Source: Szydlowski (2011)

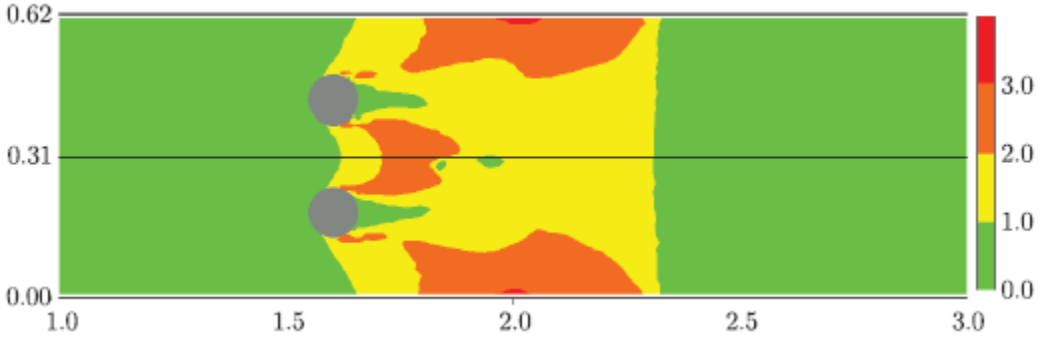

Figure 5.6: Spatial distribution of the Froude number (dimensions in metres). Source: Szydlowski (2011)

Hence, these methods, conclude that the surface roughness, geometry and porosity of the obstacle will affect the amount of energy dissipation by the flow and the flow movement.

5.2 Effect of Flow when encountering obstacle

Knowing that the different types of obstacles will affect the hydraulic response of the flow, the hydraulic response of the flow such as its flow pattern when encountering an obstacle will now be look into. In the paper by Hyung (Kim, Lee et al. 2012), the laboratory experiment was performed to study the variation in flood intensity due to structure. Numerical model was then used to verify the measured water depth from the laboratory experiment.

Figure 5.7 shows that laboratory setup of the experiment in plan and side view. The different placement of the block/s to simulate obstacle for flow shown on Figure 5.8. The experiment conditions for the flood wave propagation on Table 5.2. The location of the observation pointswith wave height gauges on the inundation area shown on Figure 5.9.

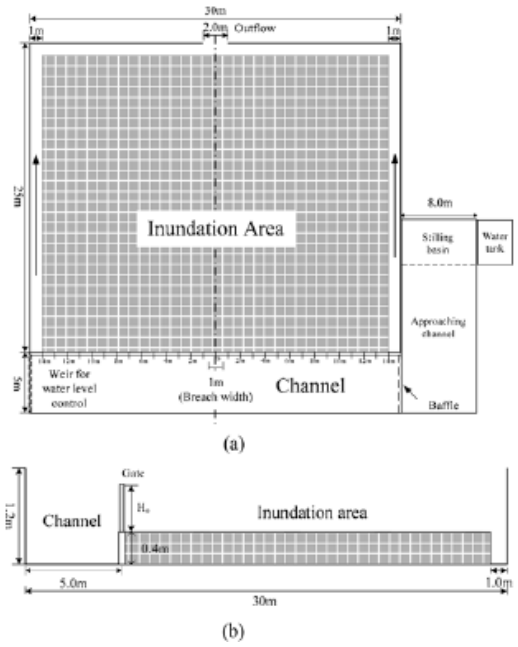

Figure 5.7: Schematic of the Flood Wave Experimental Channel: (a) Plan View, (b) Side View. Source: Kim et al (2012)

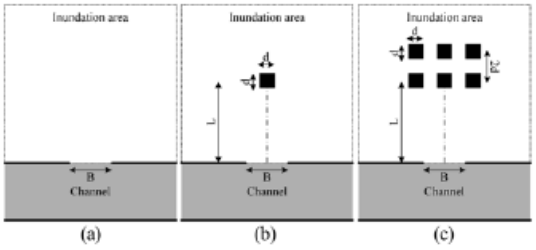

Figure 5.8: Schematic of Structure Layouts for Experiments: (a) Case1: None-structure, (b) Case 2: Single Structure, (c) Case 3: Group Structure. Source: Kim et al (2012)

Breach width B (m)	Overflow depth H0 (m)	Initial flow velocity (m/s)	Structure layout
1.0	0.55	2.3	None Single Group
	0.50	2.2	
	0.45	2.1	
	0.40	2.0	
	0.35	1.9	

Table 5.2: Experimental Conditions for Flood Wave Propagation. Source: Kim et al (2012)

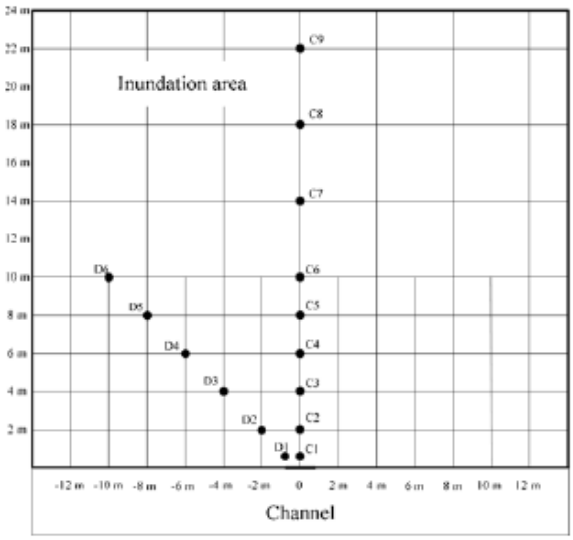

Figure 5.9: Experimental Observation Points with Wave Height Gauges. Source: Kim et al (2012)

The wave height measured in the (a) normal and (b) diagonal direction for the three cases were shown on Figure 5.10, 5.11 and 5.12, respectively.

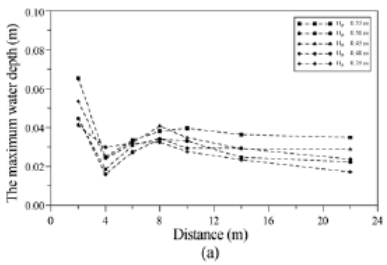

Figure 5.10: Observed Maximum Water Depth in Case 1: (a) Normal Direction, (b) Diagonal Direction. Kim et al (2012)

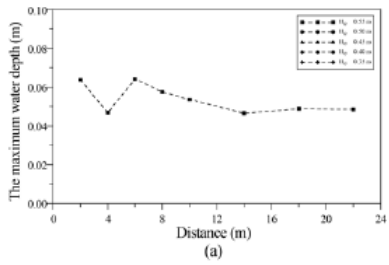

Figure 5.11: Observed Maximum Water Depth in Case 2: (a) Normal Direction, (b) Diagonal Direction. Kim et al (2012)

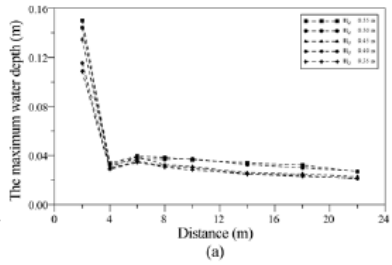

Figure 5.12: Observed Maximum Water Depth in Case 3: (a) Normal Direction, (b) Diagonal Direction. Kim et al (2012)

From these Figure, Hyung obtained the following observations:

1. When the water was released by overflow from the channel to the inundation area, its water depth was at maximum at x = 2m. This maximum water depth increase with the increase of the overflow height.
2. This maximum water depth decreases rapidly, as the flood wave velocity increase rapidly until x = 4 m.
3. After distance x = 4 m, maximum water depth increase as bottom rough cause velocity to decrease slightly.
4. If there is a obstacle, there will be water depth increase between the structure and the source of the flood wave. The water depth increase will be more for Case 3 than Case 2.
5. For flow encountering obstacle in Case 2 and 3, there were also water height increase for observation in the diagonal direction than the normal direction. This means that some of the flow instead of being reflected by the obstacle have been diverted to the sides of the obstacle.
6. Water depth is also slightly greater immediately behind the structure due to the superpositioning of the flood wave.
7. After x = 8 m, for all cases, the maximium water depth decrease as distance increase.

Figure 5.8 showns the maximum flood intensity distribution generated by the numerical model which the water depth has been verified by the experiment results.

As there are many ways of determining flood intensity, the Swiss method (OFEE et al., 1977) was adopted by the Hyung . The Swiss method defined flood intensity in term of the maximum water depth generated throughout the event and the product of the maximum velocity multiplied by the maximum depth. The flood intensity produced a quantity similar flow rate per unit wide when we consider the amount of overtopping rate.

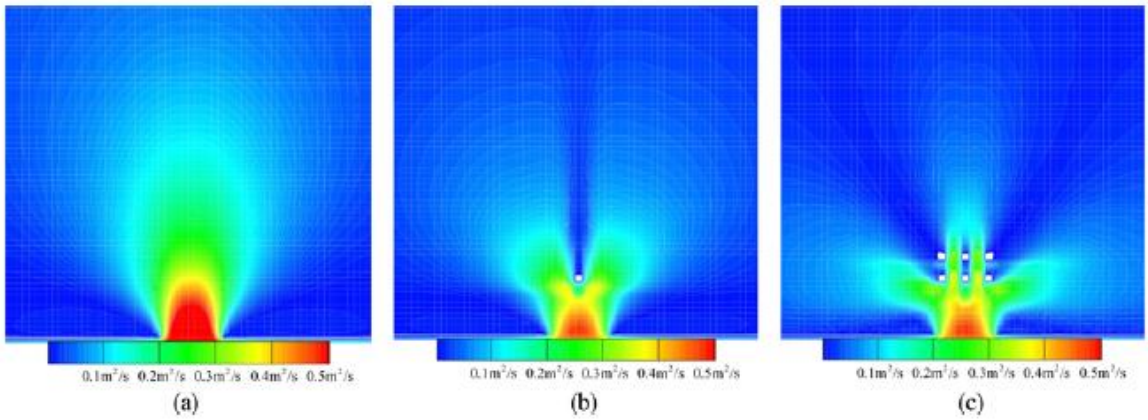

Figure 5.13: Maximum Flood Intensity Distributions: (a) None-structure, (b) Single Structure, (c) Group Structures. Source: OFFE et al (1977)

The numerical result shown was in line with the observations made from the laboratory results and it provide a more hoslistic and overview on the intensity of the flow when encountering obstacle/s. Figure 13 shows that the flood intensity was maximum when it was initially released from the opening. Without an obstacle in Figure 13(a), the flood wave will propagate, spread and reduce in its intensity as it traveled furtehr away from the source. In Figure 13(b) and 13(c), when encountering an obstacle, the flood intensity changes at the front and sides regions of the obstacle. Funneling effect also causes the increase of flood intensity at the gaps between the structures.

In addition, to analyze changes in flood intensity due to obstruction, the ratios of the maximum flood intensity increase are calculated by taking dividing the calculated flood intensity for Case 2 and 3 to that of Case 1.

Figure 5.14 shows that there is a significant increase in flood intensity in the diagonal direction. It shows that as the water depth increase, the obstacle divert more of the the wave propagation to the diagonal direction. Thus, the flood intensity behind the obstacle decreases more.

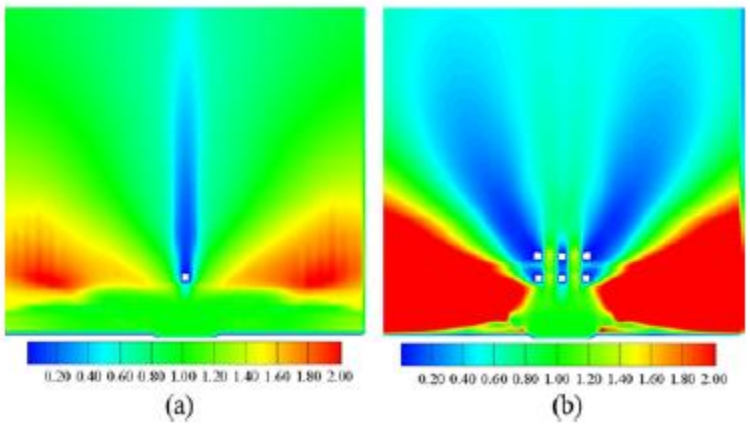

Figure 5.14: Increase Ratio of Maximum Flood Intensity: (a) Single Structure, (b) Group Structures. Source: OFFE et al (1977)

Hence, through the laboratory experiment and numerical model by Hyung (Kim, Lee et al. 2012), a better idea on the effect on flow when it encountered obstacle can be obtained.

A similar type of laboratory experiment was also done by Guido Testa (Testa, Zuccalà et al. 2007), the experimental results on the behavior of the flow when encountering obstacle/s were similar to that done by Hyung (Kim, Lee et al. 2012) as described earlier. Guido's experiment result provided an added dimension to the understanding on flow encountering obstacle.

Guido described that that the flow pattern as almost standing with a strong hydraulic jump occurred when the flow encountered the obstacle's front. This hydraulic jump propagates very slowly in the upstream direction until its intensity diminishes with time according to the inflow discharge. He added that the intensity of this hydraulic jump does not depend on any obstacles behind it. Thus the shock from the impact is equally strong whether there is any other obstacle behind it or not. This can be seen also from the results by Hyung.

Guido also mentioned that for a block layout similar to Case 3, if the spacing of the blocks is very close, this can make the obstacles to appear as a compact obstacle to the main flow.

6 REFERENCES

- CIRIA, CUR, CETMEF (2007), 'The Rock Manual. The Use of Rock in Hydraulic Engineering' . 2nd edition, C683, CIRIA, London.
- Eijgenraam, C., Brekelmans, R., den Hertog, D., Roos, K. (2010), 'Safe Dike Heights at Minimal costs: The Homogeneous Case'. Submitted to Management Science. Available on http://www.tilburguniversity.edu/research/institutes-and-research-groups/center/ graduate-school/chp/opmaast/dike1.pdf
- Inspectie Verkeer en Waterstaat (2006), 'Assessment of Primary Flood Defences in The Netherlands, National Report on 2006'. Available on http://www.safecoast.nl/editor/databank/File/Assessment%20primary%20flood%20defences%20in%20NL.pdf
- Jonkman, S., Jongejan, R., Maaskant, B., Vrijling, H. (2010), 'New Safety Standards for Coastal Flood Defences in The Netherlands'. 32nd International Conference on Coastal Engineering, ICCE 2010, June 30 – July 5 2010, Shanghai, China.
- Kim, H., Lee, J. et al (2012). 'Numerical Analysis of Flood Risk Change Due to Obstruction'. KSCE Journal of Civil Engineering 16 (2). 207-214.
- OFFE, OFAT and OFEFP (1997), 'Prise en compte des dangers dus aux dans le cadre des activities del'amenagement du territoire'. Bienne, 1997, Office Federal de l'Economie des Aux (OFFE), Office Federal de l'Amenagement du Territoire (OFAT), Office Federal de l'Environnent, Desforets, et du Paysage (OFEFP).
- Pullen, T., Allsop, N. W. H., Bruce, T., Kortenhaus, A., Schüttrumpf, H., Van der Meer, J. W. (2007), 'EurOtop – Wave Overtopping of Sea Defences and Related Structures: Assessment Manual'. Environment Agency, UK, Expertise Netwerk Waterkeren, NL and Kuratorium für Forshung im Küsteningenieurwessen, DE.
- Roos, A., Riedstra, D. (2010), 'Safety Standards in The Netherlands'. Rijkswaterstaat Centre for Water Management. Presentation of March 17th, 2010.
- Syme, W. (2008), 'Flooding in Urban Areas – 2D Modelling Approaches for Buildings and Fences'. 9th National Conference on Hydraulics in Water Engineering. Engineers Australia. Darwin Convention Centre, Australia.
- Szydlowski, M. (2011), 'Numerical Simulation of Open Channel Flow Between Bridge Piers'. TASK Quarterly 15 (3-4). 271-282.
- Testa, G., Zuccala, D. et al (2007), 'Flash Flood Flow Experiment in a Simplified Urban District'. Journal of Hydraulic Research 45 (supl. 1). 37-44.
- Lin, P.Z., Liu, P.L.F., 1999. Internal wave-maker for Navier-Stokes equations models. Journal of Waterway Port Coastal and Ocean Engineering 125 (4), 207‐215.
- Guidance on erosion resistance of inner slopes of dikes from three years of testing with the Wave Overtopping Simulator, Van der Meer, Schrijver, Hardeman, Van Hoven, Verheij and SteendamW. Allsop, MICE, T. Bruce, J. Pearson BEng and P. Besley 'Wave overtopping at vertical and steep seawalls'. Maritime Engineering 158 September 2005 Issue MA3,103–114
- Dr J.W. van der Meer (2002), 'Technical Report Wave Run-up and Wave Overtopping at Dikes', Technical Advisory Committee on Flood Defence

TU DELFT – MULTIDISCIPLINARY PROJECT CIE4061

Afsluitdijk Project
"The Monument" Location

Data Collection and Analysis

Sien Liu, Jun Huang, Sebastian Rayo, Tai Yan Lim

21/12/2012



CONTENTS

1 Introduction 2
1.1 Background 2
1.2 Problem Description 2
1.3 Document Scope 2
2 Available information 3
2.1 Received from the client 3
2.2 Other sources 3
3 Site Appreciation Analysis 4
4 Wave Climate Definition 7
5 Definition of Relevant Cross Sections 9
6 Location and Dimensions of Obstacles on Dike's Crest 11
7 Final Comments 13

1 INTRODUCTION

1.1 Background

The Afsluitdijk (Enclosure Dam) is a main dam that forms the fundamental part of the larger Zuiderzee Works that separates the Zuiderzee, a salt water inlet of the North Sea, and turning it into the fresh water lake of the IJsselmeer. It protects the central Netherlands from the effects of the North Sea. It was constructed between 1927 and 1933, and runs from Den Oever on Wieringen to the village of Zurich in Friesland. It is 32 km long and 90 meters wide, rising to 7.25 meters above sea-level, with an incline of 25% on each side.

At the location along the Afsluitdijk where the final water passage was closed ('De Vlieter'), a lookout tower known as 'The Monument' was built in 1933. It was presented by the Zuiderzee Works Construction Company and designed by architect W.M. Dudok. The site has a statue of a "Steenzetter", and also marks the inscription 'A living nation builds for its future'. A statue of Cornelis Lely has also been erected near Den Oever on the Barrier Dam itself.

The Afsluitdijk with The Monument are currently managed by the Ministry of Infrastructure and the Environment ("The client"). There is a restaurant at The Monument where the client has sublet it for private operator to manage it.

1.2 Problem Description

With the anticipation of increase storm intensity and sea level rise in the future, the client had previously engaged a consultant to analyze the existing design of Afsluitdijk for a design storm of 1:10,000 years. According to the client, the result of the study concluded that the standard cross-section of Afsluitdijk is not sufficient to withstand the design storm of 1:10,000 years, hence, modifications of it are required. The study also found that during the design storm, there is a significant overtopping over the dike.

The client is concerned about the significant overtopping found from the previous study may have adverse impact on the non-standard cross-section of the dike where The Monument is located. Therefore, the client has requested our design team to look into the dike section at The Monument location.

1.3 Document Scope

The main objectives of this document are:

1. To present a list with available information, including those that were received from the client and those available from other sources.
2. To analyse the available information, establishing those parameters that will be useful to the developing of the Afsluitdijk project.

2 AVAILABLE INFORMATION

2.1 Received from the client

Information received from the client is presented in Table 2.1.

Table 2.1. Information received from the client

Number	Item name	Type	Description
[1]	'Closure dam 20 march 2012'	Powerpoint presentation	General description of the Afsluitdijk, including details of the structure and definition of the Reconstruction Plan.
[2]	'dikprofiel met betm'	JPEG image	Cross section of improved dike considering a possible solution of increasing dike's height in order to achieve safety standard.
[3]	'Dwp-Basisreferentie'	JPEG image	Cross section of conceptual final solution of dike's improvement. It shows modification of rear slope and inclusion of revetment to increase resistance against overtopping.
[4]	'dwp-principle-overslag-ontwerpruimte'	JPEG image	Different cross section related with different possible solutions to improve safety of the dike.
[5]	'Legger-Afsluitdijk'	PDF file	Information about Afsluitdijk. Contains layouts of plan views and cross sections of different locations of the dike, including The Monument location.
[6]	'memo-DGRW-verschil-HYDRA-HR-rekenbijlagen'	Word file	Technical memorandum that includes hydraulic calculations and results about wave climate and overtopping rate on the Aflsuitdijk. Includes calculations for the year 2006 and estimation of sea level rise to the year 2050.
[7]	'Steen Toets v403 Aflsuitdijk Steenbekleding Waddenzee'	Excel file	Detailed survey of Aflsuitdijk; wave climate at different locations of the dike; list of materials.
[8]	'WG-SE20050319 DEFv3 Eindrapport'	PDF file	Afsluitdijk safety review 2005 project, executed by DHV Ruimte en Mobiliteit BV.

2.2 Other sources

Information obtained from other sources is presented in Table 2.2.

Table 2.2. Information obtained from other sources

Number	Item name	Type	Description
[9]	Site appreciation #1	Visual appreciation, pictures	First visit to The Monument during October 3rd, 2012.
[10]	Site appreciation #2	Visual appreciation.	Second visit to The Monument during October 14th, 2012.
[11]	Google Earth images	Satellite images.	Available images of The Monument location.

3 SITE APPRECIATION ANALYSIS

The field visits [9] and [10] allowed the realisation of a visual survey of The Monument location. The survey provided a general view of the location, including type of revetment, presence of walls, and location of singularities, roads and buildings, among others. Relevant information to the developing of the project is presented in Figures 3.1 to 3.6.

Figure 3.1 shows the seaside slope of the Afsluitdijk at The Monument location. Relevant characteristics observed on site are the presence of a toe made of rocks, the slope has a basalt revetment with presence of grass and on the upper part of the slope exist a steep section, which in some parts appears to be vertical. At this location, the crest of the dike has a bicycle lane, a car lane and a parking area, all made with asphalt.



Figure 3.1. Seaside slope of Afsluitdijk at The Monument location

Figure 3.2 shows the seaside slope of the Aflsuitdijk at the standard cross section, outside The Monument location. Relevant characteristics are the presence of a toe made of rocks, the slope has a partial revetment of basal (lower part) while the upper part has a revetment of grass. The crest of the dike is also has a grass revetment.



Figure 3.2. Seaside slope of Afsluitdijk at the standard cross section

The cross section at The Monument location is different than the standard cross section (presence of the wall, different width of the crest and different revetment). The Afsluitdijk has two transition sections (north and south boundaries of The Monument). Those sections are characterised by a variable height of the wall, a variable level of the bicycle lane and a variable width of the dike's crest. Figure 3.3 shows a photograph of the south transition section.



Figure 3.3. Southern transition between standard cross section and The Monument cross section

From the site visit, it could be appreciated that both transition sections (north and south boundaries of The Monument) are symmetrical.

During the visit, on the crest of the dike at The Monument location, several obstacles were found. These obstacles corresponds to a statue (A), an information wall (B), a scale dike of basalt (C) and a bridge for pedestrians (D). Figures 3.4 present photographs of these singularities.



(a)



(b)



(c)



(d)

Figure 3.4. a) Statue; b) Information wall; c) Scale dike of basalt; d) Bridge for pedestrians

On the rear slope, a highway with two double lane tracks exists. That highway does not change its configuration when it passes The Monument location. Figure 3.5 shows the highway at The Monument location.



Figure 3.5. Highway at The Monument location

Finally, the rear slope of the dike at The Monument location presents two main characteristics: the presence of a large platform that serves as a parking area for vehicles; and a building with a tower (includes a restaurant).


(a)

(b)

Figure 3.6. a) Parking area; b) Building with tower

4 WAVE CLIMATE DEFINITION

The wave climate definition (design storm of 1/10,000 years) is obtained from reference [6], which presents several definitions of wave climate. The differences among these definitions are:

- Wave propagation model (from deep water across the Wadden Sea) used.
  - HR2006
  - HYDRA-K2012 (probabilistic)
- Scenario
  - Mean sea level elevation for year 2012.
  - Projection of sea level elevation for year 2050.
- Location at the Afsluitdijk
  - East (DO – 5)
  - Middle (12 – 20)
  - West (25 – End)

Information available includes a reference sea level elevation, significant wave height, mean wave period, a calculation of overtopping flow rate and a fictitious crest level to obtain an overtopping flow rate equal to 10 l/s/m.

Tables 4.1 to 4.4 present part of the information for the different wave climate scenarios defined.

Table 4.1. Wave climate for year 2012, model HR2006

Location	Sea elevation	Significant wave height	Mean wave period
	[m+NAP]	*[m]*	*[s]*
East	5.0	2.45	6.74
Middle	5.1	2.45	6.74
West	5.2	2.45	6.74

Table 4.2. Wave climate for year 2012, model HYDRA-K2012

Location	Sea elevation	Significant wave height	Mean wave period
	[m+NAP]	*[m]*	*[s]*
East	5.04	2.62	5.17
Middle	5.11	3.40	5.62
West	5.19	2.66	5.20

Table 4.3. Wave climate for year 2050, model HR2006

Location	Sea elevation	Significant wave height	Mean wave period
	[m+NAP]	*[m]*	*[s]*
East	5.5	2.85	7.4
Middle	5.6	2.85	7.4
West	5.7	2.85	7.4

Table 4.4. Wave climate for year 2050, model HYDRA-K2012

Location	Sea elevation	Significant wave height	Mean wave period
	[m+NAP]	*[m]*	*[s]*
East	5.54	3.02	5.70
Middle	5.61	3.90	6.18
West	5.69	3.08	5.72

Considering that the current project is being developed for The Monument location and it should include a projection of the sea level rise for the next years, information of Table 4.4 will be considered. It also has a more recent model to account for the propagating waves.

Table 4.4 presents information for three locations. Neither of it includes The Monument (location approximately at 7 kilometres from the beginning of the dike). Therefore, it will be considered the "Middle" location because its related data is more conservative.

Hence, wave climate is defined as:

- Future sea level elevation = 5.61 m + NAP
- Significant wave height = 3.90 m
- Mean wave period = 6.18 s

Finally, these tables do not provide information about direction of the waves. To estimate the overtopping, a wave approaching perpendicularly to the dike will be considered, because the values under this situation are more conservative.

5 DEFINITION OF RELEVANT CROSS SECTIONS

Overtopping rate will be calculated for several relevant cross sections. Those cross sections are:

- Cross section at The Monument location (section A)
- Standard cross section (section B)
- Transition cross section 1 (closer to standard cross section) (section C)
- Transition cross section 2 (closer to The Monument cross section) (section D)

Figure 5.1 presents a plan view with the location of the defined cross sections (source [11]).

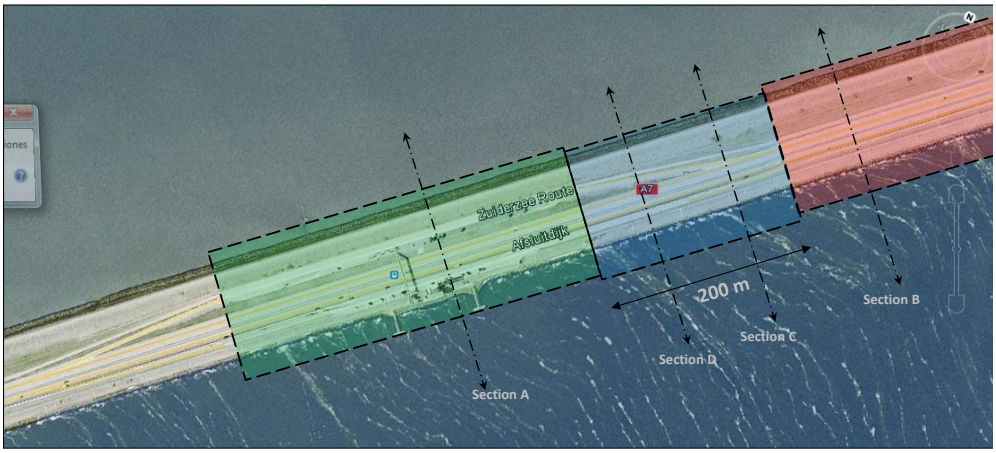

Figure 5.1. Plan view with location of cross sections.

Although section B is outside of the area of study, it is important to obtain an overtopping estimation in order to compare it with the overtopping results defined in reference [6]. Transition sections are important because they are not part of the previous study (reference [6]) and the field visit revealed that these sections are covered with grass (dike crests and rear slope) and the crest width is thinner than in the standard cross sections.

Considering that the transition area has a total length of approximately 200 m, section C is located at approximately 70 m from the standard cross section, while section D is located approximately 70 m from The Monument area. Two transition areas are distinguished: one on the north side and another on the south side of The Monument. It will be considered that both areas are symmetrical; hence, the transition sections will be defined only for the north side.

Figures 5.2 and 5.3 present typical cross sections of The Monument and standard dike, respectively (from reference [5]).

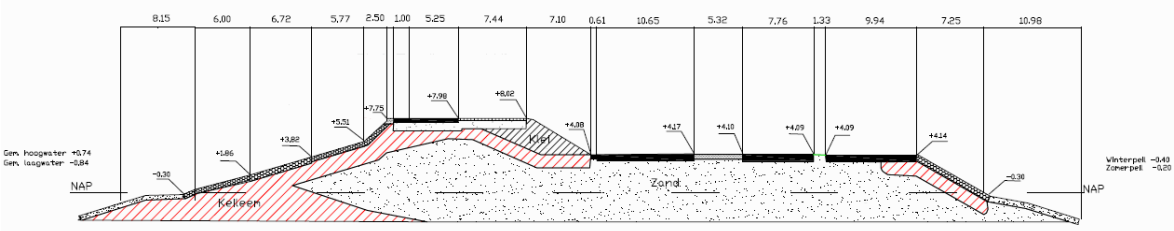

Figure 5.2.Cross section at The Monument location

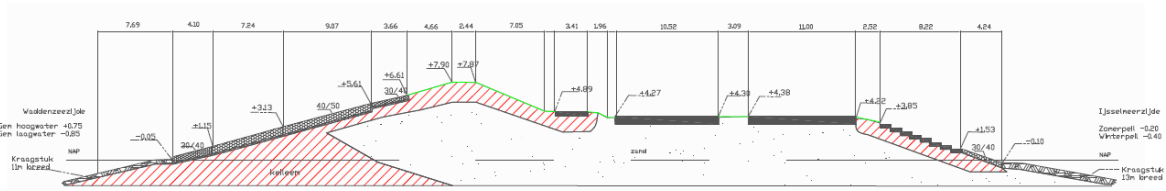

Figure 5.3. Afsluitdijk standard cross section

According with the information obtained from these Figures, at The Monument location the crest elevation is +7.75 m while the standard cross section is slightly taller (+7.9 m). Another important feature that was seen during the visit is the presence of a small wall at The Monument location, which is not present in Figure 5.2.

There is no direct information about cross sections for the transition area. Therefore, it is necessary to recreate it from the available information. The site visit allowed seeing that variation of the crest elevation, the width of the crest and the height of the seawall varied linearly from section A to section B. Hence, sections C and D were constructed assuming that linear variation between known sections. Figures 5.4 and 5.5 present the front slope of sections C and D, respectively.

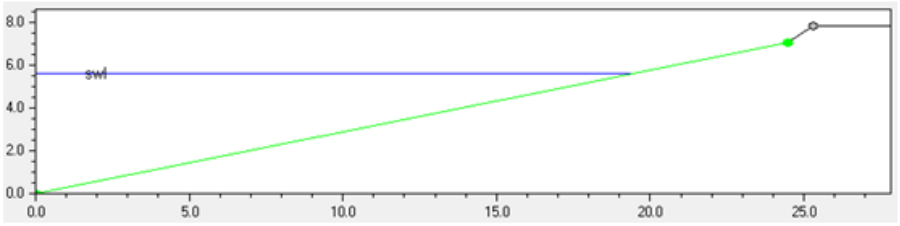

Figure 5.4. Transition cross section C

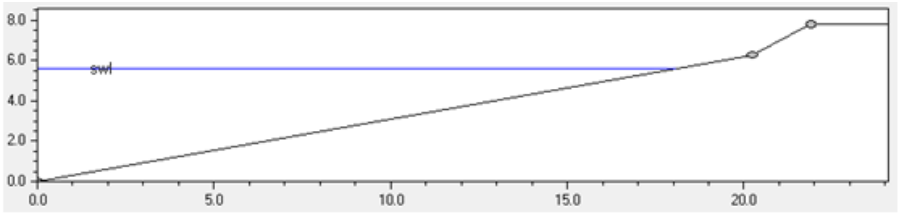

Figure 5.5. Transition cross section D

Overtopping calculation requires a proper definition of the type of revetment for each cross section. While cross sections A, C and D have basalt all over the sea slope, cross section B has a mixed revetment. Up to elevation +6.61 m, it is covered with basalt, while from elevation +6.61 to the top of the dike (+7.9 m), it is covered with grass.

6 Location and Dimensions of Obstacles on Dike's Crest

The field visits revealed the existence of several obstacles at The Monument location. These obstacles may generate a 'concentration' of overtopping flow both in the top and in the rear slope of the Afsluitdijk. The list of detected obstacles is:

- Statue
- Information wall
- Mini dike (Scale dike of basalt)
- Pedestrian bridge
- Monument Tower (Building with tower and restaurant)

The pedestrian bridge is place over some small blocks of concrete. The dimension of these blocks does not exceed 1 m, therefore, it will be assumed that these obstacles are too small to generate an important effect of flow concentration. Hence, it will not be considered in the following analysis.

Figure 6.1 shows a plan view of The Monument location. Several obstacles are highlighted: statue (A), information wall (B), scale dike of basalt (C) and building on the rear part (D).

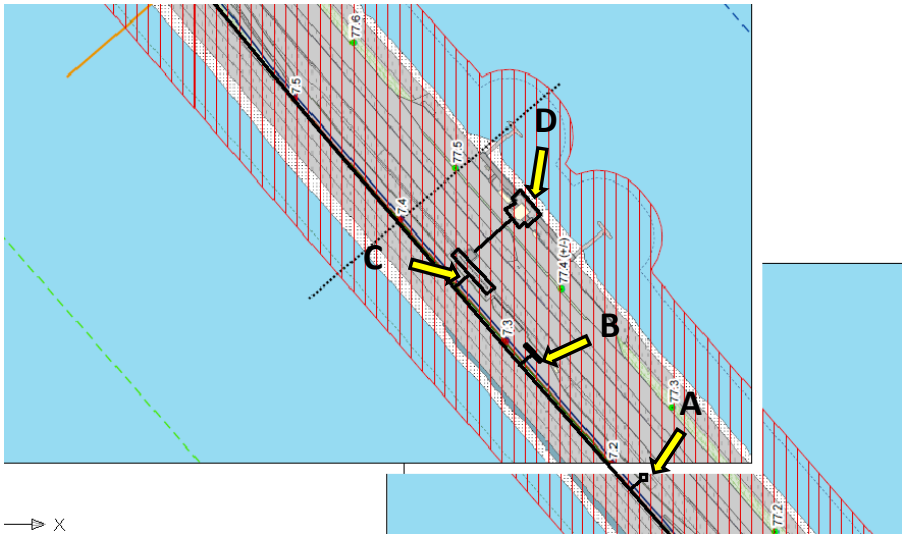

Figure 6.1. Transition cross section D. Source: reference [5]

All of these obstacles are located in the regular section of The Monument area (i.e. they are not located in any of the transition areas or the standard cross section of the Afsluitdijk). Therefore, the overtopping rate that will be produced in front of these obstacles can be considered as uniform; hence, the relative position of each obstacle along the dike is not relevant.

The important parameters related with each obstacle are the dimensions (width) and distance to the top of the dike at the defence line. While the first one will be used to define how much flow can be concentrated on the sides of the obstacle, the second will be used to define how much effective overtopping will reach the obstacle.

Dimensions were obtained with software AutoCAD and are approximated. Table 6.1 presents a summary with relevant dimensions and distances.

Table 6.1. Relevant dimensions and distances of obstacles at The Monument area

Obstacle	Denomination	Width	Distance to defence line
		[m]	*[m]*
Statue	A	5 (1)	9
Information wall	B	14	11
Mini dike	C	34	13
Monument Tower	D	21	33 (2)

(1) The statue is not aligned with the dike's axis, but it is rotated with an estimated angle of 45°. Presented width corresponds to the projection of two sides of a square, which has a side of 3.8 m.
(2) Because the building is located in the rear slope of the dike, the presented distance corresponds to the horizontal distance to the bottom of the first rear slope, which is basically the width of the highway plus the parking width plus existing tolerances.

7 FINAL COMMENTS

Regarding with the analysis of available information, the following comments are made:

- Site visits allowed the visualization and detection of several obstacles. In this analysis, only the most important (largest) obstacles were considered. Some minor obstacles, like fences, bus stops, steps and small platforms were not considered because it is considered that their effect is not significant.
- The model to estimate wave conditions under a storm of 1:10,000 years is considered to be valid. Hence, no further verification of its results will be made.
- However, it is important to emphasize that it is assumed that the results of wave propagation from deep water are considered at the top of the toe. Hence, future calculation of overtopping flow rate will consider a cross section that does not include the toe of the dike.
- Cross sections considered are obtained from a well-known reference. Nevertheless, there are some visual differences that are not perfectly explained by these cross sections. More specifically, the presence of a sea wall at The Monument area is not clearly seen in Figure 5.2, which may generate results more conservative than reality. However, in accordance with the client, this section will be considered as a basis of the hydraulic calculations.
- There are no cross sections available at the transition areas. Therefore, the linearization procedure is the best possible assumption that can be made. However, there are uncertainties about these cross sections, which can generate errors in overtopping estimation. A future definition of overtopping at these locations necessarily will need a proper survey of these sections.
- Location and dimensions of the obstacles are on the basis of reference [5] and the field visits. However, there is no detailed information about these obstacles. Therefore, dimensions are only approximations based on available information.
- Finally, the available information does not include anything related with foundations of the structures. Considering that dimensions of the visible part of these structures are only approximations, it is not possible to assume any dimension and/or shape of their foundations. Therefore, a calculation of resistance against overturning will be possible to make only in future stages of engineering.

TU DELFT – MULTIDISCIPLINARY PROJECT CIE4061

Afsluitdijk Project
"The Monument" Location

Problem Analysis

Sien Liu, Jun Huang, Sebastian Rayo, Tai Yan Lim

21/12/2012



CONTENTS

1 Introduction 2
1.1. Background 2
1.2. Problem Description 2
1.3. Document Scope 2
2 Overtopping 3
2.1 Cross-section selection 3
2.2 Overtopping rate 3
2.3 Flow depth and flow velocity 5
3 Flow distribution 7
3.1 Assumptions 7
3.2 Figures of places of interest 9
3.2.1 Statue 9
3.2.2 Monument tower 10
3.3 Information Wall 11
3.4 Mini dike 12
4 Diagnosis 14
4.1 Critical Spots Definition 14
4.2 Analysis 15
4.2.1 Spot A: transitions 15
4.2.2 Spot B: Front defence at The Monument 16
4.2.3 Spot C: Rear slope at The Monument 17
4.2.4 Spot D: Sides of tower building 18
4.3 Recommendations 18
5 Final comments 19

1 INTRODUCTION

1.1. Background

The Afsluitdijk (Enclosure Dam) is a main dam that forms the fundamental part of the larger Zuiderzee Works that separates the Zuiderzee, a salt water inlet of the North Sea, and turning it into the fresh water lake of the IJsselmeer. It protects the central Netherlands from the effects of the North Sea. It was constructed between 1927 and 1933, and runs from Den Oever on Wieringen to the village of Zurich in Friesland. It is 32 km long and 90 meters wide, rising to 7.25 meters above sea-level, with an incline of 25% on each side.

At the location along the Afsluitdijk where the final water passage was closed ('De Vlieter'), a lookout tower known as 'The Monument' was built in 1933. It was presented by the Zuiderzee Works Construction Company and designed by architect W.M. Dudok. The site has a statue of a "Steenzetter", and also marks the inscription 'A living nation builds for its future'. A statue of Cornelis Lely has also been erected near Den Oever on the Barrier Dam itself.

The Afsluitdijk with The Monument are currently managed by the Ministry of Infrastructure and the Environment ("The client"). There is a restaurant at The Monument where the client has sublet it for private operator to manage it.

1.2. Problem Description

With the anticipation of increase storm intensity and sea level rise in the future, the client had previously engaged a consultant to analyze the existing design of Afsluitdijk for a design storm of 1:10,000 years. According to the client, the result of the study concluded that the standard cross-section of Afsluitdijk is not sufficient to withstand the design storm of 1:10,000 years, hence, modifications of it are required. The study also found that during the design storm, there is a significant overtopping over the dike.

The client is concerned about the significant overtopping found from the previous study may have adverse impact on the non-standard cross-section of the dike where The Monument is located. Therefore, the client has requested our design team to look into the dike section at The Monument location.

1.3. Document Scope

The main objectives of this document are:

1. To calculate the overtopping flow rate and velocity of each cross – section with certain software.
2. To analysis the flow distribution of each obstacle trying to figure out the largest flow rate.
3. The 4 critical spots are defined and analysed to figure out which of the spots are most dangerous.

2 OVERTOPPING

2.1 Cross-section selection

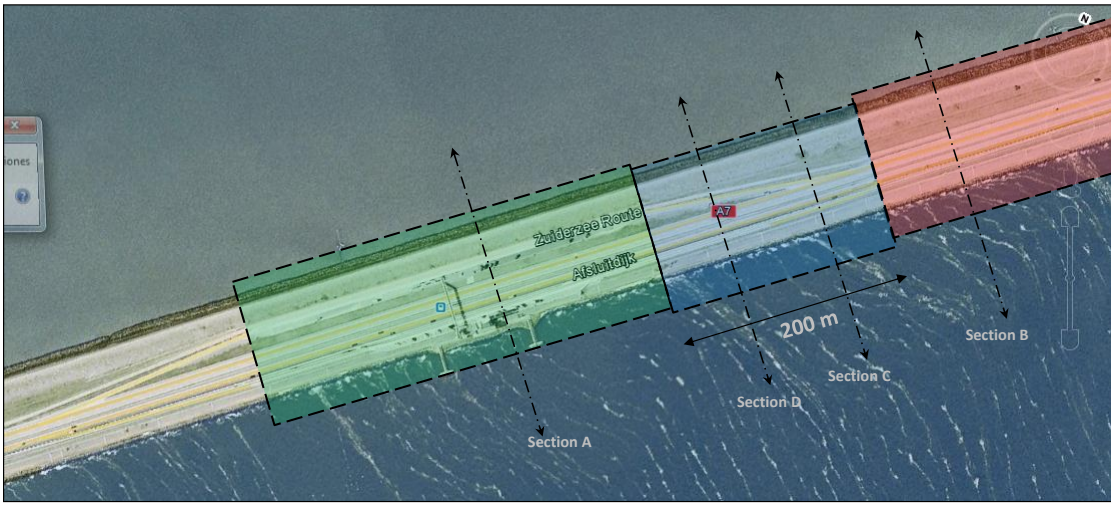

Figure 2.1 Plan view with location of cross sections.

In this procedure, 4 cross-sections are chosen to calculate based on the particular shape respectively.

The first cross-section is the standard cross-section, the second cross-section is the monument cross-section, and the third and the fourth cross-section are two transition cross-sections from the standard cross-section to the monument cross-section.

2.2 Overtopping rate

The overtopping rates and maximum wave overtopping volume are calculated by using computer program 'PCOverslag', which can be downloaded from :

http://www.helpdeskwater.nl/onderwerpen/applicaties-modellen/@28822/pc-overslag/

Overtopping rates at four locations are calculated based on the data that have been given. Standard cross-section and monument cross-section can be seen from two pictures below (plan views are shown in Figure 1.1):

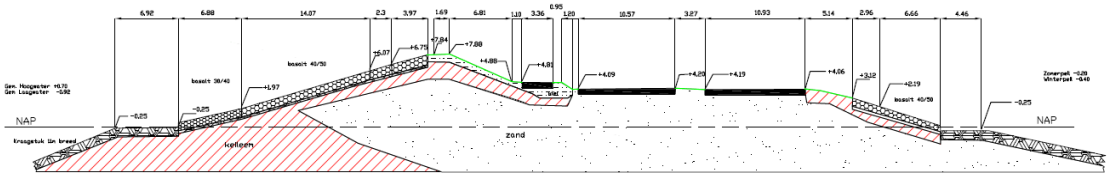

Figure2.2 cross-section of standard segment (*LEGGER AFSLUITDIJK, 2009*)

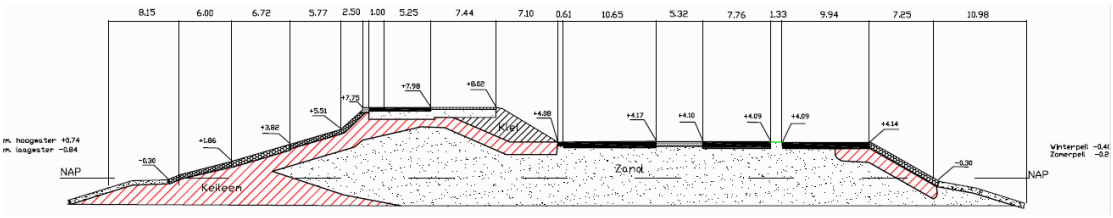

Figure 2.3 cross-section of monument segment (*LEGGER AFSLUITDIJK*, *2009*)

The cross-sections of transition 1 and transition 2 are interpolation at two locations in between monument cross-section and standard cross-section. Simplified slope drawings of cross-sections with design water level are shown in following four pictures:

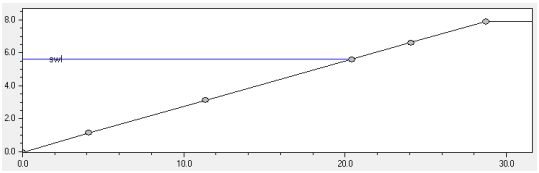

Figure 2.4 standard cross-section

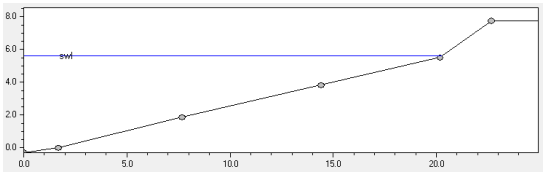

Figure 2.5 monument cross-section

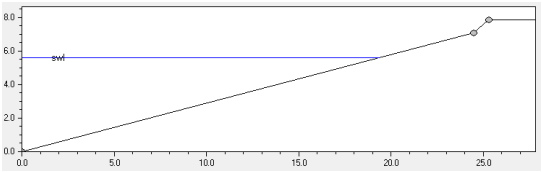

Figure 2.6 transition 1 cross-section

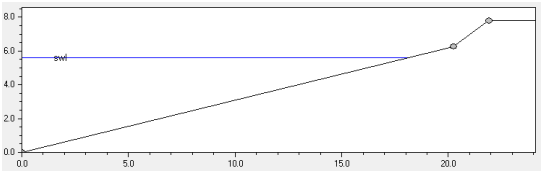

Figure 2.7 transition 2 cross-section

The design conditions are 1 in 10,000 years, which are tabulated as follows:

Dijkvak	Toetspeil H [M+NAP]	Golfhoogte Hs [m]	Golfperiode $T_{m-1,0}$ [s]
West (DO – 5)	5,54	3,02	5,70
Midden (12-20)	5,61	3,90	6,18
Oost (25-Frlh)	5,69	3,08	5,72

Table 2.1 design conditions of 1:10,000 years

It can be clearly seen that, the design conditions are different from location to location in the whole Afsluitdijk. Considering that our interest area is in the middle of the Afsluitdijk, the design condition of H=5.62 m, H_s=3.9 m, $T_{m-1,0}$=6.18 s will be selected for wave overtopping calculation. The storm duration is considered to be 6h, and the incident wave angles are considered to be 0 in order to obtain a conservative result.

There are only two different kinds of materials on the seaward slope, basalt and grass. The influence factors of roughness are $\gamma_f = 0.9$ and $\gamma_f = 1$ respectively. The seaward slopes consist of several segments with different $\tan\alpha$, this effects are also taken into consideration in 'PCOverslag'.

The results in the table show the output of 'PCOverslag'. Several important parameters like wave run-up, mean wave overtopping rates and maximum wave overtopping volume are selected. The maximum wave overtopping volume has high uncertainty and highly depends on the storm duration. However, it an important parameter to evaluate the hazard on buildings and infrastructure caused by wave overtopping.

parameters	Standard cross section	Monument cross section	Transition 1	Transition 2
R_c (m+NAP)	7.90	7.75	7.90	7.75
$Z_{2\%}$ (m+NAP)	12.48	14.2	14.163	12.635
$Z_{2\%}$- R_c	4.58	6.45	6.263	4.885
q (l/s/m)	270.88	579.82	549.036	289.168
V_{max} (l/m)	32349.17	59066.09	56573.1	33503.66

Table 2.2 PC overtopping software results

2.3 Flow depth and flow velocity

The flow depth and flow velocity are important to estimate the erosion rate of the grass and clay which will be the cause of dike breaching. Base on the newly developed theory by Bosman (see in document of literature review), the overtopping flow depth and flow velocity can be calculated, but under following assumptions:

- Dike crest is horizontal.
- Vertical flow velocity to the dike slope can be neglected.
- Pressure term is constant over dike crest.
- Viscous effects in flow direction are small and bottom friction is constant over dike crest.

The formula that we use to calculate the flow depth and flow velocity are further development by Bosman based on formula of Schüttrumpf and Van Gent (2003). However, these formulas are developed from experiments with only two kinds of dike slope (1:4 and 1:6). So the results besed on these formulas have certain uncertainties but they offer us a good view of overtopping flow.

The results with some important parameters are shown in the table (more details are in appendix 1). Same consideration is taken to obtain conservative results, so the influence factors of roughness are considered to be 1.

parameters	Standard cross section	Monument cross section	Transition 1	Transition 2
$H_{(0)}$ [m]	0.46	0.41	0.40	0.41
$V_{(0)}$ [m/s]	6.6	6.2	6.1	6.2
Crest width [m]	2.5	19	18	3
$H_{(end)}$ [m]	0.24	0.03	0.004	0.19
$V_{(end)}$ [m/s]	4.3	0	0	3.2

Table 2.3 flow depth and flow depth on crest

3 FLOW DISTRIBUTION

Based on the result from the data analysis, the flow distributions through the following obstacles were calculated:

- Statue,
- Monument Tower (Building with restaurant and tower),
- Information Wall and
- Mini- Dike (Scale dike of basalt)

These obstacles around The Monument location were the only possible obstacles from the analysis to generate a 'concentration' of overtopping flow both in the top and in the rear slope of the Afsluitdijk.

3.1 Assumptions

The following five assumptions were made on the flow of the water after it overtop the crest and travel through the inner and encounter obstacles.

- Flow reduction of 1/2 L is used to estimate the overtopping flow just in front of obstacle, q_2.
- Flow distribution coefficient, W_1/W_2 varies to max 1.00. => $q_3 = 2 \times q_2$, where Max W_2 = 5m
- For long obstacle, flow from edge to W_1 m is assumed to be diverted to the sides of obstacle.
- For long obstacle, flow that is between W_1 m away from both edges is assumed to be reflected.
- For Monument Tower, no flow reduction is applied to q_2 (i.e. 61.03 l/s/m), after it passes down from the inner slope.

One important point to note is that these assumptions were conservative in nature and thus will overestimate the actual amount of flow that passed the obstacle. More research is required in future to validate these assumptions and obtain a more cost effective design.

After overtopping, the water will flow from the dike's crest down on inner slope till it encounters an obstacle. Overtopping water flowing over a distance will lose kinetic energy due to friction losses with the surface it had travelled. According to the guideline given by the Eurotop manual, this effective discharge (q_2) just when encountered an obstacle can be approximated by reducing the overtopping discharge (q_1) by a factor of the distance between the obstacle and seawall crest (L) such that $q_2 = q_1/L$, where L vary with a range of 5 to 25m. The calculated q1 for the Monument area is 579.82 l/s/m. This reduction factor L is dependent on the type of surface where the overtopping water flows over before encountering an obstacle. For a less porous surface in this study, this reduction factor L should be reduced. Thus a 1/2 L reduction factor is assumed instead of L under the first assumption.

The second assumption described the amount of overtopping water flowing at the side of the obstacle (q_3). See the red arrow in figure 1 below. This flow (q_3) consists of flow from q_2 and the diverted flow when encountering obstacle. The amount of flow diverted at the sides of the obstacle depends on the flow condition such as the flow speed, approach angle and also on the geometry, surface roughness and porosity of the obstacle. Based on the observation from the literature, this flow (q_3) is always less than twice the original amount of flow just when encountered the obstacle (q_2). Thus the contribution from the diverted flow is at most $1xq_2$ such that $q_3 = \max(2xq_2)$.

Based on the third assumption, W_1 is defined as the width of flow that will be diverted to the sides of obstacle. In the case of a long obstacle, its length is much greater than its width and W_1 is assumed to be 1m. The rest of the flow encountering the obstacle that is in between W_1 away from both edges, is assumed to be directly reflected as shown by the purple arrow in figure 1 under fourth assumption. Hence, the different amount of q_3 due to the different W_2 expressed as a flow distribution coefficient, W_1/W_2 can be determined. Thus, the amount of flow at obstacle's side (q_3) = flow just encountering obstacle (q_2) + flow diverted to obstacle's side => $q_3 = q_2(1+W_1/W_2)$. In addition, the amount of spreading of q_3 (W_2) observed from the literature is always less than 5m from the edge of the obstacle (i.e. W_2 = max 5m). Hence, $Q_3 = q_3 \times W_2$ can be found.

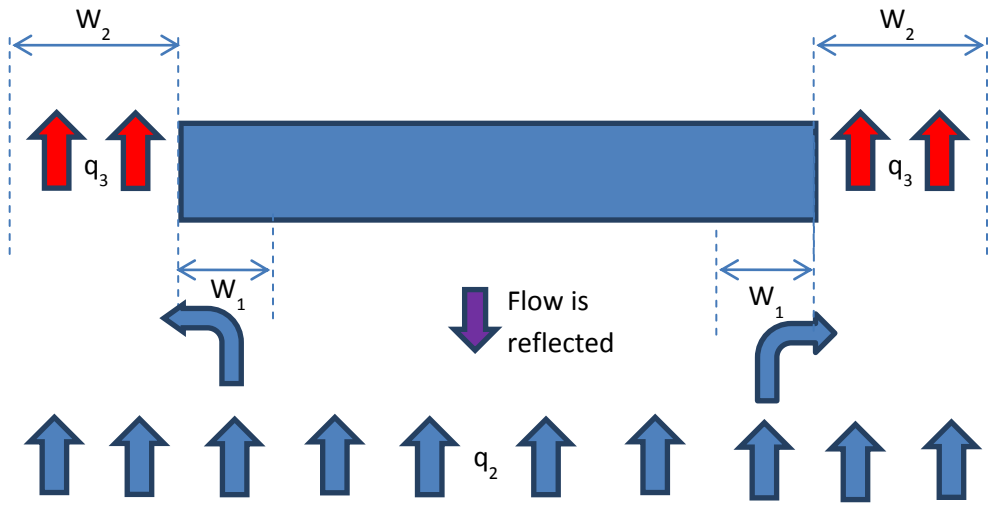

Figure 3.1: Figure showing the definition of q2, q3, W1 and W2.

The fifth assumption, overwrite the 1/2L reduction factor assumed under the first assumption in computing q_2. This fifth assumption is only applied for the computation of q_2 for the Monument Tower. This assumption is used is because the distance between the dike crest and the Monument Tower is more than 33m. A 1/2L reduction factor if used will reduce q_2 to 35.14l/s/m than 61.03 l/s/m which is less conservative. Since, the effect of the flow when encountering a specified obstacle (I.e. Monument Tower) is not properly understood and study at this moment, a more conservative value is recommended and thus the fifth assumption is adopted.

In the following section, the results of flow distribution through the following obstacles were shown:

- Statue,
- Monument Tower (Building with restaurant and tower),
- Information Wall and
- Mini- Dike (Scale dike of basalt)

3.2 Figures of places of interest

3.2.1 Statue

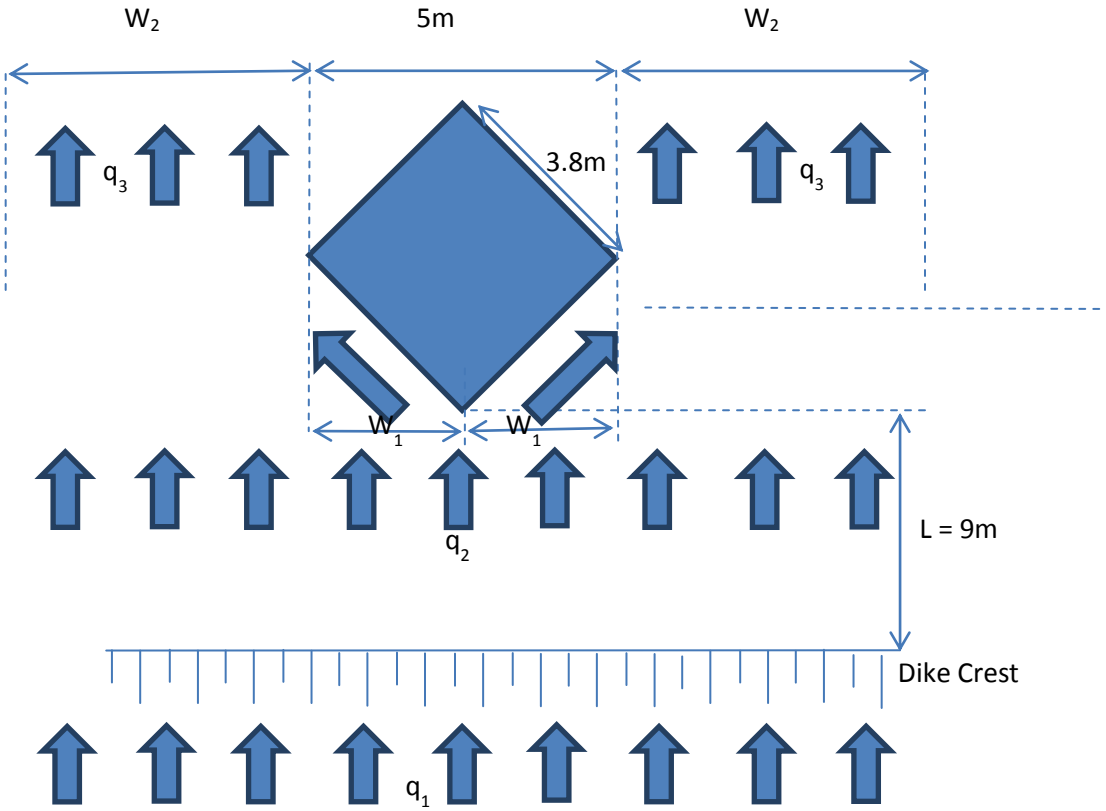

Figure3.2 Flow distribution of statue

The corresponding data is listed in the table below.

q1	579.82	l/s/m
L	9.00	m
x	0.50	
q2	128.85	l/s/m

W1	2.50	m
W2	2.5 - 5	m
W1/W2	0.5 - 1	
q3	193.27 -257.70	l/s/m

Table 3.2.1 relevant parameter for location of statue

3.2.2 Monument tower

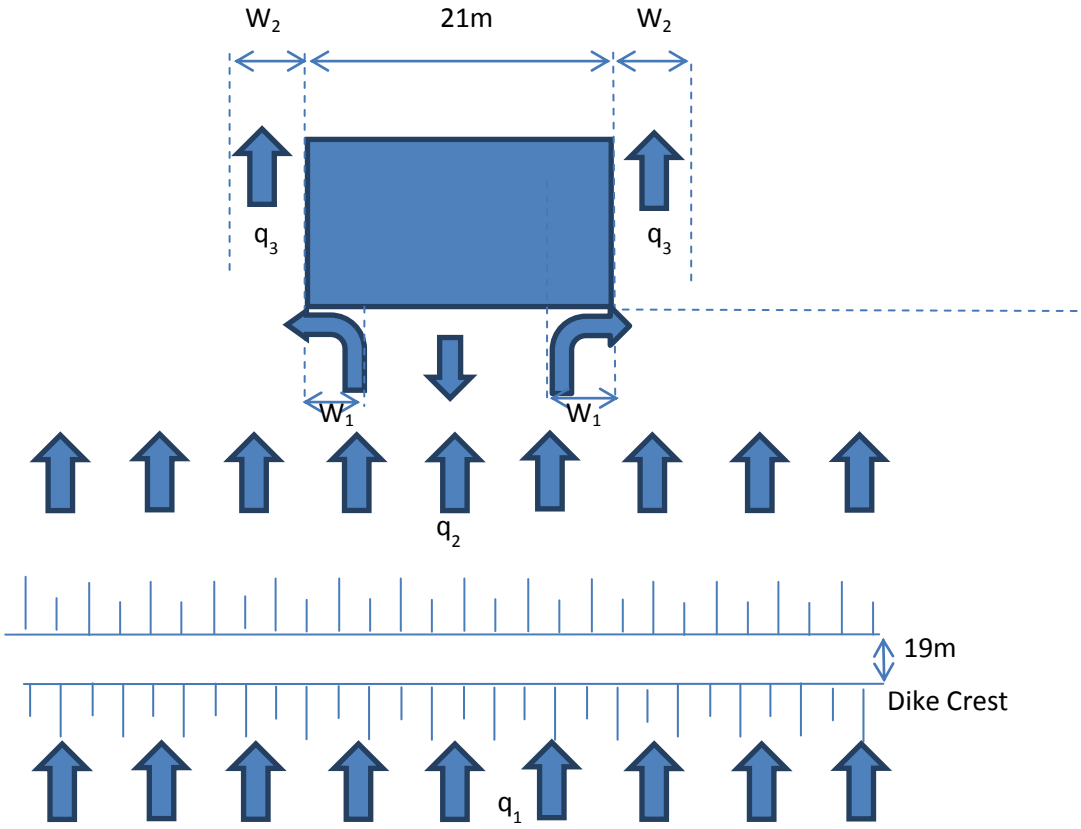

Figure3.3 Flow distribution of Monument tower

The corresponding data is listed in the table below.

q1	579.82	l/s/m
L	19.00	m
x	0.50	
q2	61.03	l/s/m

W1	1.00	m
W2	1.0 - 5.0	m
W1/W2	0.2 - 1.00	
q3	73.24 - 122.07	l/s/m

Table 3.2.2 relevant parameter for location of monument tower

3.3 Information Wall

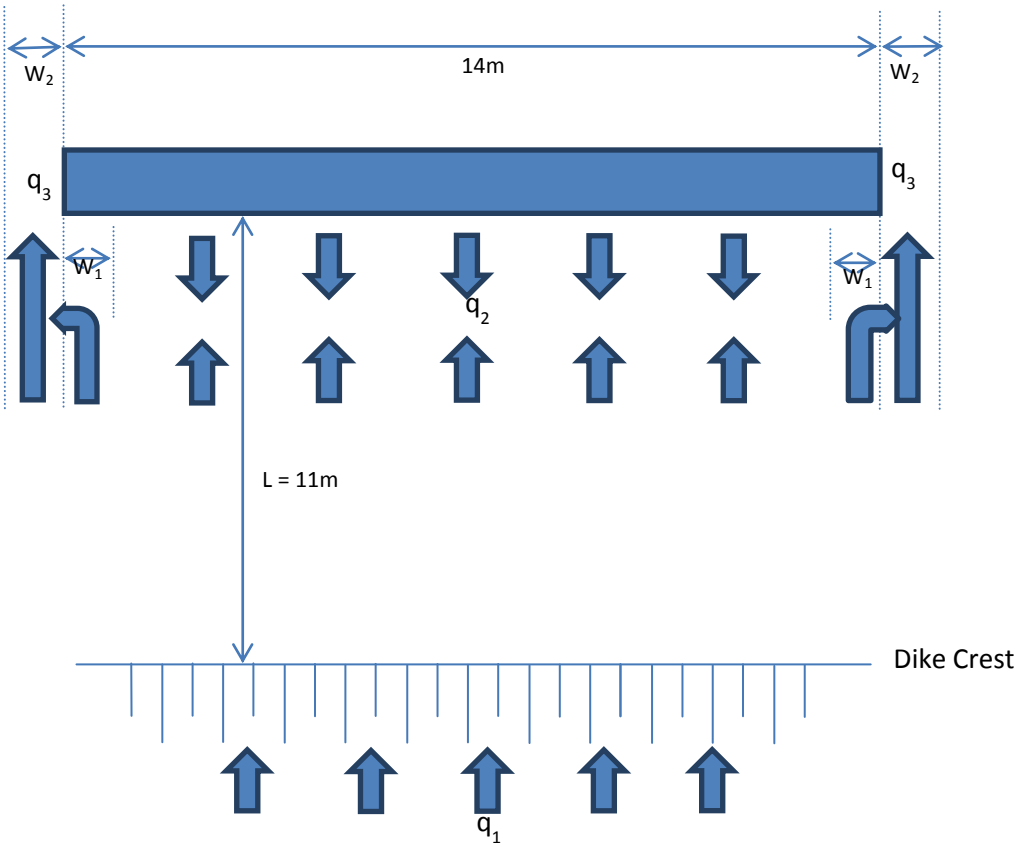

Figure3.4 Flow distribution of Information Wall

The corresponding data is listed in the table below.

q1	579.82	l/s/m
L	11.00	m
x	0.50	
q2	105.42	l/s/m
W1	1.00	m
W2	1.0 - 5.0	m
W1/W2	0.2 - 1.00	
q3	126.51 - 210.84	l/s/m

Table 3.2.3 relevant parameter for location of information wall

3.4 Mini dike

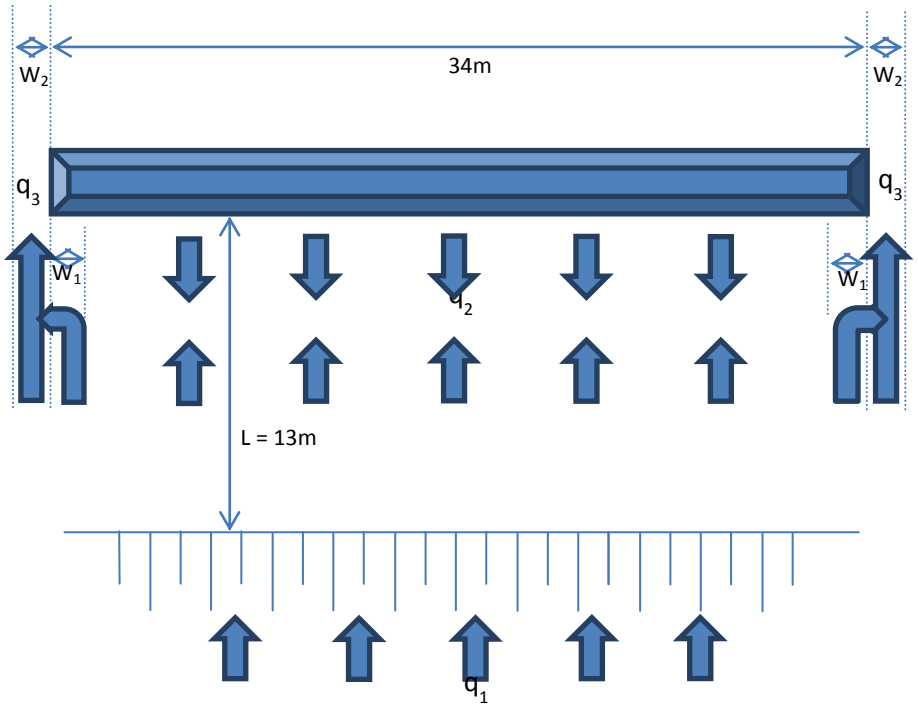

Figure3.5 Flow distribution of mini dike

The corresponding data is listed in the table below.

q1	579.82	l/s/m
L	13.00	m
x	0.50	
q2	89.20	l/s/m
W1	1.00	m
W2	1.0 - 5.0	m
W1/W2	0.2 - 1.00	
q3	107.04 - 178.41	l/s/m

Table 2.2.4 relevant parameter for location of mini dike

4 DIAGNOSIS

4.1 Critical Spots Definition

The calculation of overtopping flow rate and its spatial distribution at the top of the dike have revealed several areas that might be in risk of breaching if there is a storm of 1:10,000 years. The critical spots are presented in Figure 4.1.

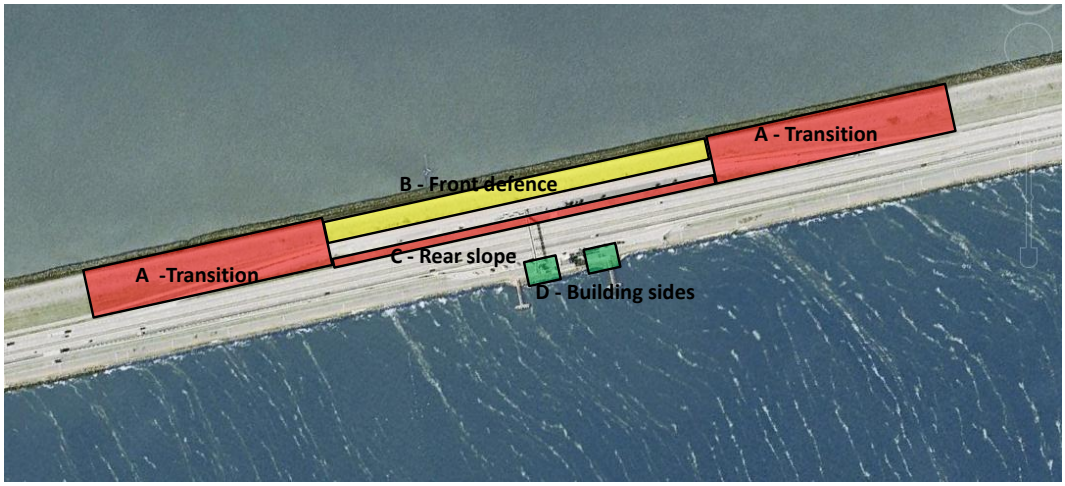

Figure 4.1. Critical spots at The Monument location

The critical spots are:

- Spot A: both transitions (north and south sides) from The Monument cross section to standard cross section.
- Spot B: front defence at The Monument area (part of the high parking area closer to the seaside slope).
- Spot C: rear slope at The Monument area (from parking area to highway platform).
- Spot D: sides of the tower building (rear slope from low parking area to lake side).

Figures 4.2 and 4.3 show photographs of the critical spots.


(a)


(b)

Figure 4.2. a) Spot A: transitions from The Monument to standard dike; b) Spot B: front defence at The Monument


(a)

(b)

Figure 4.3. a) Spot C: rear slope at The Monument; b) Spot D: sides of tower building

4.2 Analysis

4.2.1 Spot A: transitions

The analysis presented is the same for both transitions because it is considered that they are symmetrical between them, hence, the geometry of the cross sections is the same. In addition, the wave field is the same at both locations. Therefore, the overtopping flow rate distribution can be considered as unique.

Previously the overtopping flow rate was calculated at two different cross sections (transition 1 and 2). The values obtained were 549 l/s/m and 289 l/s/m, respectively. Considering that the boundaries of both transitions are The Monument and the standard dike, the overtopping flow rate at those points is 271 l/s/m and 580 l/s/m, respectively.

At both transitions, on the front slope the dike has a revetment with basalt. Nevertheless, the top and rear slope of the dike has grass revetment. Figure 4.4 presents a photo of one of the transition spots.



Figure 4.4. Photograph of one of the transition spots

The strength of grass is quite small, especially when there are large velocities of overtopping. Calculations of overtopping velocities are in the range of 6 to 6.5 m/s, which are larger than the maximum allowed velocities for grass. Figure 4.4 shows the maximum permissible duration of grass coverage depending on the flow velocity and the quality of the grass coverage.

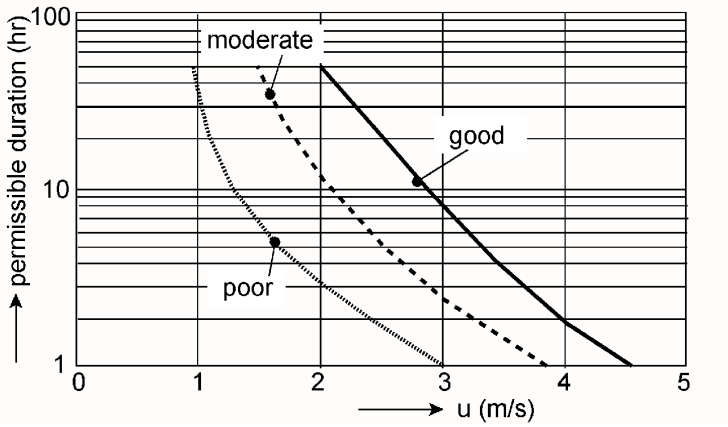

Figure 4.5. Permissible flow duration on grass cover. Source: Schiereck, G. J., 'Introduction to Bed, Bank and Shore Protection'

The overtopping velocities exceed the maximum allowed in this graph, which means that the permissible duration of a storm will be less than one hour. Therefore, it can be concluded that the resistance of the grass for overtopping flow rate in the range 271 to 580 l/s/m is very limited.

Below the grass cover there is a clay layer. If there is no grass cover anymore, the clay layer will have a limited resistance against overtopping load. Applying the Parthenade method (suitable for cohesive soils) and assuming the clay layer has a critical shear stress equal to 5 Pa, the erosion process in this layer will take about 1.5 hours. Hence, it can be stated that the resistance of this layer is low when the outer protection has been removed.

Considering that the resistance of both the grass cover and the clay layer are quite low against the overtopping loads, diagnosis indicates that an improvement in this spot is required.

4.2.2 Spot B: Front defence at The Monument

The overtopping flow rate is fixed and is equal to 590 l/s/m. In this spot, the dike's rear slope has a basalt revetment, while on top of the dike there is a small concrete wall. Figure 4.6 presents a photograph of part of this area.



Figure 4.6. Photograph of front defence at The Monument

The overtopping rate is large but there is a strong revetment at this location. The main assumption is that behaviour of concrete and asphalt against large overtopping flow rates (especially for erosion) is good. Hence, no further improvements are considered to protect the front defence.

It is important to emphasize that further research of asphalt under very large flow velocities is required, in order to define if this material may have risk of failure.

4.2.3 Spot C: Rear slope at The Monument

The rear slope located behind the high parking area at The Monument has a variable overtopping flow rate, which is influenced by the presence of obstacles at The Monument area. These obstacles generate flow concentrations at some areas. In addition, there are some other areas that does not have overtopping flow rate because they are just behind this obstacles.

The overtopping flow rate is variable, from 0 l/s/m to 260 l/s/m. The average overtopping flow rate along the rear slope is equal to 60 l/s/m.

The rear slope has grass coverage. Figure 4.7 shows a photograph of the rear slope at The Monument area.



Figure 4.7. Photograph of rear slope at The Monument

Characteristics overtopping flow rate (average and maximum) are larger than the maximum allowed overtopping flow rate for a grass cover (30 l/s/m).

Considering that the resistance of the grass cover is limited, diagnosis indicates that an improvement in this spot is required.

4.2.4 Spot D: Sides of tower building

At both sides of the tower building, overtopping flow rate is concentrated. The maximum overtopping flow rate will be 120 l/s/m.

On this spot, the rear slope of the dike has a revetment made of basalt. Figure 4.8 shows a photograph of the sides of the tower building.



Figure 4.8. Photograph of sides of tower building

The strength of the rear slope of the dike at this location is sufficient for a overtopping flow rate of 120 l/s/m. Therefore, improvement at this spot is not required.

4.3 Recommendations

Based on the previous diagnosis, several recommendations should be considered:

- Both transition areas and the rear slope behind the high parking area at The Monument require improvements to withstand a design storm of 1:10,000 years.
- Improvements should be an increase of dike's resistance, a diminishing of the load (reduction of overtopping flow rate) or a combination of both measures.
- The diagnosis is made on the basis of several assumptions made to determine distribution of overtopping flow rate at The Monument.
- Diagnosis considers the limit state of the dike is the removal of the outer protection (grass cover, asphalt or concrete). The resistance of the clay layer can be considered as very small, which means that in case of the design storm, the erosion of the clay layer will be sufficiently rapid to generate a breaching on the dike.

5 FINAL COMMENTS

- When calculating the overtopping flow rate on top of the dike, different roughness caused by the 2 material of basalt and grass is taken into consideration and revealed in the program "PCoverslag".
- Flow depth and velocity calculation is based on some assumptions which makes the calculation simple and remain the model a 2D model.
- In the overtopping manual 2007 the flow reduction rate is the distance from the transition part form the slope to the dike crest. This equation is made for permeable protection layers while in the monument area, the dike crest is impervious. A correction factor of 2 is used here to illuminate the uncertainty caused by the protection type.
- The distribution pattern and proportion of flow distributed is based on assumptions, for detailed and précised distribution of flow around the monument, a physical model is needed.

Appendix 1

The details of calculation procedure for wave overtopping rate and overtopping flow velocity &depth have been tabulated below and the theory of calculation can be referred to theoretical research:

Parameters	Standard cross section	Monument cross section	Transition 1	Transition 2
R_c (m+NAP)	7.9	7.75	7.9	7.75
$Z_{2\%}$ (m+NAP)	12.48	14.2	14.163	12.635
$z_{2\%} - R_c$	4.58	6.45	6.263	4.885
q (l/s/m)	270.88	579.82	549.036	289.168
V_{max}(l/m)	32349.17	59066.09	56573.1	33503.66
C'(v)	1.112636142	0.8856887	0.8856887	1.0131754
H_s	3.9	3.9	3.9	3.9
$\sqrt{gH_s}$	6.182232606	6.1822326	6.1822326	6.1822326
$R_{u,2\%} - z_A$	4.58	6.45	6.263	4.885
V(a) [m^3]	7.454163937	7.0416428	6.9388155	7.0101929
design water level [m]	5.61	5.61	5.61	5.61
tan(alpha)	0.28	0.36	0.36	0.31
C'(h)	0.123795918	0.0784444	0.0784444	0.1026524
H(a) [m]	0.566985306	0.5059667	0.4912976	0.5014572

Flow velocity and flow depth at the beginning of the dike crest

Parameters	Standard cross section	Monument cross section	Transition 1	Transition 2
C(trans,h)	0.81	0.81	0.81	0.81
H(a)	0.4592581	0.409833	0.397951	0.40618
f	0.02	0.02	0.02	0.02
C''(h)	15	15	15	15
C''(v)	0.042	0.042	0.042	0.042
V(0)	6.57662597	6.212669	6.121947	6.184921

Appendix 2

The details of calculation procedure for erosion rate of inner grass slope have been tabulated below and the theory of calculation can be referred to theoretical research. Besides, this calculation is very rough with several assumptions:

- Overtopping flow is considered as the uniform flow with same flow depth and flow velocity.
- The Chazy Coefficient is based on the typical value for river with C=50. Another two values of Chazy Coefficient around 50 is also considered in order to estimate the sensitivity of this parameter.

parameters	Standard cross section	Transition 1	Transition 2
CD	1.00E-02	1.00E-02	1.00E-02
$H_{(a)}$	0.459258	0.409833	0.397951
$u_{(mean)}$	6.576626	6.212669	6.121947
g	9.8	9.8	9.8
C	50	60	40
ρ_{sw}	1030	1030	1030
u*	0.411762	0.324145	0.479118
shear stress	174.6343	108.2224	236.4408
ρ_c	1600	1600	1600
critical shear stress	5	5	5
M	2.2528	2.2528	2.2528
Erosion rate	76.43044	46.50789	104.278
q(mean overtopping)	0.27088	0.27088	0.27088
q(single overtopping)	3.020369	3.020369	3.020369
coefficient	0.089684	0.089684	0.089684
T	1.7	2.8	1.2
Te	548.8686	904.0189	387.4367
Erosion Mass (kg/m)	41950.27	42044.01	40401.11
Erosion Mass (m^3/m)	26.21892	26.27751	25.25069
geometry of caly layer			
crest width	2.5	2.5	2.5
depth of clay	3	3	3
length of crest	15	15	15

TU DELFT – MULTIDISCIPLINARY PROJECT CIE4061

Afsluitdijk Project
"The Monument" Location

Definition of Alternatives

Sien Liu, Jun Huang, Sebastian Rayo, Tai Yan Lim

21/12/2012



CONTENTS

1 Introduction 2
1.1 Background 2
1.2 Problem Description 2
1.3 Document Scope 2
2 Alternatives 3
2.1 Reinforcing of Outer Protection 3
2.2 Wall on Top 3
2.3 Berm 4
2.4 Submersed Breakwater 4
2.5 Reinforced Grass with Small Wall 5
2.6 Energy Converter Device 6
2.7 Increase in Roughness 7
3 Pre-Dimensioning 8
3.1 Reinforcing of Outer Protection 8
3.1.1 Transition 8
3.1.2 Rear slope at The Monument 8
3.2 Wall on Top 8
3.2.1 Transition 8
3.2.2 Rear slope at The Monument 8
3.3 Berm 8
3.3.1 Transition 8
3.3.2 Rear slope at The Monument 9
3.4 Submersed Breakwater 9
3.4.1 Transition 9
3.4.2 Rear slope at The Monument 9
3.5 Reinforced Grass with Small Wall 9
3.5.1 Transition 9
3.5.2 Rear slope at The Monument 9
3.6 Energy Converter Device 10
3.6.1 Transition 10
3.6.2 Rear slope at The Monument 10
3.7 Increase in Roughness 10
3.7.1 Transition 10
3.7.2 Rear slope at The Monument 10
4 Investment Cost 11
4.1 General Information 11
4.2 Cost Estimation 11

1 INTRODUCTION

1.1 Background

The Afsluitdijk (Enclosure Dam) is a main dam that forms the fundamental part of the larger Zuiderzee Works that separates the Zuiderzee, a salt water inlet of the North Sea, and turning it into the fresh water lake of the IJsselmeer. It protects the central Netherlands from the effects of the North Sea. It was constructed between 1927 and 1933, and runs from Den Oever on Wieringen to the village of Zurich in Friesland. It is 32 km long and 90 meters wide, rising to 7.25 meters above sea-level, with an incline of 25% on each side.

At the location along the Afsluitdijk where the final water passage was closed ('De Vlieter'), a lookout tower known as 'The Monument' was built in 1933. It was presented by the Zuiderzee Works Construction Company and designed by architect W.M. Dudok. The site has a statue of a "Steenzetter", and also marks the inscription 'A living nation builds for its future'. A statue of Cornelis Lely has also been erected near Den Oever on the Barrier Dam itself.

The Afsluitdijk with The Monument are currently managed by the Ministry of Infrastructure and the Environment ("The client"). There is a restaurant at The Monument where the client has sublet it for private operator to manage it.

1.2 Problem Description

With the anticipation of increase storm intensity and sea level rise in the future, the client had previously engaged a consultant to analyze the existing design of Afsluitdijk for a design storm of 1:10,000 years. According to the client, the result of the study concluded that the standard cross-section of Afsluitdijk is not sufficient to withstand the design storm of 1:10,000 years, hence, modifications of it are required. The study also found that during the design storm, there is a significant overtopping over the dike.

The client is concerned about the significant overtopping found from the previous study may have adverse impact on the non-standard cross-section of the dike where The Monument is located. Therefore, the client has requested our design team to look into the dike section at The Monument location.

1.3 Document Scope

The main objectives of this document are:

1. To present a list of different alternatives that improves the safety of the transition areas and the rear slope at The Monument location.
2. To define preliminary dimensions for each defined alternative.
3. To estimate investment cost (in a pre-feasibility level of engineering) for each alternative.
4. To pre-select the most convenient alternatives (in terms of investment cost), which will be analysed in a multi-criteria workshop.

2 ALTERNATIVES

According with the diagnosis of The Monument area, there are two spots that requires an improvement in its level of safety. These spots are the transitions between the standard dike and The Monument location; and the rear slope behind the high parking area at The Monument location.

General improvements may be an increase of the dike's strength, a diminishing of the overtopping flow rate (reduced load) or a combination of both. A brainstorm workshop and suggestion from the Client defined several alternatives for both spots.

2.1 Reinforcing of Outer Protection

This alternative considers that the outer protection of the dike (grass cover) should be improved by replacing it with a material that stands for very large overtopping flow rate, especially without erosion. It is considered that some materials that have an important resistance against large overtopping flow rates are block revetment and asphalt.

Figure 2.1 shows a scheme with the outer protection's reinforcing. On the transition areas, grass cover of the top and rear slope of the dike are replaced by block revetment; on The Monument area, grass cover of the rear slope is replaced by block revetment.

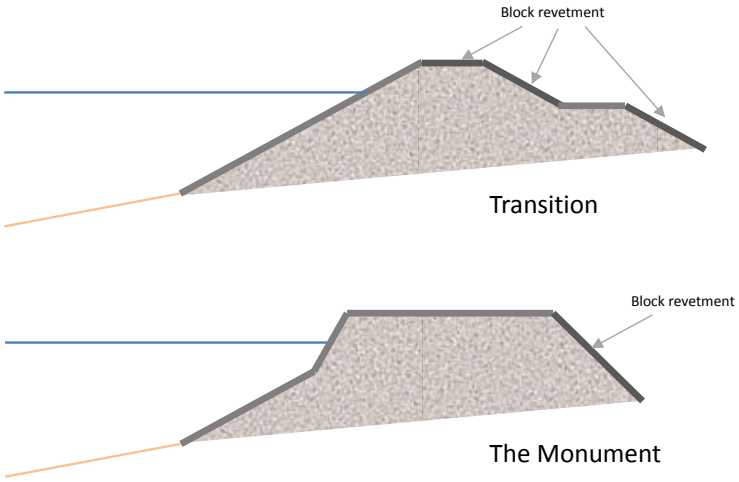

Figure 2.1. Scheme of reinforcing of outer protection

Considering that this alternative does not reduce the load, then the overtopping flow rate at the transition areas and the rear slope of The Monument are those defined in the diagnosis.

2.2 Wall on Top

This alternative considers that the overtopping flow rate on the dike will be reduced by the construction of a wall on top of the dike. Reduction of the overtopping flow rate will be to values that a grass cover can stand without significant damage. According to literature review, the selected maximum overtopping flow rate for a grass cover is 30 l/s/m.

Figure 2.2 shows a scheme with the location of the constructed wall. The wall should be constructed with a material with large resistance against direct impacts of overtopping, like concrete. On both areas, the existing grass covers are not modified.

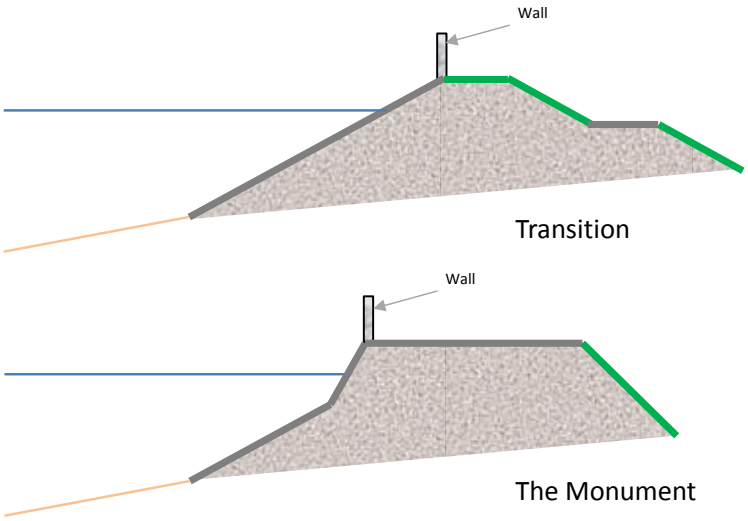

Figure 2.2. Scheme of wall on top

2.3 Berm

This alternative considers that the overtopping flow rate on the dike will be reduced by the construction of a berm on the sea side slope of the dike. Reduction of the overtopping flow rate will be to values that a grass cover can stand without significant damage. According to literature review, the selected maximum overtopping flow rate for a grass cover is 30 l/s/m.

Figure 2.3 shows a scheme with the location of the berm. The berm should be constructed with a material with large resistance against waves, like rocks. On both areas, the existing grass covers are not modified.

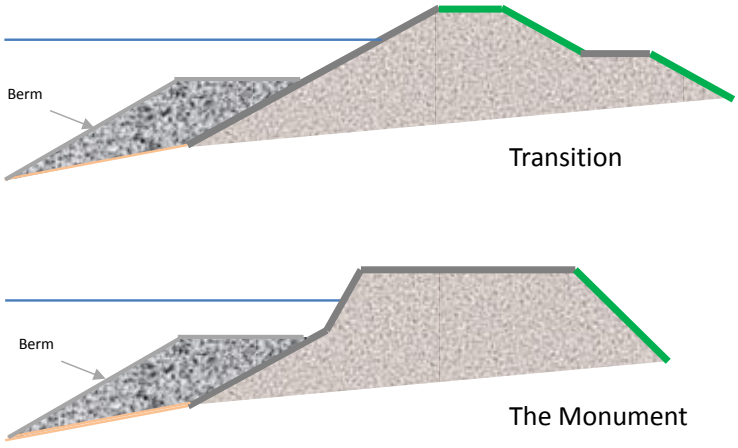

Figure 2.3. Scheme of berm

2.4 Submersed Breakwater

This alternative considers that the significant wave height will be reduced by the presence of a submersed breakwater. The transmitted waves will have a significant wave height smaller, which will finally reduce the overtopping flow rate on the dike. Final reduction of the overtopping flow rate will be to values that a grass cover can stand without significant damage. According to literature review, the selected maximum overtopping flow rate for a grass cover is 30 l/s/m.

Figure 2.4 shows a scheme with the location of the submersed breakwater. It is important to emphasize that during the design storm (1:10,000 years), the sea level will rise to a certain elevation. The proposed breakwater will be 'submersed' only during this type of events. The rest of the time the crest of the breakwater will be over the sea surface, which means that the armour layer of this structure must be designed for direct wave impacts.

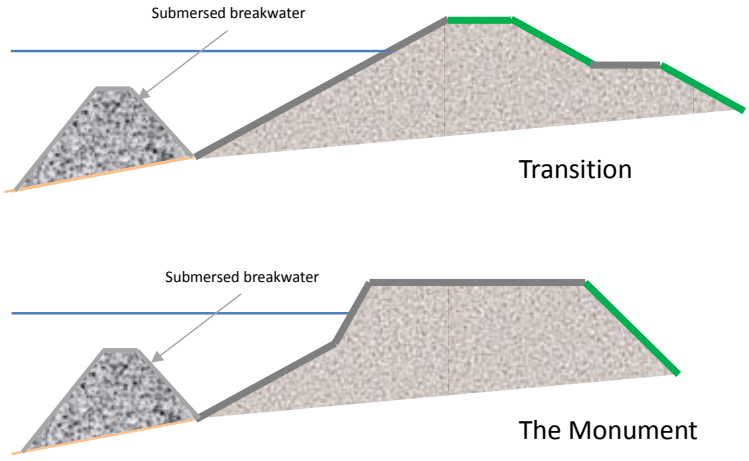

Figure 2.4. Scheme of submersed breakwater

2.5 Reinforced Grass with Small Wall

This alternative considers that the strength of the outer protection of the dike will be increased and, at the same time, the load on the dike will be reduced (partially). The existing grass cover will be replaced by a reinforced grass cover (with geo-membrane) that has a better behaviour against erosion caused by overtopping flow rate. Nevertheless, there is no available information about maximum overtopping flow rates for this type of protection. Maximum allowed overtopping flow rate will be estimated based on the increase of the maximum significant wave height and its relation with overtopping flow rate.

Figure 2.5 presents a graph that indicates increase of allowed significant wave height in terms of the grass cover status.

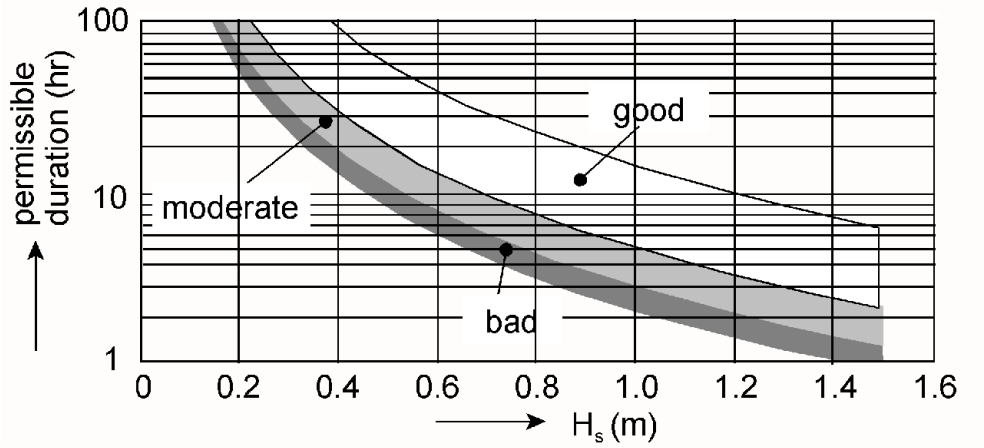

Figure 2.5. Permissible flow duration on grass cover. Source: Schiereck, G. J., 'Introduction to Bed, Bank and Shore Protection'

Assuming typical storm duration of 5 hours, an increase of the grass status from moderate to good is reflected in an increase of the maximum significant wave height from 1.0 m to 1.5 m, which is an increment of 50%. By using software 'PCOverslag', it is possible to estimate that the maximum overtopping flow rate increases from 30 to 150 l/s/m when there is an increment of maximum allowed significant wave height of 50%. Nevertheless, it is important to emphasize that this method is only an assumption and further research should be made in order to estimate more accurately the real resistance of reinforced grass.

Because the maximum overtopping flow rate for reinforced grass is smaller than the overtopping flow rate estimations, it is necessary to reduce the load on the dike. This partial reduction will be made by constructing a small wall on top of the dike.

Figure 2.6 shows a scheme with the location of the reinforced grass and the small wall. While the reinforced grass will have a geo-membrane to increase resistance against erosion, the wall will be made of a material with sufficient resistance against overtopping flow, like concrete.

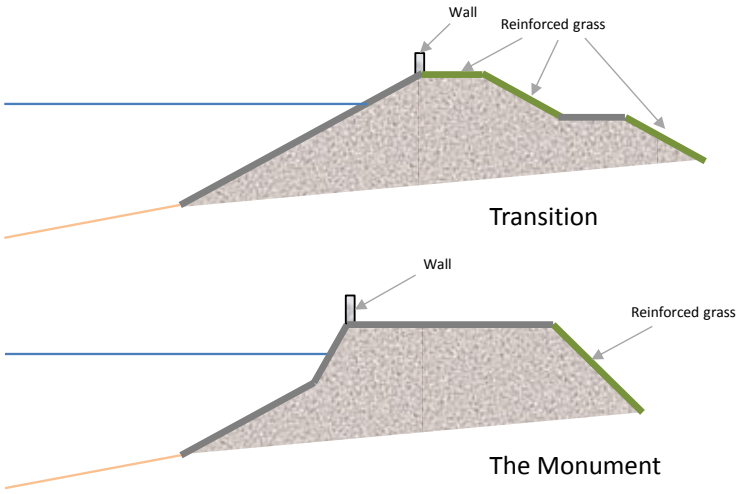

Figure 2.6. Scheme of reinforced grass and small wall

2.6 Energy Converter Device

This alternative considers that the load on the dike will be reduced by several energy converter devices. These devices extract part of the wave energy, transform it into electric energy and reduce the wave energy that reaches the dike. Therefore, the significant wave height is reduced and in this way, the overtopping flow rate also reduces. Final reduction of the overtopping flow rate will be to values that a grass cover can stand without significant damage. According to literature review, the selected maximum overtopping flow rate for a grass cover is 30 l/s/m.

Figure 2.7 shows a scheme with the location of the energy converter device. Considering that there are many different type of energy converter (floating or bottom-placed units), the pre-selected units will be Oyster (bottom-placed units). On both areas the existing grass covers are not modified.

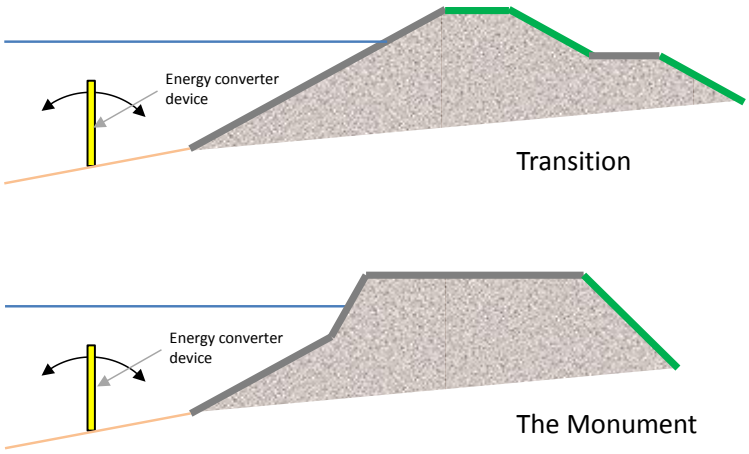

Figure 2.7. Scheme of energy converter device

2.7 Increase in Roughness

This alternative considers that the overtopping flow rate on the dike will be reduced by an increase of the roughness at the dike's seaside slope. A larger roughness generates a reduction in the overtopping flow rate. Nevertheless, the reduction in the overtopping flow rate is not sufficient to obtain values smaller than the maximum allowed for the grass covers. An increase in roughness will be obtained by replacing the basalt cover with a more rough material, for example, rocks.

Because the maximum overtopping flow rate for reinforced grass is smaller than the overtopping flow rate, it is necessary to reduce the load on the dike. This partial reduction will be made by constructing a small wall on top of the dike.

Figure 2.8 shows a scheme with the location of the increased roughness of the dike. On both areas the existing grass covers are not modified.

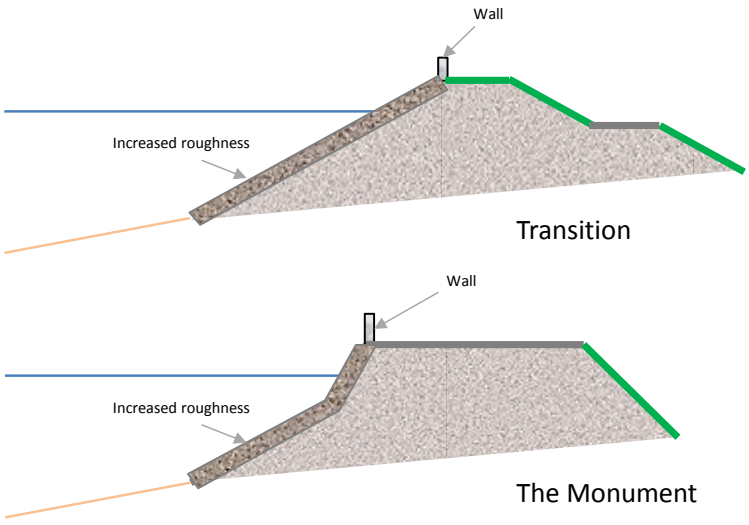

Figure 2.8. Scheme of increased roughness in seaside slope

3 PRE-DIMENSIONING

To evaluate the different alternatives, a rough dimensioning for each one is completed. A summary of these dimensions (for transition and rear slope critical spots) is presented forward.

It is important to notice that both transition areas are symmetrical. In addition, each one is divided into two equal sectors: one closer to The Monument and another close to the standard section of the dike.

3.1 Reinforcing of Outer Protection

3.1.1 Transition

The area of the sector closer to The Monument has a length of 240 m and a width of 18 m. The area of the sector closer to the standard section of the dike has the same dimensions. Therefore, the total area to be covered is **8,640** m^2. It is considered the utilisation of block revetment on this entire area.

3.1.2 Rear slope at The Monument

The area has a length of 350 m and a width of 8 m. Therefore, the total area to be covered is **2,800** m^2. It is considered the utilisation of block revetment on this entire area.

3.2 Wall on Top

3.2.1 Transition

On the sector closer to The Monument, the total length is 240 m. Preliminary dimensions of the seawall are a height of 0.9 m and a width of 0.4 m. Considering a foundation factor equal to 2 (i.e. the foundation will have the same volume than the part of the wall above the terrain), the total volume of the wall is 173 m^3.

On the sector closer to the standard dike, the total length is 240 m. Preliminary dimensions of the seawall are a height of 0.6 m and a width of 0.4 m. Considering a foundation factor equal to 2 (i.e. the foundation will have the same volume than the part of the wall above the terrain), the total volume of the wall is 115 m^3.

Chosen material is concrete. Therefore, the total volume of concrete is equal to **288** m^3.

3.2.2 Rear slope at The Monument

The area has a length of 350 m. Preliminary dimensions of the seawall are a height of 0.8 m and a width of 0.4 m. Considering a foundation factor equal to 2 (i.e. the foundation will have the same volume than the part of the wall above the terrain), the total volume of the wall is **224** m^3. Chosen material is concrete.

3.3 Berm

3.3.1 Transition

On the sector closer to The Monument, the total length is 240 m. Preliminary dimensions of the berm indicates a width of 35 m and a height of 3.5 m. Total volume is **29,400** m^3.

On the sector closer to the standard dike, the total length is 240 m. Preliminary dimensions of the berm indicates a width of 30 m and a height of 3.5 m. Total volume is 25,200 m^3.

Chosen material is rocks. Therefore, the total volume of rocks is equal to **54,600** m^3.

3.3.2 Rear slope at The Monument

The area has a length of 350 m. Preliminary dimensions of the berm indicates a width of 35 m and a height of 3.5 m. Total volume is **42,875** m^3. Chosen material is rocks.

3.4 Submersed Breakwater

3.4.1 Transition

On the sector closer to The Monument, the total length is 240 m. Preliminary dimensions of the submersed breakwater indicates a height of 4.6 m, a crest width of 3 m and slopes of 1:3. Total volume is 18,547 m^3. These dimensions are the same considered for the area closer to the standard dike.

The chosen material is rocks. During normal operation of the breakwater, its height will be above the water level, thus it will operate as a regular breakwater. The armour material must have sufficient stability to resist the direct impact of waves. Hence, chosen material is rocks. Total volume is **37,094** m^3.

3.4.2 Rear slope at The Monument

For the area for the rear slope at The Monument, it has a length of 350 m. Preliminary dimensions of the submersed breakwater required a height of 4.6 m, a crest width of 3 m and slopes of 1:3. Total volume is **18,547** m^3. Like in the transition spot, chosen material is rocks.

3.5 Reinforced Grass with Small Wall

3.5.1 Transition

The area of the sector closer to The Monument has a length of 240 m and a width of 18 m. The area of the sector closer to the standard section of the dike has the same dimensions. Therefore, the total area to be covered is **8,640** m^2. It is considered the utilisation of reinforced grass on this entire area.

Because the overtopping flow rate exceeds the maximum allowed overtopping flow rate for reinforced grass, it is necessary to include a small seawall. On the area closer to The Monument it will have a height of 0.3 m and a width of 0.4 m. On the area closer to the standard dike it will have a height of 0.2 m and a width of 0.4 m. Total volume for the small seawall (including foundations) is **140** m^3. Chosen material is concrete.

3.5.2 Rear slope at The Monument

The area has a length of 350 m and a width of 8 m. Therefore, the total area to be covered is **2,800** m^2. It is considered the utilisation of reinforced grass on this entire area.

Because the overtopping flow rate exceeds the maximum allowed overtopping flow rate for reinforced grass, it is necessary to include a small seawall. It will have a height of 0.2 m and a width of 0.4 m. Total volume for the small seawall (including foundations) is **56** m^3. Chosen material is concrete.

3.6 Energy Converter Device

3.6.1 Transition

Total length of both areas (closer to The Monument and closer to the standard dike) is 480 m. Energy converter devices like Oyster has a width of 15 m. Hence, the total required units are **56**.

3.6.2 Rear slope at The Monument

Total length of this area is 350 m. Energy converter devices like Oyster has a width of 15 m. Hence, the total required units are **40** m.

3.7 Increase in Roughness

3.7.1 Transition

In order to increase roughness of the seaside slope, it is considered to replace existing basalt with natural rocks. On the transition spot, the total length of both areas (closer to The Monument and closer to the standard dike) is 480 m, while total width is 26 m. Considering a conservative value for rocks dimension equal to 0.4 m, total volume of rocks is equal to **5,000** m^3.

Because the overtopping flow rate exceeds the maximum allowed overtopping flow rate for reinforced grass, it is necessary to include a small seawall. On both areas (closer to The Monument and closer to the standard dike), it will have a height of 0.1 m and a width of 0.4 m. Total volume for the small seawall (including foundations) is **56** m^3. Chosen material is concrete.

3.7.2 Rear slope at The Monument

In order to increase roughness of the seaside slope, it is considered to replace existing basalt with natural rocks. Total length is 350 m, while total width is 26 m. Taking a conservative value for rocks dimension equal to 0.4 m, total volume of rocks is equal to **3,640** m^3.

Because the overtopping flow rate exceeds the maximum allowed overtopping flow rate for reinforced grass, it is necessary to include a small seawall. It will have a height of 0.1 m and a width of 0.4 m. Total volume for the small seawall (including foundations) is **28** m^3. Chosen material is concrete.

4 INVESTMENT COST

4.1 General Information

To estimate the investment cost for each alternative, the following unitary prices are assumed:

- Block revetment: 7 US$/yd^2 = **58** euros/m^2. Source: US Army Corps of Engineers, 'Design of Coastal Revetments, Seawalls and Bulkheads'.
- Concrete: 260 US$/m^3 = **200** euros/m^3. Source: own assumption.
- Rocks: 60 US$/yd^3 = **55** euros/yd^3. Source: US Army Corps of Engineers, 'Design of Coastal Revetments, Seawalls and Bulkheads'.
- Reinforced grass: **14** euros/m^2. Source: own assumption.
- Energy converter device: 33 x 10^6 euros/unit. Source: www.aquamarinepower.com

4.2 Cost Estimation

Table 4.1 presents a summary with the cost estimation per alternative per critical spot.

Table 4.1. Summary of investment cost estimation

Spot	Alternative	Quantity	Total cost *(euros)*
Transition	A1 – Reinforcing of outer protection	Block revetment: 8,640 m^2	500,000
	A2 – Wall on top	Concrete: 288 m^3	35,000
	A3 – Berm	Rocks: 54,600 m^3	3,000,000
	A4 – Submersed breakwater	Rocks: 37,094 m^3	2,000,000
	A5 – Reinforced grass with small wall	Reinforced grass: 8,640 m^2 Concrete: 140 m^3	150,000
	A6 – Energy converter device	Oyster: 56 units	1,850,000,000
	A7 – Increase in roughness	Rocks: 5,000 m^3 Concrete: 56 m^3	550,000
The Monument	B1 – Reinforcing of outer protection	Block revetment: 2,800 m^3	162,000
	B2 – Wall on top	Concrete: 224 m^3	58,000
	B3 – Berm	Rocks: 42,875 m^3	2,400,000
	B4 – Submersed breakwater	Rocks: 18,547 m^3	1,500,000
	B5 – Reinforced grass with small wall	Reinforced grass: 2,800 m^3 Concrete: 56 m^3	50,000
	B6 – Energy converter device	Oyster: 40 units	1,350,000,000
	B7 – Increase in roughness	Rocks: 3,640 m^3 Concrete: 28 m^3	400,000

5 FINAL COMMENTS

Regarding with the definition of alternatives and its investment costs, the following comments are made:

- Most of the proposed alternatives are improvements that by themselves solve the overtopping problems at the critical spots (transition areas and rear slope of The Monument). Nevertheless, the utilisation of reinforced grass and an increase in roughness of the seaside slope of the Afsluitdijk necessarily require a partial reduction of the load. This partial reduction is obtained with the construction of a small seawall.
- Dimensioning of each alternative is preliminary. It obeys to an intention to estimate roughly the investment cost, information that is necessary in order to discard any possible alternative because of economic unfeasibility.
- For the transition spot, the cheapest alternatives are A2 (wall on top) and A5 (reinforced grass with small wall), with investment costs equal to 35,000 and 150,000 euros, respectively. The investment cost for the rest of the alternatives exceeds several times the cheapest costs, therefore, the rest of the alternatives are considered as economical unfeasible and discarded from this analysis.
- For The Monument spot, the cheapest alternatives are B1 (reinforcing of outer protection), B2 (wall on top) and B5 (reinforced grass with small wall), with investment costs equal to 162,000, 58,000 and 50,000 euros, respectively. The investment cost for the rest of the alternatives exceeds several times the cheapest costs, therefore, the rest of the alternatives are considered as economical unfeasible and discarded from this analysis.
- Pre-selected alternatives (A2 and A5; B1, B2 and B5) will be analysed in a Multi-Criteria workshop. Results of this workshop will define the best alternative for each spot.

TU DELFT – MULTIDISCIPLINARY PROJECT CIE4061

Afsluitdijk Project
"The Monument" Location

Multi – Criteria Analysis

Sien Liu, Jun Huang, Sebastian Rayo, Tai Yan Lim

21/12/2012



CONTENTS

1 Introduction 2
1.1 Background 2
1.2 Problem Description 2
1.3 Document Scope 2
2 Methodology 3
3 Criteria Definition 3
4 Alternatives 4
5 Evaluation 4
6 Result 5
7 Final Comments 7

1 INTRODUCTION

1.1 Background

The Afsluitdijk (Enclosure Dam) is a main dam that forms the fundamental part of the larger Zuiderzee Works that separates the Zuiderzee, a salt water inlet of the North Sea, and turning it into the fresh water lake of the IJsselmeer. It protects the central Netherlands from the effects of the North Sea. It was constructed between 1927 and 1933, and runs from Den Oever on Wieringen to the village of Zurich in Friesland. It is 32 km long and 90 meters wide, rising to 7.25 meters above sea-level, with an incline of 25% on each side.

At the location along the Afsluitdijk where the final water passage was closed ('De Vlieter'), a lookout tower known as 'The Monument' was built in 1933. It was presented by the Zuiderzee Works Construction Company and designed by architect W.M. Dudok. The site has a statue of a "Steenzetter", and also marks the inscription 'A living nation builds for its future'. A statue of Cornelis Lely has also been erected near Den Oever on the Barrier Dam itself.

The Afsluitdijk with The Monument are currently managed by the Ministry of Infrastructure and the Environment ("The client"). There is a restaurant at The Monument where the client has sublet it for private operator to manage it.

1.2 Problem Description

With the anticipation of increase storm intensity and sea level rise in the future, the client had previously engaged a consultant to analyze the existing design of Afsluitdijk for a design storm of 1:10,000 years. According to the client, the result of the study concluded that the standard cross-section of Afsluitdijk is not sufficient to withstand the design storm of 1:10,000 years, hence, modifications of it are required. The study also found that during the design storm, there is a significant overtopping over the dike.

The client is concerned about the significant overtopping found from the previous study may have adverse impact on the non-standard cross-section of the dike where The Monument is located. Therefore, the client has requested our design team to look into the dike section at The Monument location.

1.3 Document Scope

The main objectives of this document are:

1. To explain the methodology of multi – criteria method here used and define every criteria.
2. To analyse the alternatives with the method and derive the result needed.

2 METHODOLOGY

The multi-criteria analysis is a sub-discipline of operations research that explicitly considers multiple criteria in decision-making environments. Various criteria are taken into consideration; cost can be the most important criterion.

We consider 10 criteria which are listed below: Investment costs, Maintenance costs, Common practice , Aesthetic , Environment , Ease of construction , Overtopping reduction , Flexibility , Additional benefit, Public safety. And for each criterion, a certain weight factor is given based on the importance and preference of it. The weight varies from 0 to 1.

For each criterion, different methods are evaluated and given certain scores based on how much the criterion is fulfilled. The scores vary from 0 to 1 and have a sum of 1.

From the basic analysis, 3 alternatives for position A, and 2 alternatives for position B. For position A, the 3 alternatives are A1 reinforced dike, A2 wall in top and A5 reinforced grass and wall respectively, and for position B, B2 wall in top and B5 reinforced grass and wall are chosen.

After the procedures, each method is evaluated by adding the score multiplied by the weight together. The method with the largest value is the best one.

3 CRITERIA DEFINITION

Investment cost

The total investment cost is very important for the designer and stakeholder to take into concern.

Maintenance cost

Maintenance should be reduced to as low as possible, and for some alternatives, it is quite difficult to maintain, so the cost will be very high.

Common practice

Common practice measures whether the alternative is commonly used by the public, if it is, it will reduce the difficulty of construction.

Aesthetic

Aesthetic is a very important criterion since the monument place is also a very famous tourist place.

Environment

Environment is always an important around coastal areas including factors like sediment transport, it should be concerned.

Ease of construction

The ease of construction is defined to measure how easy it is to construct the certain construction or to install the particular devices. Including the adjustment of the design and construction technology for the certain location; the amount of waste and abortive work; the ease for the local construction industry participants are able to read construction documentation, including all drawings and specifications.

Overtopping reduction

Large overtopping rate will increase the failure probability of the inner slope and also will largely affect the monument and the restaurant. So the criteria of the overtopping reduction is essential here to measure the influence of the allowable overtopping.

Flexibility

With time increase, the construction will need some maintenance as well as some improvement. Even the construction will be replaced by some more effective ones with modern technology. Here the criteria is to measure the ease of that.

Additional benefits

For methods with special devices there will be some additional benefits such as income from wave energy converter.

Public safety

The public safety concerns about people who may be in danger caused by overtopping, as well as the vehicles in the parking area, and the restaurant's safety.

4 ALTERNATIVES

Based on the diagnosis the section A and the section B are chosen to be analyzed.

For section A, six methods are analyzed, which are:

- A1: reinforce dike with revetment
- A2: seawall in dike's crest
- A3: construct a berm,
- A4: construct a submerged breakwater
- A5: replace grass with reinforced grass and construct seawall in dike's crest
- A6: install energy converter device
- A7: increase of roughness

For section B, the alternatives are the same.

According to the previous document in alternatives, A1, A2 and A5 are selected for location A; B2 and B5 are selected for location B.

5 EVALUATION

Investment costs: Wall on top has a lower investment cost than reinforced grass and wall. For position A, A2 and A5 get the highest value. For position B, B2 gets the higher value.

Maintenance costs: Reinforced grass requires a continuous checking of the status of the grass. Hence, its maintenance costs are more expensive than the other alternatives. A dike's reinforcing and a wall in top do not require too

much maintenance. A1, A2 have the same high score and A5 has the lower score. For location B, B2 has a lower maintenance cost so the score is lower.

Common practice: The most common practice to face overtopping is to make revetment or put walls. The methods A1 and A2 have the high score while A5 has a low score since it is comparably rare. Of course for location B, B2 is more common to see.

Aesthetic: Solutions that do not modify the cross section have a better score. The worst solution is to place a revetment all along the dike, because there will be no grass anymore.A5 and B5 have high scores since they don't rather change the original profile.

Environment: Dike reinforcement will remove all the grass, affecting that environment. A2 has the highest score and A1 has the lowest value. For location B, B2 has a higher value since unlike reinforced grass and wall, it changes the environment less.

Ease of construction: Build a wall is the easiest of solutions, so that A2 and B2 have the highest value.

Overtopping reduction: All solutions can reduce overtopping rate, among which the wall in top is the most effective. A2 has the higher value and for location B, B2 has the higher value.

Flexibility: A wall on top of the dike reduces the overtopping to a minimal value. Reinforced grass with a small wall also reduces it, but partially. Dike's reinforcing does not reduce the overtopping flow rate. So A2 and A5 share the higher score while A1 has the lower value. For location B, increasing wall's height is the easiest way to increase resistance against possible rises in overtopping, which is similar for both alternatives.

Additional benefit: Neither of this alternatives has an additional benefit. So the score for each alternative is the same.

Public safety: Overtopping reduction alternatives are safer for possible pedestrians and vehicles during a major storm. Thus A2 and B2 have the higher score.

For section B, the methods are the same while the score for each criterion is more or less the same.

6 RESULT

For the multiple criteria analysis the weight and the score are put in in Tables 6.1 and 6.2.

Table 6.2. Results of total score for location A

Criterion	Weight	Methods	
		A2	A5
Investment costs	1.0	0.60	0.40
Maintenance costs	1.0	0.60	0.40
Common practice	0.7	0.65	0.35
Aesthetic	0.5	0.40	0.60
Environment	0.7	0.55	0.45
Ease of construction	0.8	0.65	0.35
Overtopping reduction	0.2	0.60	0.40
Flexibility	0.5	0.50	0.50
Additional benefit	0.3	0.50	0.50
Public safety	0.8	0.60	0.40
Total Score		**3.76**	**2.74**

Table 6.1. Results of total score for location B

Criterion	Weight	Methods		
		B1	B2	B5
Investment costs	1.0	0.12	0.44	0.44
Maintenance costs	1.0	0.37	0.37	0.26
Common practice	0.7	0.38	0.38	0.24
Aesthetic	0.5	0.20	0.30	0.50
Environment	0.7	0.13	0.50	0.38
Ease of construction	0.8	0.31	0.38	0.31
Overtopping reduction	0.2	0.15	0.50	0.35
Flexibility	0.5	0.20	0.40	0.40
Additional benefit	0.3	0.33	0.33	0.33
Public safety	0.8	0.13	0.50	0.38
Total Score		**1.52**	**2.68**	**2.30**

It can be seen clearly from the table above, build a wall on top of the dike for both locations can be found to be the chosen choices.

7 FINAL COMMENTS

- The methodology of multi – criteria is used here to make sure each important criterion is considered and weighed properly.
- Altogether 10 criteria are defined. Including investment cost, maintenance cost, common practice, aesthetic, environment, ease of construction, overtopping reduction, flexibility, additional benefit and public safety. The criterion which weighs the most is the investment cost and the maintenance cost which makes sense since cost has always the priority, among the options the final alternative "wall on top of the dike" has the least investment and maintenance cost.
- The criterion of additional benefit is set for alternative 6: install energy convertor device, since it has already been cancelled due to high investment cost, the value for this criterion of each alternative in Table 6.1 and 6.2 are the same.
- Based on the description in document "Definition of alternatives", there are seven alternatives to be chosen. After the selection of rough estimate of cost, 2 alternatives for location A and 3 alternatives for location B are left. Each alternative is valued of the 10 criteria, multiplied by the weight and add together. The final alternative for both location turn out to be the same: wall on the top of the dike.

TU DELFT – MULTIDISCIPLINARY PROJECT CIE4061

Afsluitdijk Project
"The Monument" Location

Overtopping Wall Design

Sien Liu, Jun Huang, Sebastian Rayo, Tai Yan Lim

21/12/2012



CONTENTS

1 Introduction 1
1.1 Background 1
1.2 Problem Description 1
1.3 Document Scope 1
2 Overtopping retaining wall 2
2.1 Gravity wall 2
2.2 Design of Cantilever Retaining Wall 2
3 Construction of cantilever retaining wall 6
4 final comments 8

1 INTRODUCTION

1.1 Background

The Afsluitdijk (Enclosure Dam) is a main dam that forms the fundamental part of the larger Zuiderzee Works that separates the Zuiderzee, a salt water inlet of the North Sea, and turning it into the fresh water lake of the IJsselmeer. It protects the central Netherlands from the effects of the North Sea. It was constructed between 1927 and 1933, and runs from Den Oever on Wieringen to the village of Zurich in Friesland. It is 32 km long and 90 meters wide, rising to 7.25 meters above sea-level, with an incline of 25% on each side.

At the location along the Afsluitdijk where the final water passage was closed ('De Vlieter'), a lookout tower known as 'The Monument' was built in 1933. It was presented by the Zuiderzee Works Construction Company and designed by architect W.M. Dudok. The site has a statue of a "Steenzetter", and also marks the inscription 'A living nation builds for its future'. A statue of Cornelis Lely has also been erected near Den Oever on the Barrier Dam itself.

The Afsluitdijk with The Monument are currently managed by the Ministry of Infrastructure and the Environment ("The client"). There is a restaurant at The Monument where the client has sublet it for private operator to manage it.

1.2 Problem Description

With the anticipation of increase storm intensity and sea level rise in the future, the client had previously engaged a consultant to analyze the existing design of Afsluitdijk for a design storm of 1:10,000 years. According to the client, the result of the study concluded that the standard cross-section of Afsluitdijk is not sufficient to withstand the design storm of 1:10,000 years, hence, modifications of it are required. The study also found that during the design storm, there is a significant overtopping over the dike.

The client is concerned about the significant overtopping found from the previous study may have adverse impact on the non-standard cross-section of the dike where The Monument is located. Therefore, the client has requested our design team to look into the dike section at the Monument location.

1.3 Document Scope

The main objectives of this document are:

- Design a retaining wall to make an overtopping rate reduction from 588 l/m/s to 60 l/m/s. Design dimensions of the wall and check the stability of the wall against the wave overtopping.
- Make a construction proposal with rough estimation only to provide an initial overview of the construction sequence and the duration required.

2 OVERTOPPING RETAINING WALL

2.1 Gravity wall

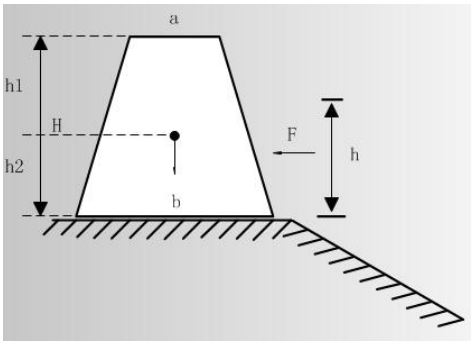

Figure 2.1 gravity wall

Table 2.1 rough calculation of dimension of gravity wall

Parameter	Value
F [N]	20639
a [m]	0.5
B [m]	0.8
G [N]	13759
f [N]	4128
Conclusion : f << F	

It can be seen from the first estimation of dimensions of gravity wall, the friction force is much less than the flow force ($F \approx 5f$). In addition, the dimension of gravity wall is already very large with a=0.5 m and b=0.8m. If a gravity wall is designed as a solution for overtopping reduction, a large structure will be required and it can be very costly due to the huge amount of material required. Consequently, a smaller structure with a strong resistant to wave overtopping is preferred. Cantilever Retaining Wall structure is thus chosen as a good system for overcoming overtopping flow from the wave for this design.

2.2 Design of Cantilever Retaining Wall

There are three main failure mechanisms for cantilever retaining wall, they are sliding, overturning and bearing (see figures below).

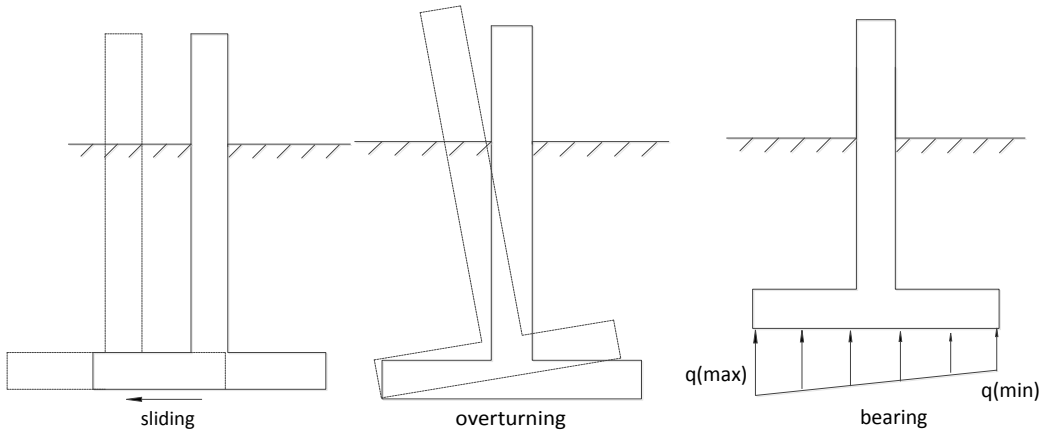

Figure 2.2 failure patterns

First, a force diagram is drawn for design of Cantilever Retaining Wall as shown in Figure 3. Figure 3 shows all the main forces acting on the structure and table 2 shows the interpretation of each force.

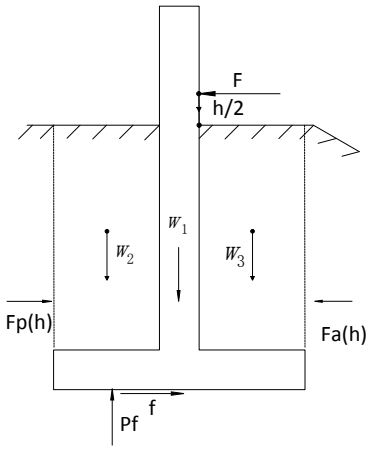

Figure 2.3 force diagram

Table 2.2 Interpretation of force

parameter	**Interpretation**
F	Flow impact force
W1	Gravity of structure
W2 & W3	Gravity of clay
Fa(h)	Active force Fa
Fp(h)	Passive force Fp
f	Friction force
Pf	Uplift force

For considering failure pattern of sliding, the balances of horizontal forces and vertical forces are important such that the net horizontal force and net vertical force must be zero, which are shown as follows:

$$\sum_{i=1}^{n} F_{X(i)} = 0$$

$$\sum_{i=1}^{n} F_{Y(i)} = 0$$

For considering failure pattern of overturning, the balance on the sum of moment around heel is important, which is shown as follows:

$$M_{driving} + M_{resisting} = 0$$

For considering failure pattern of bearing, the loss of strength for the soil below the footing of the wall becomes the cause of failure (see figure 1 c), which can be calculated by following equations:

$$q_{max} = \left(\frac{W}{B}\right) * \left(1 + \frac{6e}{B}\right)$$

$$q_{min} = \left(\frac{W}{B}\right) * \left(1 - \frac{6e}{B}\right)$$

Where:

q_{max} – maximum pressure executed on bottom.

q_{min} – minimum pressure executed on bottom.

W – glossary weight of structure (plus earth weight).

e – distance from heel to center of under footing.

B – length of under footing.

Retaining wall design is an iterative process. An initial geometry is usually assigned to the wall and the appropriate forces are calculated. The actual forces are then checked using acceptable factors of safety and the geometry is revised until satisfactory factors of safety are reached. There are however, common dimensions for walls that are available that can be used as a first cut.

Based on the theory given above, after several trial and error, the final dimension of the structure has been determined as follows.

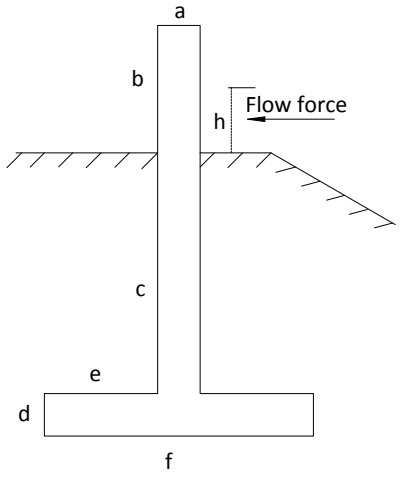

Figure 2.4 dimensions of retaining wall

Table 2.3 Dimensions of Cantilever Retaining Wall

Parameter	Value
a [m]	0.3
b [m]	0.9
c [m]	1.7
d [m]	0.3
e [m]	0.8
f [m]	1.9

The final stability is checked and the procedure of calculation is tabulated as follows:

Table 2.4 stability of structure

SECTION	AREA	ρ	W_i	Arm of force	M_i
1	1.35	2400	19110	0.95	18154.5
2	1.36	1800	23990	0.4	9596
3	1.36	1800	23990	1.5	35985
$\sum Mi$ =63735.5					
Lateral earth pressure (Left side)					
D	K_p	P_p	F_p	Arm of force	M_p
2	2.62	963	963	0.67	645.2
Lateral earth pressure (Right side)					
D	K_a	P_a	F_a	Arm of force	M_a
2	0.38	140	140	0.67	93.8
Overturning					
$M_r = M_p + \sum Mi = 645.2 + 63735.5 = 64380.7$ $M_d = M_F + M_a = 20639 \cdot 2.23 + 93.8 = 46118.8$ Safty factor $= M_r/M_d =$ **$\mathbf{1.40}$ (limit 1.3)**					
W_1	W_2	W_3	μ	F	P_f
19110	23990.4	23990.4	0.4	20639	67090.8
Sliding					
$F_{net} = F + F_a - F_p = 20639 + 140 - 963 = 19816$ $f = \mu \cdot P_f = 26836.3$ Safety of factor $= f/F_{net} =$ **$\mathbf{1.35}$ (limit 1.3)**					
Bearing					
$q_{max} = q'_{max} + q' = 35311 + 142698 = 178009 = 178$kPa $q_{allowable} = 300kPa$ (Source: British Code) Safety factor $= q_{allowable}/q_{max} =$ **$\mathbf{1.68}$ (limit 1.5)**					

3 CONSTRUCTION OF CANTILEVER RETAINING WALL

A rough estimation of the construction time is given; the starting time of the whole project is set to be on 20th, March, 2013.

The whole project construction contains two phases. The first phase starts from 20th, March, 2013 and ends at 23rd, April, 2013, including the task of construction preparation, foundation excavation, gravel cushion, steel processing, the scaffold ride demolition template group demolition, concrete pouring. The second part starts from 25th, May, 2013 and ends at 11th, May, 2013, including wall the Backfill compacted, mortared rubble slope protection, Mortar rubble draining system, and concrete curing.

Table 3.1 Construction procedure of cantilever retaining wall

Name of procedure	Duration
Preparation for construction	3 days
Reinforced steel bending preparation	9 days
Foundation excavation	7 days
Gravel mattress	7 days
Concrete stepping stone layer	4 days
Steel banding	14 days
Scaffolding erection	6 days
Template installation	11 days
Pouring concrete	9 days
Template removal	3 days
Backfill compacted	10 days
Mortar rubble slope protection	16 days
Mortar rubble draining system	16 days
Cleaning the area	2 days

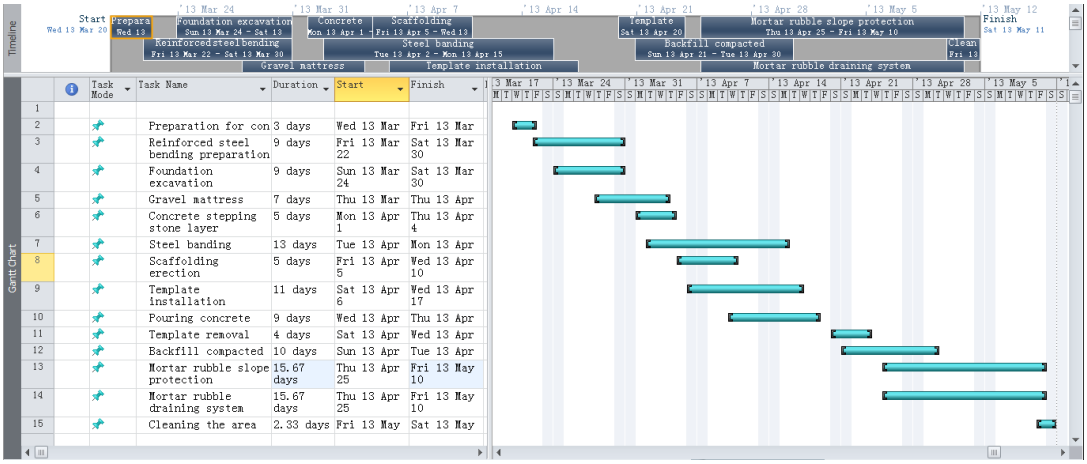

Figure 3.1 construction sequence

4 FINAL COMMENTS

1. Two kinds of retaining walls have been considered in this design, Gravity Wall and Cantilever Retaining Wall. However, it requires too much material of concrete for Gravity Wall. Hence, the Cantilever Retaining Wall is chosen as the optimum alternative.
2. The height of wall (b=0.9m) above the ground is determined by certain degree of overtopping rate reduction. This is calculated by PCOverslag software and not included in the part of wall design.
3. The foot of the wall is symmetric as a simple design. It is suggested to adjust the foot of the structure to make further design.
4. Three failure patterns are checked in the wall design including overturning, sliding, and bearing of earth. However, the bending failure of the structure is not considered in the design. This kind of failure pattern can always be avoided by increasing the number of rebar in the wall.